CHAPTER 2. SURFACE WATER HYDROLOGY

2.1. INTRODUCTION

Surface water hydrology is one of the key driving variables in river ecosystems. The natural characteristics of a river ecosystem are (1) influenced by the underlying geology and tectonics; (2) created and maintained by geomorphic and hydrologic processes that result from energy and material interactions between flowing water and sediment supply; and in some cases (3) influenced by riparian vegetation. The complexity of river ecosystems can be simplified somewhat by a hierarchical conceptual model of how the interaction of water and sediment (the basic independent variables that influence shorter-term channel processes and form) cascade down to the biota (Figure 2-1). This conceptual model illustrates how water and sediment interact to cause fluvial geomorphic processes that are responsible for creating and maintaining channel form (morphology). Correspondingly, the channel morphology provides aquatic and terrestrial habitat within the river corridor, and thus influences the abundance and distribution of riverine biota. Each tier of the hierarchical model can be described as having the following components:

- SUPPLY: Primary natural components of supply are water and sediment, with some influence by logs delivered from eroding banks and the upstream watershed. Changes to water and sediment in this conceptual system cascade down to the biota, but this cascading perspective is often not adequately considered before the management change is imposed on the system.
- PROCESS: The primary natural components of the processes tier are sediment transport, sediment deposition, channel migration, channel avulsion, nutrient exchange, and surface water-groundwater exchange. Sediment transport and deposition form alluvial features, including alternate bars and floodplain surfaces. These processes typically occur during high flow events, which occur over a relatively small percentage of the year.
- FORM: In turn, processes create the channel and floodplain features that define aquatic and terrestrial habitat along the river corridor. Form provides the physical location and suitable conditions that define habitat for aquatic organisms, including native fish species. Channel morphology is thus a critical linkage between fluvial processes and the native biota that use the river corridor.
- BIOTA: Typically the management target, the biota responds to changes cascading from Supply, Process, and Form. Changes to water and sediment in this conceptual system cascade down to the biota, but this cascading perspective is often not adequately considered before the management change is imposed on the system.

Humans are also part of river ecosystems. Within this natural hierarchical framework, there are human components that influence each hierarchy (Figure 2-1). Management of supply, such as dams changing the flow and sediment regime of a river, causes changes to processes and form that influence biota. Additionally, there are constraints within human management infrastructure or policy, such as dam outlet works or property damage avoidance that influence this hierarchy.

This chapter provides background on the Water component of the SUPPLY tier and discusses how changes in water routing and inundation have changed as a result of human management in the San Joaquin River. Chapter 3 provides background on the Sediment component of the SUPPLY tier and addresses how changes in Water and Sediment have caused cumulative changes to PROCESS and FORM. These two chapters are intended to provide the physical foundation for better understanding changes to the biota of interest, and provide insights that may improve the success of the Restoration Study.

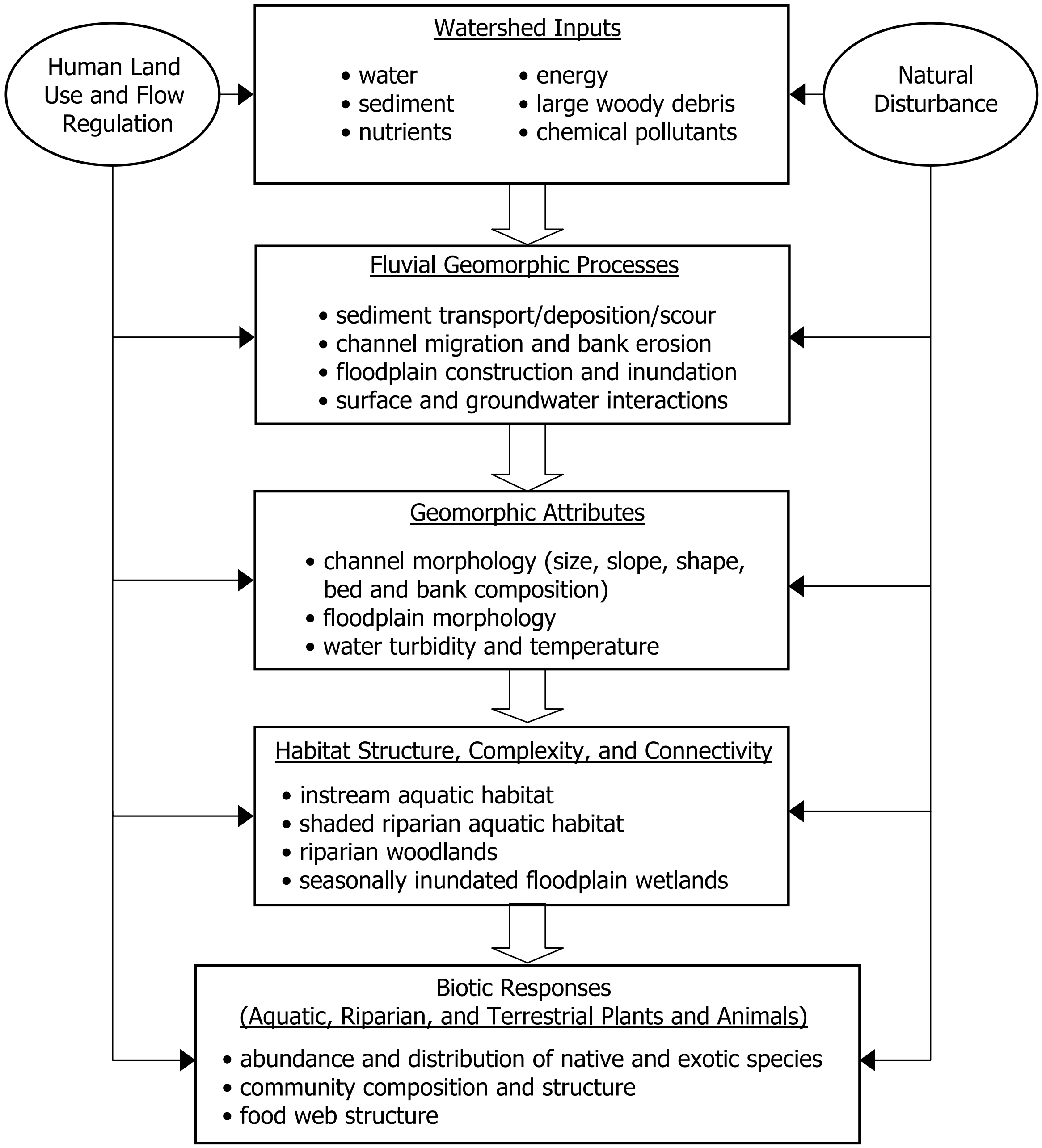

Figure 2-1. Conceptual physical framework of alluvial river ecosystems, showing how natural fluvial geomorphic components and human components cascade to changes in biota.

2.2. OBJECTIVES

The goal of this chapter is to describe the historical flow regime, explain how the flow regime has changed, and provide information that will enable us to hypothesize how these changes to the flow regime have led to changes in biota. The objective IS NOT to provide an argument to returning to the historical flow regime but will establish a framework upon which linkages to the health and productivity of priority biota can be made. It will enable the following questions to be posed (among many others):

- How did spring-run Chinook salmon evolve and adapt their life history to the natural hydrograph?
- How have changes to the natural hydrograph interfered with the spring-run Chinook salmon life history?
- How important are certain hydrograph components to the health, productivity, and survival of spring-run Chinook salmon?
- What geomorphic processes occurred during wetter years and what processes occurred during drier years?

This evaluation of surface flow hydrology will provide insight on certain portions of the flow regime that were more important than others for several species (discussed in subsequent chapters), and may help prioritize portions of the flow regime to improve as part of the Restoration Study. The chapter also gives an overview of historical and present-day flow routing through the system, as well as examples of how infrastructure has changed flood flow magnitude, duration, and inundation areas. Objectives below are summarized from the scope of work:

- Compile and evaluate historical and existing surface water data on the San Joaquin River and tributaries pertinent to the Restoration Study planning process.
- Describe historical and existing longitudinal surface water flow trends from Friant Dam to the Merced River by developing a reach-by-reach water budget of seasonal inflows and outflows along the San Joaquin River using gaging stations, diversion rates, other quantitative data, and qualitative estimates where no quantitative data is available. Describe how longitudinal differences in gaining and losing reaches may have influenced salmonid production.
- Prepare a hydrograph component analysis that describes pre-Friant and post-Friant seasonal flows at mainstem San Joaquin River gaging stations that can be used in other chapters to link life history.
- Assess impact of levees, bypasses, and other infrastructure on flood peak attenuation compared to pre-development conditions.
- Analysis and description of changes in the area and inter-annual variability in areas flooded by the pre-dam events shown on the 1914 CDC maps, and comparable post-dam events of similar flood frequency using the post-dam flood frequency distribution. The purpose of this analysis is to characterize the frequency, duration, and reclining limb of over-bank flows and the areas frequently inundated during both the pre- and post-Friant Dam period, and the pre- and post- flood control period.

2.3. STUDY AREA

The study area for this chapter is defined by the watershed boundary of the San Joaquin River. Under historical conditions, this study area would have included the Tulare Lake basin because during periods of high lake elevations and/or high flows from the Kings River, flows periodically spilled from the Tulare Lake basin through Fresno Slough into the San Joaquin River. Under present conditions, Tulare Lake no longer exists (except during very wet years), but flows still periodically enter the San Joaquin River from the Fresno River via James Bypass and Fresno Slough. Therefore, for discussion purposes, the study area will extend into the Tulare Lake basin. For quantitative purposes, the study area is the San Joaquin River from Friant Dam downstream to the confluence with the Merced River, including selected tributaries to the San Joaquin River (Figure 2-2 and Figure 2-3).

2.4. DATA SOURCES

All of the data discussed in this technical memorandum were obtained from the various agencies that collect data within the project reach. These agencies include the following:

- U.S. Geological Survey (USGS);
- U.S. Bureau of Reclamation (Bureau);
- California Department of Water Resources (DWR);
- San Joaquin River Exchange Contractors;
- Statistical Analysis of Kings River flows to estimate unimpaired San Joaquin River flows (Madeheim, 1999).

Table 2-1 summarizes the gaging stations available in the San Joaquin Valley, although not all were used in the discussion or analysis in Chapter 2. Several individuals conducted the analyses done for this chapter, and the period of record used for the analyses varies to some degree. The date of the most recent data used in an analysis depends on when the analysis was done, and varies from an end date of 1997 at the earliest, with some analyses using data through 2001. The date chosen for defining the pre-Friant Dam to post-Friant Dam transition varies by analysis. Some analyses begin the post-Friant Dam period as 1950 to accommodate completion of the Friant-Kern and Friant-Madera canals, while other analyses begin the post-Friant Dam period as 1944 with the beginning of regulation. The period of record used in each analysis is delineated.

Table 2-1. Summary of flow records available for the project reach of the San Joaquin River from Friant Dam to the confluence with the Merced River.

Gage # (see Fig. 2-2)	Gage Name, Drainage Area	Gage Stn # or CDEC ID	Agency	Data Type	Data Used in Water Budget Analysis[1]	Period of Record[2]
1A	San Joaquin River release from Friant Dam (DA=1,640 sq mi)	MIL	USBR	mean daily	X	1944 - present
1B	San Joaquin River below Friant Dam (DA= 1,676 sq mi)	11251000	USGS	mean daily	X	1908 - present
				annual peaks		
2	Cottonwood Creek near Friant (DA= 35.6 sq mi)[1]	11250500	USGS	mean daily annual peaks		1942 – 1951[3]
		CTK	USBR	mean daily		1951- present
3A	Little Dry Creek near Friant (DA= 57.9 sq mi)	11251500	USGS	mean daily annual peaks		1942 - 1956
		LDC	USBR	mean daily		1951- present
3B	Little Dry Creek near mouth (DA= 77.4 sq mi)[2]	11251600	USGS	mean daily annual peaks		1957 – 1961[4]

Table 2-1. cont.

Gage # (see Fig. 2-2)	Gage Name, Drainage Area	Gage Stn # or CDEC ID	Agency	Data Type	Data Used in Water Budget Analysis[1]	Period of Record[2]
4	San Joaquin River @ Donny Bridge (DA= not published)		USBR	mean daily		1984-1999
5	San Joaquin River @ Skaggs Bridge (DA= not published)		USBR	mean daily		1984-1999
6	San Joaquin River at Gravelly Ford (DA= not published)	GRF	USBR	mean daily	X	1987[5] - present
	San Joaquin River near Biola (DA= 1,811 sq mi)	11253000	USGS	mean daily annual peaks		1953-1961
7	San Joaquin River below Bifurcation (DA= not published)	SJB	USBR	mean daily		1986 - present
8	Chowchilla Bypass at Head (DA= not published)	CBP	DWR	mean daily	X	1980 - 1991
			USBR	mean daily	X	1986 - present
9	James Bypass (Fresno Slough) near San Joaquin (DA= not published)	11253500	USGS	mean daily	X	1948 - present
10	San Joaquin River near Mendota (DA= 3,940 sq mi)	11254000	USGS	mean daily		1940 - 1954
				annual peaks		1940 - 1954
			USBR	mean daily	X	1986 - present
11	Arroyo Canal (DA= not applicable)		Exchange Contractors	mean daily	X	1990 - present
12	San Joaquin River near Dos Palos (DA=4,669 sq mi)	11256000	USGS	mean daily		1941 - 1954
				annual peaks		1941 - 1954
			USBR	mean daily	X	1986, 1987, 1995
13	San Joaquin River near El Nido (DA=6,443 sq mi)	11260000	USGS	mean daily		1940 - 1949
				annual peaks		1940 - 1949
14	Eastside Bypass near El Nido (DA= not applicable)	ELN	DWR	mean daily	X	1980 - present
15	Mariposa Bypass near Crane Ranch (DA= not applicable)		DWR	mean daily	X	1980 - 1994
16	Eastside Bypass below Mariposa Bypass (DA = not applicable)		DWR	mean daily	X	1980 - present
17	Bear Creek below Eastside Canal (DA= not published)		DWR	mean daily	X	1980 - present
18	San Joaquin River near Stevinson (DA= not published)	SJS	DWR	mean daily	X	1980 - present
19	Salt Slough at HW 165 near Stevinson (DA = not applicable)	11261100	USGS	mean daily	X	1986 - 1994, 1996- present
				annual peaks		1986 - present
			DWR	mean daily	X	1980 - present
20	San Joaquin River at Fremont Ford Bridge (DA= 7,619 sq mi)	11261500	USGS	mean daily	X	1937 - 1989
				annual peaks		1937 - 1989
21	Mud Slough near Gustine (DA = not applicable)	11262900	USGS	mean daily	X	1986 - present
				annual peaks		1986 - present

Table 2-1. cont.

Gage # (see Fig. 2-2)	Gage Name, Drainage Area	Gage Stn # or CDEC ID	Agency	Data Type	Data Used in Water Budget Analysis[1]	Period of Record[2]
22	Merced River near Stevinson (DA= 1,273 sq mi)	11272500	USGS	mean daily	X	1941 - 1995
				annual peaks		1924, 1941 - 1995
23	Merced River Slough near Newman (DA = not applicable)	11273000	USGS	mean daily		1942 - 1972
				annual peaks		1951 - 1972
24	San Joaquin River near Newman (DA= 9,520 sq mi)	11274000	USGS	mean daily	X	1912 - present
				annual peaks		1914 - present

[1] Water budget analyses used data through WY 1999.

[2] Water years - may contain missing periods

[3] USBR/DWR re-started station (CDEC code CTK), period of record: 2/98-present; electronic data from USBR 1986- present

[4] USBR/DWR re-started station (CDEC code LDC), period of record: 2/98-present; electronic data from USBR 1986- present

[5] Earlier records may be available from USBR

2.5. BACKGROUND

The San Joaquin River and tributaries drain approximately 13,500 mi^2 (measured at the USGS gaging station at Vernalis) along the western flank of the Sierra Nevada and eastern flank of the Coast Range, and flow northward into the Sacramento-San Joaquin delta, (where it is joined by the Calaveras and Mokelumne River before combining with the Sacramento River). Typical of Mediterranean climate catchments, flows vary widely seasonally and from year to year. Three major tributaries join the San Joaquin from the east: the Merced, Tuolumne, and Stanislaus rivers. Smaller tributaries include the Fresno River, Chowchilla River, Bear Creek, and Fresno Slough (from the Kings River). Precipitation is predominantly snow above about 5,500 to 6,000 feet in the Sierra Nevada, with rain in the middle and lower elevations of the Sierra foothills and in the Coast Range. As a result, the natural hydrology reflected a mixed runoff regime, dominated by winter-spring rainfall runoff and spring-summer snowmelt runoff. Most flow is derived from snowmelt from the Sierra Nevada, with relatively little runoff contributed from the western side of the drainage basin in the rain shadow of the Coast Range. Watershed elevation ranges from sea level near Vernalis to over 14,000 ft at the crest of the Sierra Nevada. Precipitation averages from 5 to 15 inches/year in the floor of the San Joaquin Valley, up to 80 inches/year at higher elevations of the Sierra Nevada (USGS 1998). The unimpaired average annual water yield (WY 1906-2002) of the San Joaquin River as measured immediately above Millerton Reservoir is 1,801,000 acre-ft (USBR 2002); the post-Friant Dam average annual water yield (WY 1950-2000) to the lower San Joaquin River is 695,500 acre-ft (USGS, 2000). As average precipitation decreases from north to south, the San Joaquin River basin (including the Stanislaus, Tuolumne, and Merced rivers) contributes only about 22% of the total runoff to the Delta (DWR 1998).

The following sections describe components of the natural flow regime, tributaries, and water management infrastructure within the study reach. Additional information on water management infrastructure can be found in Chapter 5.

2.5.1. The Natural Flow Regime

The flow regime of a river or stream describes the temporal variability of runoff at two scales: that within a single hydrologic year (*intra-annual,* e.g., an annual hydrograph depicting winter floods,

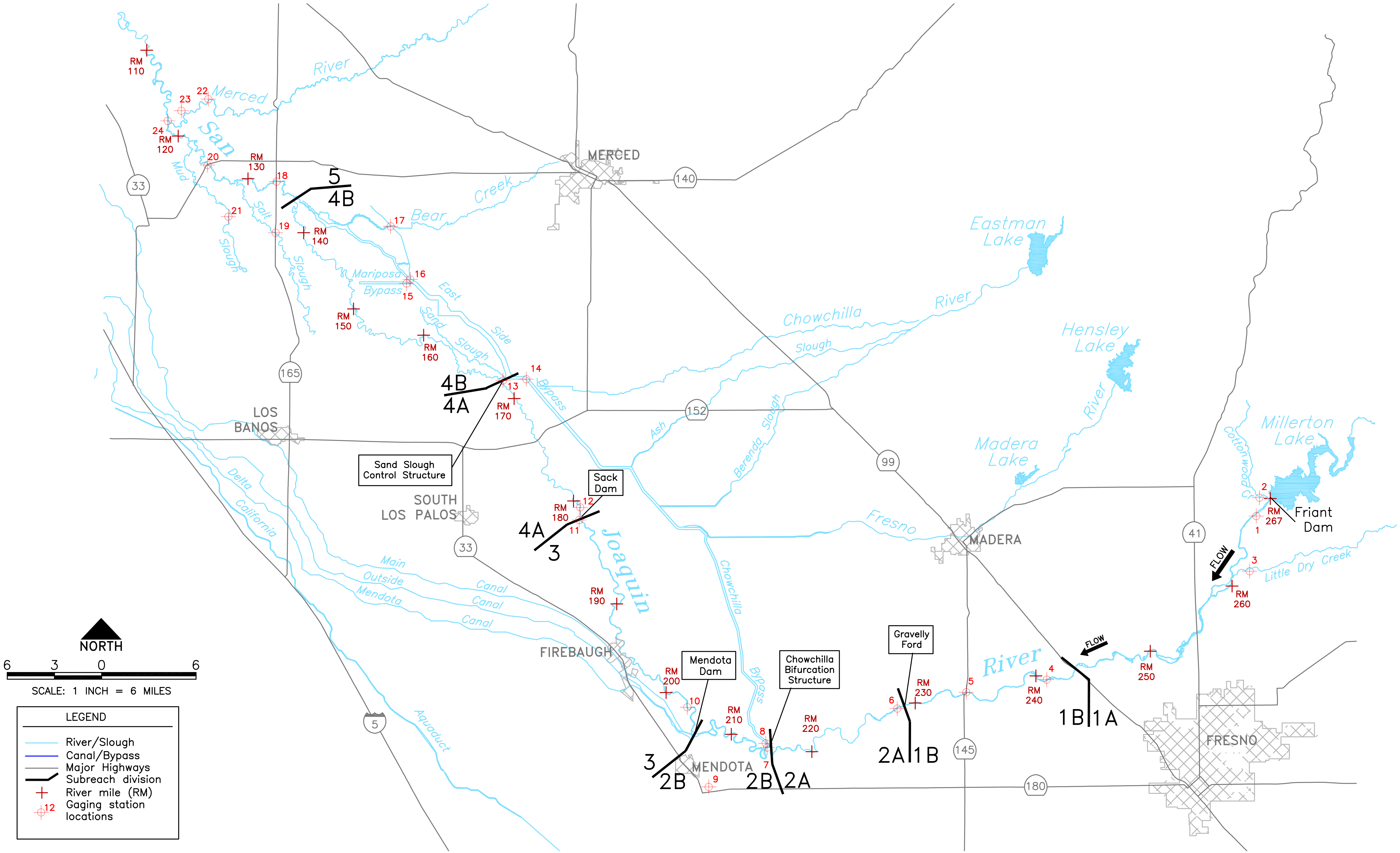

Figure 2-2. Project area of the San Joaquin River Restoration Plan showing Reach and Subreach Boundaries, and gaging stations.

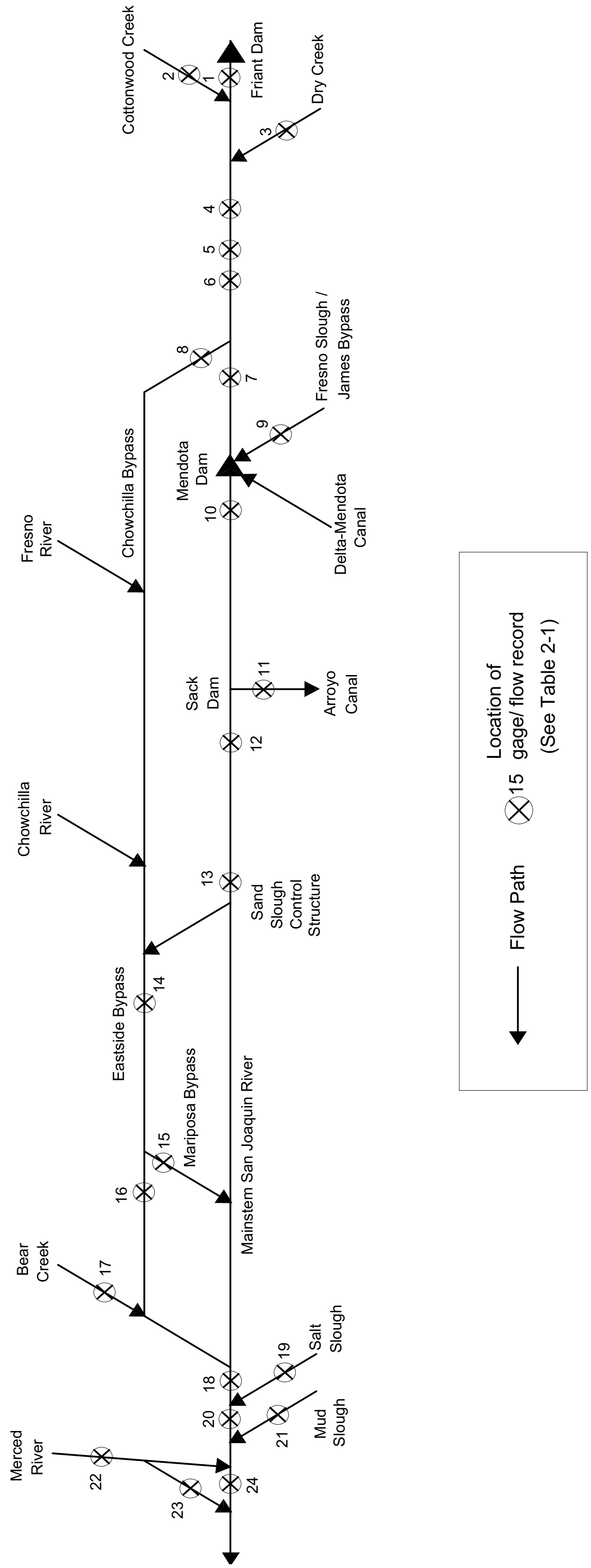

Figure 2-3: Schematic of San Joaquin River showing location of gaging stations presented in Table 2-1 and Table 2-3.

spring snowmelt runoff, recession, and baseflow) and that from year-to-year (*inter-annual,* e.g., dry years, wet years, and multi-year cycles of alternating drought and high water yield). Both temporal scales are important to fluvial processes, channel morphology, and ecosystem functions. The natural (unimpaired) flow regime of any given stream is unique to that stream, and is a primary determinant of the size, shape, and character of the stream. It is a function of a variety of factors, including the magnitude, duration, frequency, and timing of precipitation; the form of precipitation (rain versus snow); and the properties of the watershed that control how precipitation translates into streamflow (geology, soils, vegetative cover, elevation, aspect, gradient, development, etc.).

The concepts of *magnitude, duration, frequency,* and *timing* are useful for describing hydrological phenomena, for comparing flow regimes of different streams, and for comparing unimpaired with impaired flow regimes for a single stream before and after flow regulation.

- *Magnitude* refers to the rate of discharge of either high flows or low flows of geomorphic or biological significance, such as peak discharges and dry season low flows.
- *Duration* refers to the length of time a river carries a specific flow rate, or the percent of time over a specific period that a specific discharge is equaled or exceeded (information that can be derived from a flow-duration curve).
- *Frequency* describes the rate of occurrence of a particular flow, for example, the 100-year flood occurs, on average, once every 100 years (information that can be derived from a flood frequency curve).
- *Timing* of low and high flows is also important for supporting riparian and aquatic ecosystem processes. Species are adapted to natural cycles of high and low flows that provide hydrologic conditions necessary for key life history stages.

The natural or "unimpaired" flow regime historically provided large variation in the magnitude, timing, duration, and frequency of streamflows, both inter-annually and seasonally. Variability in streamflows was essential in sustaining ecosystem *integrity* (long-term maintenance of biodiversity and productivity) and *resiliency* (capacity to endure natural and human disturbances) (Stanford, et al. 1996). Restoring the natural flow variability of a river is now recognized as a fundamentally sound approach to initiating river ecosystem restoration (Poff, et al. 1997). Historic river restoration efforts have not tended to restore flow variability due to a variety of reasons, primarily due to poor understanding of the ecological links to a variable flow regime. One of the goals of this chapter is to provide the hydrology foundation to be able to establish these ecological links in the Restoration Study.

2.5.2. Definition of Hydrologic Records

Various terms are used to describe periods of the hydrologic record that can lead to confusion for the readers. Water storage development in the San Joaquin River watershed began in the 1850's with the gold rush, and has increased in scale to the present day (Table 2-2). The following terms are defined to provide consistency in hydrology descriptor, and to explain what information is being used.

2.5.2.1. Unimpaired runoff

Unimpaired runoff represents the flow that would occur absent any diversions or reservoir regulation, and is directly derived from the measured flows. Although it is sometimes referred to as the full natural runoff or full natural flow, the unimpaired runoff does not reflect fully natural conditions since it does not account for changes in natural watershed runoff characteristics that have occurred in the past 200 years due to land use alterations and vegetation conversion. It is assumed, however, that the

Table 2-2. Cumulative water storage facilities in the upper San Joaquin River watershed.

Year Completed	Dam Name	Stream	Storage capacity (acre-ft)[1]	Storage as % of annual unimpaired runoff	Cumulative storage (acre-ft)	Cumulative storage as % of annual unimpaired runoff[2]
1896	No. 1 Forebay	Tributary of North Fork San Joaquin River	69	0.004%	69	0.004%
1906	No. 3 Forebay	Tributary of North Fork Willow Creek	20	0.001%	89	0.005%
1910	Crane Valley (Bass Lake)	North Fork Willow Creek	45,410	2.5%	45,499	2.5%
1912	No. 2 reservoir	North Fork Willow Creek	103	0.0%	45,602	2.5%
1913	Dam 4	Big Creek	60	0.0%	45,662	2.5%
1918	Huntington Lake	Big Creek	88,834	4.9%	134,496	7.5%
1920	Kerckhoff Diversion	Mainstem San Joaquin River	4,200	0.2%	138,696	7.7%
1921	Dam 5	Big Creek	49	0.0%	138,745	7.7%
1923	Big Creek #6	Mainstem San Joaquin River	993	0.1%	139,738	7.8%
1926	Florence Lake	South Fork San Joaquin River	64,406	3.6%	204,144	11.3%
1927	Shaver Lake	Stevenson Creek	135,283	7.5%	339,427	18.8%
1927	Bear Creek Diversion	Bear Creek	103	0.0%	339,530	18.9%
1942	Friant/Millerton	Mainstem San Joaquin River	520,500	28.9%	860,030	47.8%
1951	Big Creek #7 Redinger	Mainstem San Joaquin River	26,000	1.4%	886,030	49.2%
1954	Vermillion Valley Thomas Edison	Mono Creek	125,000	6.9%	1,011,030	56.1%
1955	Portal Powerhouse Forebay	Tributary of South Fork San Joaquin River	325	0.0%	1,011,355	56.2%
1960	Mammoth Pool	Mainstem San Joaquin River	123,000	6.8%	1,134,355	63.0%
1986	Balsam Meadow Forebay	West Fork Balsam Creek	2,872	0.2%	1,137,227	63.1%

[1] Division of Safety of Dams, Bulletin 17-00, July 2000; USBR Millerton Lake Operations Report (for Big Creek #7)
[2] Unimpaired runoff = 1,801,000 acre-ft, from USBR computed full natural flows 1906-2002.

cumulative effect of those alterations on the seasonal runoff is relatively minor and the unimpaired runoff is a satisfactory representation of natural runoff. This report estimates unimpaired runoff using data developed by Madeheim (1999) from extrapolating the Kings River data to the San Joaquin River. This report also uses full natural runoff or full natural flow estimates provided by USBR. These estimates are computed from upstream gaging stations and inflow into Millerton Reservoir, and consider reservoir evaporation and upstream storage.

2.5.2.2. Pre-Friant Dam flows

Construction of Friant Dam began in 1939, and flows were moderately regulated by Friant Dam between 1942 and 1951 when the Friant-Kern and Friant-Madera canals were completed. Pre-Friant Dam flows are measured at the San Joaquin River at Friant gaging station (STN #11-251000), and the 1908-1942 period of record was used. As shown in Table 2-2, there was increasing flow regulation in the upper watershed prior to completion of Friant Dam that would affect flows measured at the Friant gaging station; therefore, these flows are not considered unimpaired. While the flows were impaired by upstream dams prior to the completion of Friant Dam, the degree of impairment was small compared to the flow regime after completion of Friant Dam.

2.5.2.3. Post-Friant Dam flows

Friant Dam was completed in 1942; however, because the Friant-Kern canal and Friant-Madera canal was not fully completed until 1951, the degree of flow regulation downstream of Friant Dam differed as the canals were constructed. Therefore, to use a consistent time period where operations, diversions, and downstream releases were consistent, the 1950-present period of record is used to represent post-Friant Dam flows for most analyses. The flood frequency analysis uses 1944-present for Post-Friant Dam flows because the reservoir was used for flood control purposes immediately after the dam was completed. Flows are measured at the San Joaquin River at Friant gaging station (STN #11-251000).

2.5.3. Hydrologic Features

The hydrologic network of the approximately 150 miles of the San Joaquin River between Friant Dam and the Merced River is formed and influenced by confluences, diversions, and flood control features. This infrastructure is discussed in more detail in Chapter 5; a shorter summary is provided below.

Instream flows in the San Joaquin River are controlled by releases from Friant Dam. Two small intermittent tributaries join the river immediately downstream from Friant Dam: Cottonwood Creek and Little Dry Creek. Numerous gravel pits are present in the river and floodplain along the approximately 35-mile gravel-bedded reach of the mainstem downstream from Friant Dam. Because of the effects of channel percolation losses and diversions, flow varies significantly along the reach between Friant Dam (RM 270) and Gravelly Ford (RM 230). A bifurcation structure at RM 216 controls a flow split between the mainstem San Joaquin River and the Chowchilla Bypass. Mendota Dam at RM 204.5 provides the headworks for distributing water that is brought into the system through the Delta-Mendota Canal. A portion of the imported water is distributed into several canals that connect to Mendota Pool upstream from the dam, and a portion is passed into the river for downstream delivery to the Arroyo Canal. Flows are diverted from the San Joaquin River into the Arroyo Canal at Sack Dam (RM 182.1). The Sand Slough Control Structure at RM 168.5 controls the flow split between the mainstem San Joaquin River and the Eastside Bypass. The Mariposa Bypass delivers flow back into the river from the Eastside Bypass near RM 148. The remaining flows in the Eastside Bypass downstream from the Mariposa Bypass and inflows from Bear Creek enter the river near RM 136. A schematic of the flood control system is shown on Figure 5-5. Salt Slough and Mud Slough enter the San Joaquin River from the west near RM 129.5 and RM 121.3, respectively. The Merced River enters the San Joaquin River near RM 119. A line diagram of the main features of the hydrologic network of the San Joaquin River between Friant Dam and the Merced River is presented in Figure 2-3 and a summary of the available gage records is presented in Table 2-1. The following sections describe each of the major components of the network.

2.5.3.1. Friant Dam Releases

Instream flows are released to the San Joaquin River from Friant Dam. Both the Bureau of Reclamation and USGS maintain a record of flows downstream from Friant Dam. The Bureau of Reclamation records represent calculated flow releases from the dam outlet works (including flows to the Friant Hatchery), while the USGS flows are obtained from a continuously monitored gaging station that is located downstream from the dam and hatchery release. A summary of inflows, typical diversions, and typical instream releases is shown on Figure 5-2.

2.5.3.2. Tributaries: Cottonwood Creek and Little Dry Creek

Two intermittent tributaries join the San Joaquin River downstream from Friant Dam. Cottonwood Creek enters from the north immediately downstream from Friant Dam, and has a drainage area of 35.6 mi^2 at the former USGS gaging station. Little Dry Creek enters from the south approximately 6 miles downstream from the dam, and has a drainage area of 57.9 mi^2 at the former USGS gaging station. These tributaries are very small and contribute very little to the overall runoff volume in the San Joaquin River. However, during periods of low flow releases from Friant Dam in the winter months, these tributaries can contribute significantly to the flow during storm events. The ACOE recommended San Joaquin River flow limit of 8,000 cfs includes these tributaries, so high flows from these tributaries reduce the flood release from Friant Dam. Flows in Little Dry Creek are augmented by flows from Big Dry Creek through a secondary spillway from the Big Dry Creek flood control reservoir. Cottonwood Creek and Little Dry Creek have been gaged by USGS and USBR, and are described further in Section 2.6.2.4 and 2.6.2.5.

2.5.3.3. Gravel Pits

Numerous gravel pits are present in the river and floodplain along the approximately 35-mile gravel bedded reach of the San Joaquin River downstream from Friant Dam. Based on the 1997 aerial photography, the total surface area of the pits is approximately 1,360 acres, of which the San Joaquin River is directly connected to approximately 190 acres of gravel mining pits. The remainder of the pits are located in the floodplain adjacent to the river. These pits are hydrologically connected to the river (separated by permeable gravel berms), and create significant ponding and associated evaporation losses. Gravel pits directly connected to the main channel can significantly attenuate flow release changes from Friant Dam.

2.5.3.4. Diversions and Losses

There are two primary sources of water loss in the study reach (Friant Dam to the Merced River confluence): riparian water diversions, and infiltration losses. Riparian diversions vary considerably, from small individual pumps or diversion canals, to large volume water delivery canals (e.g., Arroyo Canal). These riparian diversions are discussed further in Section 2.7.2.3 and Chapter 5, and a list of diversions mapped by CDFG in 2001 is shown in Table 5-2. Larger diversions are shown on Figure 2-2. Under historical conditions, the San Joaquin River gained flows from the shallow groundwater table in most reaches (see Chapter 4). Groundwater pumping over the last 150 years has reduced the shallow groundwater table in most reaches, such that instream flows infiltrate into the shallow groundwater table and instream flows decrease with distance downstream. Because of the effects of infiltration losses and riparian diversions, flow in the San Joaquin River varies significantly along the reach between Friant Dam and Gravelly Ford, particularly when the flow release from Friant Dam is less than about 500 cfs. Significant flow losses also occur between Gravelly Ford and the Chowchilla Bifurcation Structure, primarily because of percolation losses (Figure 2-4). The measured flow loss for the Friant Dam to Gravelly Ford reach indicates that flow does not reach Gravelly Ford when the discharge at the "below-Friant-Dam" gage is less than about 100 cfs, and that about 150 cfs or more is lost when Friant Dam releases are greater than about 200 cfs. Similarly, no flow reaches the Chowchilla Bifurcation Structure when the discharge at Gravelly Ford is less than about 75 cfs, and the amount of flow loss between Gravelly Ford and Chowchilla Bifurcation Structure increases to about 200 cfs at higher flows (Figure 2-2). These flow losses assume steady-state condition (i.e., losses computed during prolonged periods of steady flows); flow losses can be greater during the initial days of a new flow release or an increasing flow release as the shallow groundwater is recharged by infiltration from the San Joaquin River flows. Seasonal loss estimates are described in Section 2.7.2.6. During normal conditions, the San Joaquin River is dry from just downstream of Gravelly Ford to Mendota Pool, and from Sack Dam to the Mariposa Bypass.

2.5.3.5. Operation of the Chowchilla Bifurcation Structure

A Bifurcation Structure is located at RM 216 that controls a flow split between the mainstem San Joaquin River and the Chowchilla Bypass. Operation of the structure is based on 1 of 2 conditions: (1) Initial flow to the San Joaquin River and (2) initial flow to the Chowchilla Bypass (The Reclamation Board 1969). Review of daily average flows of actual operations during the 1986 and 1995 high flow event suggests that a modified version of condition 1 is usually followed (see Figure 5-13). The actual operations of the bifurcation structures during a flood event depend greatly on three primary factors:

- Flood flows from the Kings River system through Fresno Slough.
- Water Demands from Mendota Pool (thus determining whether check boards are in place at Mendota Dam).
- Seasonality (will seepage/flooding problems affect agricultural practices on adjacent lands).

In all cases, water from the Kings River system (via Fresno Slough) has priority to available capacity on the San Joaquin River below Mendota Pool. When flood flows are below channel capacities, the Lower San Joaquin Levee District is provided the latitude to best utilize the design capacities of the Lower San Joaquin River Flood Control Project.

The first 1,500 cfs at the Chowchilla Bifurcation Structure should be routed to Mendota Pool, as long as flood flows from the Fresno Slough to the Mendota Pool are below 3,000 cfs. Since the rated channel capacity of the San Joaquin River is 4,500 cfs downstream of Mendota Dam, incremental flow from the Kings River above 3,000 cfs should be equally reduced at the Chowchilla Bifurcation Structure and routed to the Chowchilla Bypass. If flows from Fresno Slough are substantially below 3,000 cfs, the check boards at Mendota Pool can remain in place and the pool elevation targeted for 14.2 feet. The bifurcation structures are typically operated to route as steady a flow as possible to Mendota Pool (minimize flow variation).

Based on the assumption of 1,500 cfs being routed to the San Joaquin River at the Chowchilla Bifurcation Structure, the next increment of flood flows on the San Joaquin River from 1,500 cfs to 7,000 cfs (i.e., the next 5,500 cfs) should be routed to the Chowchilla Bypass. The next 1,000 cfs,

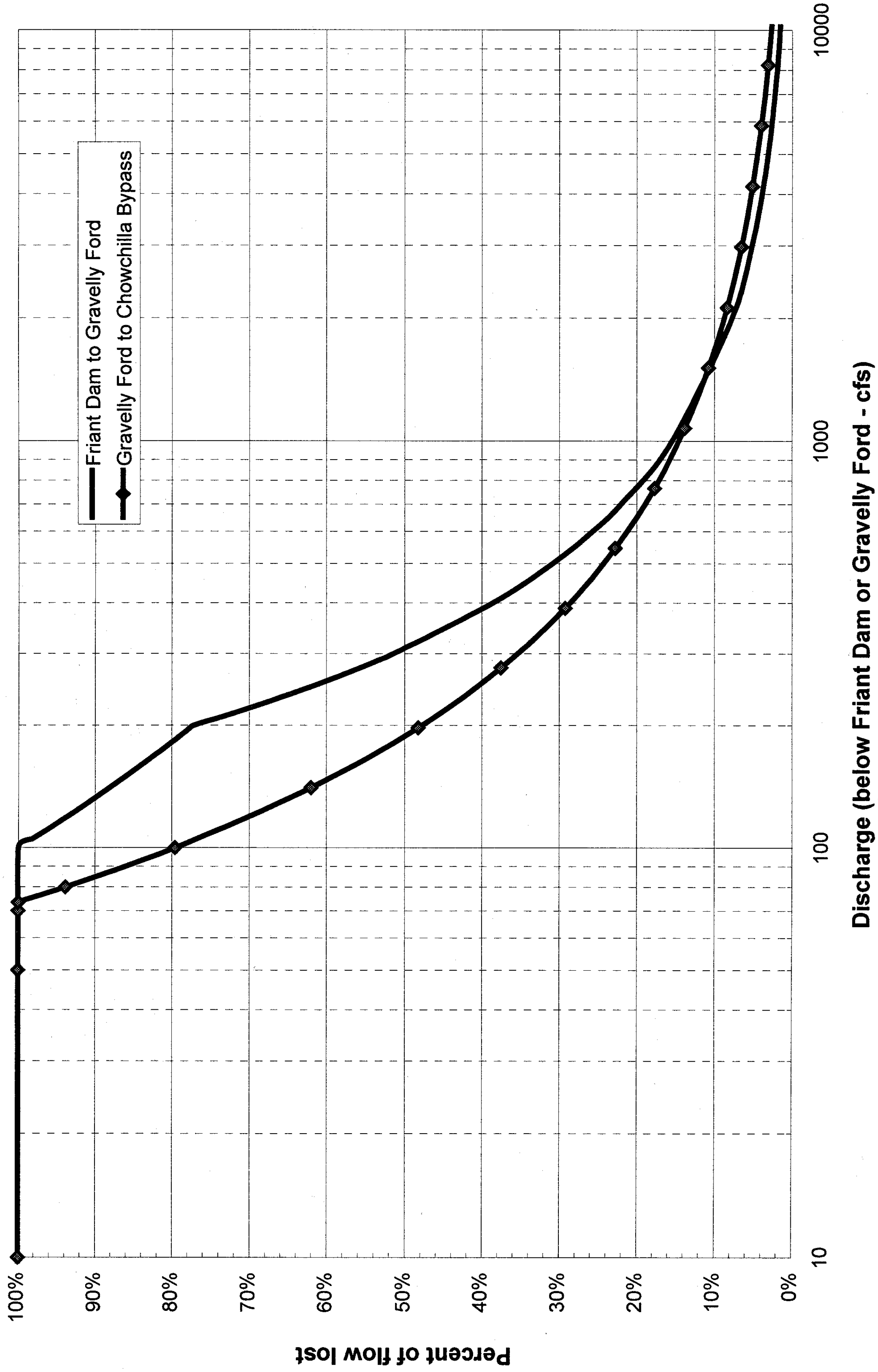

Figure 2-4. Estimated flow loss curves for the San Joaquin River between Friant Dam and Gravelly Ford, and between Gravelly Ford and the Chowchilla Bifurcation Structure.

or flood flows at the Chowchilla Bifurcation Structure of 7,000 cfs to 8,000 cfs, should be routed to the Mendota Pool. At this point, all check boards at Mendota Dam have typically been removed. A total of 2,500 cfs would be routed to Mendota Pool as long as flows from Fresno Slough are 2,000 cfs or lower. If the Fresno Slough contribution is greater than 2,000 cfs, then the channel below Mendota Pool could be subjected to flows greater than the maximum capacity of 4,500 cfs unless flows from the Chowchilla Bifurcation Structure are reduced. Should the flows exceed 8,000 cfs at the Chowchilla Bifurcation Structure or 10,000 cfs total between the San Joaquin River and Fresno Slough, the Lower San Joaquin Levee District is to operate the bifurcation structures at their own discretion with the objective of minimizing damage to the flood control project and protected area.

2.5.3.6. Mendota Dam

Mendota Dam is located at RM 204.5 and provides the headworks for distributing water that is brought into the system through the Delta-Mendota Canal. A portion of the imported water is distributed into several canals that connect to Mendota Pool upstream from the dam, and a portion is passed into the river for downstream delivery to the Arroyo Canal. Figure 5-4 illustrates typical seasonal operation of the Mendota Pool. In addition, during flood periods, flows enter Mendota Pool from the Kings River North via the James Bypass and Fresno Slough. Flows in the Kings River North are controlled by the operation of Pine Flat Dam, where a weir directs flows to the north up to the channel capacity, and then directs any additional flows into the south channel. Although early studies indicated that the capacity of the Kings River North was about 4,500 cfs, flows up to 6,000 cfs have passed through the reach (ACOE 1993).

2.5.3.7. Sack Dam and Arroyo Canal

Flows are diverted from the San Joaquin River into the Arroyo Canal at Sack Dam (RM 182.1), which is a low head earth and concrete structure with wooden flap gates. Flow is provided to Arroyo Canal by releases of Delta Mendota Canal water from Mendota Dam. The Exchange Contractors recorded daily diversions into the Arroyo Canal for the period 1990 to 1999. Typically, all flows less than 600 cfs is diverted from the San Joaquin River at this point, such that the downstream reaches are either dry or supplied by agricultural return flows.

2.5.3.8. Sand Slough Control Structure

The Sand Slough Control Structure, located at RM 168.5, controls the flow split between the San Joaquin River and the Eastside Bypass. There are no known operating rules for the structure during low flows, but the rules limit downstream flows in the San Joaquin River downstream of the structure to the flood control design discharge of 1,500 cfs. Because the present capacity of the San Joaquin River channel is severely limited, current operations limit downstream flows to 300 to 400 cfs. However, it appears that actual operations no longer open the gates to allow flows into the San Joaquin River, including during the 1997 flood. The San Joaquin River downstream of the Sand Slough Control Structure is dry until agricultural return water begins to allow positive flow to occur again.

2.5.3.9. Eastside Bypass

The Eastside Bypass begins at the confluence of the Chowchilla Bypass and the Fresno River, and extends downstream approximately 36 miles to the confluence with the San Joaquin River at the downstream end of Reach 4B. The Mariposa Bypass splits from the Eastside Bypass approximately 26 miles downstream from the confluence of the Fresno River and Chowchilla Bypass.

2.5.3.10. Mariposa Bypass

The Mariposa Bypass delivers flow back into the San Joaquin River from the Eastside Bypass near RM 148. The official operating rules for the Mariposa Bifurcation Structure require all flow to be diverted back into the San Joaquin River at discharges in the Eastside Bypass up to 8,500 cfs, with any higher flows to remain in the Eastside Bypass (San Luis Canal Company 1969). Review of flow data in the Mariposa Bypass indicates that actual operations released less flow into the river through the Mariposa Bypass than would be required by the operating rules (see Figure 5-14).

2.5.3.11. Bear Creek

The remaining flows in the Eastside Bypass and tributary inflows from Bear Creek re-enter the San Joaquin River near RM 136. The Department of Water Resources (DWR) has operated stream gages on Bear Creek just upstream from its confluence with the Eastside Bypass, and on the Eastside Bypass just downstream from the Mariposa Bypass since 1980.

2.5.3.12. Tributaries: Salt Slough and Mud Slough

Salt Slough and Mud Slough enter the San Joaquin River from the west side of the San Joaquin Valley near RM 129.5 and RM 121.3, respectively. Gage records are available from the USGS on both Salt Slough (at the Highway 165 Bridge) and Mud Slough since 1986. The DWR has also operated a gage on Salt Slough since 1980.

2.5.3.13. Merced River

The Merced River enters the San Joaquin River near RM 119. The USGS gage records are available for the Merced River from 1941 through 1995, and for Merced Slough, which is a bypass channel that carries a portion of the Merced River flows to the San Joaquin River at high flow, from 1942 through 1972.

2.5.3.14. Eastside Tributaries

The Eastside Bypass presently intercepts several significant tributaries that historically connected to the San Joaquin River. These tributaries include the Fresno River, Ash Slough, Berinda Slough, the Chowchilla River, Owens Creek, and Bear Creek. These tributaries historically entered the flood basin in Reach 3-5 rather than the mainstem San Joaquin River itself, and contributed to the prolonged inundation of the flood basins, particularly during winter storm events and spring snowmelt floods.

The Fresno River, with an average annual unimpaired discharge of 76,800 acre-ft (USGS, 1975), is now controlled by Hidden Dam located approximately 38 miles upstream from the San Joaquin River. Based on review of USGS gaging records, flow is released during the summer months for agricultural used downstream. There are no gaging stations near the confluence of the San Joaquin River, but field review suggests that little to no flow reaches the San Joaquin River under normal conditions. The Fresno River connects to the Chowchilla Bypass approximately 15 miles downstream from the Chowchilla Bifurcation Structure, and flows can be directed back into the old Fresno River channel downstream of the bypass through a headgate known as the Road 9 Structure. However, only the amount of flow necessary to satisfy riparian water rights on properties between the Chowchilla Bypass and the San Joaquin River are directed into the river; so little or no Fresno River flows reach the mainstem under the present operating system.

The Chowchilla River, with an unimpaired average annual flow of approximately 71,000 acre-ft (USGS 1975), is controlled by Buchanan Dam, located about 32 miles upstream from the San Joaquin

River. Flood control releases from the Chowchilla River enter the Eastside Bypass. As with the Fresno River, flow is released during the summer months for agricultural used downstream. Again, there are no gaging stations near the confluence of the San Joaquin River (Eastside Bypass), but field review suggests that little to no flow reaches the San Joaquin River under normal conditions. Flood control releases from the Chowchilla River enter the Eastside Bypass system and are routed to the San Joaquin River through either the Mariposa Bypass or Eastside Bypass (Figure 2-2).

In addition to these tributaries, Lone Willow Slough served as a distributary channel of the San Joaquin River between the present location of the Chowchilla Bifurcation Structure and approximately the confluence of the Fresno River. The historical slough intercepted several minor tributaries that drain from the east. Lone Willow Slough was also used as a diversion for the Columbia Canal Company, and the headgates are still in place at the head of the slough. At present, the channel of Lone Willow Slough remains somewhat intact but does not completely connect any longer, and the headgates are no longer opened because irrigation water is supplied to the Columbia Canal Company through a diversion from Mendota Pool. The Chowchilla Bypass and Eastside Bypass presently intercept the tributaries (Fresno River, Chowchilla River).

2.6. HISTORIC AND EXISTING HYDROLOGY

A variety of gaging stations are used to illustrate historic and existing surface water hydrology. For example, changes in surface water hydrology due to cumulative flow regulation dams is best illustrated using the USGS gaging station at Friant immediately downstream of Friant Dam (Figure 2-2). The USGS gaging station near Newman is also used to illustrate changes from upstream dams, including those on those on the Merced River, since the gage is downstream of the Merced River confluence. Key tributaries immediately below Friant Dam are also used to illustrate potential importance of these tributaries to restoration efforts (e.g., possibly supporting steelhead or providing geomorphic flows). The gaging stations listed in Table 2-1 are only a partial list of gages within the study area; however, those stations are the most important to the Restoration Study.

There are many tools to analyze surface water hydrology (e.g., flood frequency analysis, flow duration analysis). Rather than doing a blanket analysis using all the available and/or standard analysis tools, a few specific analyses are carefully applied that are most useful for illustrating linkages to the biological and geomorphological components that are integral to the San Joaquin River Restoration Study. This section presents the following analyses: (1) water year analysis at the Friant gaging station, (2) flood frequency computations of important gaging stations within the study area, (3) hydrograph component analysis at the Friant and Newman gaging stations to illustrate hydrograph trends at the upstream and downstream ends of the study reach, and (4) present example hydrographs of several key upstream tributaries.

2.6.1. Water Year Analysis

Streamflow is often described in terms of the average annual water yield (e.g., acre-feet per year) over a number of years, or an average flow duration curve over a number of years. While this may describe a long-term average water yield from a stream, this averaging masks inter-annual variability that strongly influences river ecosystem processes. By classifying the distribution of water years, the inter-annual flow variability can be better illustrated. Water managers use water year classifications for water delivery forecasting and management. A water year classification is also useful to describe correlations between river ecosystem processes and wetter and drier years.

There are many water year classifications in use on the different Central Valley watersheds. Other classifications (e.g. DWR/SWRCB) are for water supply purposes and also include precipitation and previous year's runoff. To guide some of the analyses in this section, we use a simple classification to describe inter-annual flow variability. This classification system is not meant to replace other systems, but simply to illustrate some important aspects of the inter-annual variability in runoff. The measuring point used is the computed unimpaired water year yield at Friant, which has been computed for the period 1896 to 1999 by Madeheim (1999). The annual water yield volumes are plotted cumulatively from wettest to driest against exceedence probabilities, with water year classes divided symmetrically into five equally weighted classes separated by annual exceedence probabilities (p) of 0.20, 0.40, 0.60, and 0.80. Thus, the five classes can be named "Extremely Wet" (p = 0 to 0.20), "Wet" (p = 0.20 to 0.40), "Normal" (p = 0.40 to 0.60), "Dry" (p = 0.60 to 0.80), and "Critically Dry" (p = 0.80 to 1.00). The boundaries of the classes do not necessarily have to be in 0.20 increments; it is important that they are symmetrical around the median value (p=0.50) to ensure that wetter and drier years are weighted equally. This classification system helps depict the range of variability in the annual water yield and provides an equal probability for each class that a given water year will fall into that category (equally distributed around the mean), which in turn allows simpler interpretation of comparisons between water year types. The result of this analysis at Friant is illustrated in Figure 2-5.

While this analysis is useful for comparing years, other specific ecological objectives (e.g., flows for fish migration) require focusing on a specific portion of the year. Differences among and within water year classes have meaningful geomorphic and biological consequences, and will be discussed later in this section with examples.

2.6.2. Flood Frequency

A flood frequency analysis predicts frequency that a given flood magnitude would occur, and a certain flood magnitude (e.g., 50,000 cfs) is labeled an "X-year flood" (e.g., 100-year flood, which has a 1% chance of occurrence any given year). These relationships were developed for selected San Joaquin River gaging stations based on their location and on their available peak flow record. Flood frequency analyses provide a useful tool to hydrologists and geomorphologists because they describe the flows responsible for geomorphic work. A probability distribution is fitted to the record of instantaneous annual maximum floods at a given station, and the estimated parameters of the distribution are then used to predict the average recurrence interval of floods of a given magnitude (Dunne and Leopold 1978). In this section, flood frequency computations performed by the ACOE (1999) for available gages in the study area are presented, as well as additional computations performed by the authors for certain stations important to describing the San Joaquin River hydrology that were either not computed by the ACOE, or the ACOE used only rainfall data in their computations. For these latter stations chosen for additional analyses, they were selected because they contribute high flows to the San Joaquin River that may influence restoration efforts. Cottonwood Creek and Little Dry Creek were chosen because they are in Reach 1, which will be important for salmonid spawning and rearing. James Bypass was included because it measures the amount of flow actually delivered to the San Joaquin River from the Fresno River. The San Joaquin River near Newman gage was included because it provides a pre-and post-Friant Dam comparison at the downstream end of the Study Reach. With the exception of the James Bypass gaging station, the raw data for the annual maximum series is plotted. Annual maximum data is not available for the James Bypass gaging station, so annual maximum daily average values were used. A log-Pearson Type III distribution is then fitted to the raw data. Flood frequency curves and flood magnitudes with recurrence intervals of 1.5, 5, 10, 25, and 50 years are summarized for both the unimpaired and regulated periods of record. The log-Pearson curve fitting was performed using standard procedures (USGS 1982); however, the curve fitting to measured data for several of the gaging stations is poor, and predicted flood magnitudes for floods greater than the 10-year flood should be viewed with caution.

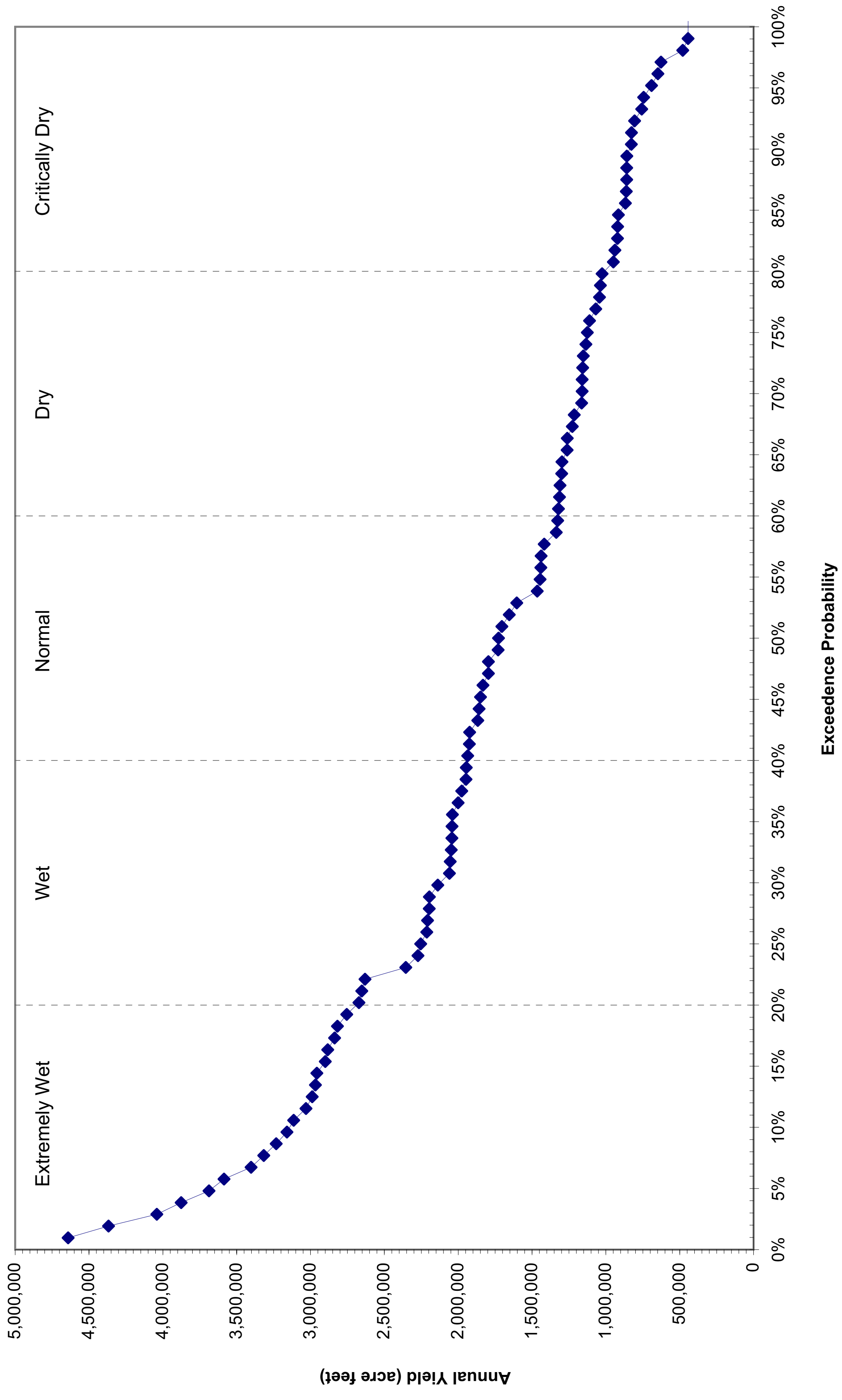

Figure 2-5. Water year classification at Friant Dam using computed unimpaired flow data from Madeheim (1999). This water year classification is used only for describing the hydrograph component analysis. ``

The ACOE performed flood frequency analyses at the San Joaquin River near Friant gaging station and San Joaquin River at Gravelly Ford gaging station (ACOE 1999). The ACOE analysis was performed as part of a post-flood assessment in response to the widespread regional flooding of 1997, and the emphasis of their analysis is placed on generating representative probabilistic flooding relationships as they pertain to the contemporary regulated flow regime. The ACOE flood frequency was developed using a combination of actual and hypothetical data to create a "regulated flood flow frequency curve." The actual and hypothetical data are based on rainfall generated flood events rather than all potential floods (e.g., snowmelt floods); thus results are different from those generated by a standard flood frequency analysis of post-Friant Dam data (as done in Section 2.6.2.1). The actual data include only post-dam (regulated) annual peak streamflow series from 1949 to 1997, and the hypothetical data include modeled large flood events. The modeled hypothetical data were added to the actual peak flow data set to offset the "minimal amount of historical data," thereby allowing for larger-scale, less-frequent flood events to be included in the analysis.

The results of the flood frequency analyses are summarized in Table 2-3, and are discussed in more detail below. The gaging stations used for the flood frequency analyses are shown on Figure 2-2 and Figure 2-3.

Table 2-3. Summary of frequency analysis results for selected streamflow gaging stations within the project reach.

Gaging station name and USGS or CDEC I.D. (from Table 2.1)	***Period of Record***	***Drainage Area (mi²)***	***1.5-Year Recurrence Interval Flow (cfs)***	***10-Year Recurrence Interval Flow (cfs)***	***100-Year Recurrence Interval Flow (cfs)***
Background Report analysis					
San Joaquin River below Friant. USGS: 11-251000	1908-1943 (pre-Friant)	1,676	11,400 [a]	34,400 [a]	80,700 [a]
San Joaquin River below Friant. USGS: 11-251000	1944-2000 (post-Friant)		400 [a]	8,950 [a]	64,400 [a]
San Joaquin River nr Newman. USGS: 11-274000 [c]	1914-1943 (pre-Friant)	9,520	9,150 [a]	20,400 [a]	52,200 [a]
San Joaquin River nr Newman. USGS: 11-274000 [c]	1944-2001 (post-Friant)		2,160 [a]	25,000 [a]	86,500 [a]
Cottonwood Creek nr Friant. USGS: 11-250500	1941-1951	35.6	40 [a]	520 [a]	N/A [b]
Little Dry Creek nr Friant. USGS:11-251500	1942-1956	57.9	190 [a]	1,770 [a]	N/A [b]
James Bypass (Fresno Slough) near San Joaquin, USGS: 11-253500	1948-2001	N/A			
ACOE analysis					
San Joaquin River below Friant. USGS: 11-251000	1949-1997 (post-Friant)	1,676	220	8,000	70,000
San Joaquin River at Gravelly Ford. CDEC: GRF	1949-1997 (post-Friant)	1,805	110	9,000	65,000

Table 2-3. cont.

Gaging station name and USGS or CDEC I.D. (from Table 2.1)	Period of Record	Drainage Area (mi²)	1.5-Year Recurrence Interval Flow (cfs)	10-Year Recurrence Interval Flow (cfs)	100-Year Recurrence Interval Flow (cfs)
Fresno River below Hidden Valley Dam. USGS: 11-258000	1976-1998	234	250	3,700	5,000
Chowchilla River below Buchanan Dam. USGS: 11-2590	1976-1998	235	470	3,700	7,000
Ash Slough below Chowchilla River (no gage given)	1976-1998	268	340	2,600	5,000
Berenda Slough below Chowchilla River (no gage given)	1976-1998	268	135	1,050	2,000
Eastside Bypass near El Nido. CDEC: ELN	1965-1998	5,630	230	17,000	21,000

[a] Estimated from Log-Pearson III fit of raw data, flood recurrences greater than 10-yr should be viewed with caution due to poor curve fitting.

[b] Insufficient raw data to extrapolate flow estimate.

[c] Includes flow from the Merced River (see Section 2.6.2.3).

[d] Flood frequency computed from maximum daily average flow, no instantaneous peaks available

2.6.2.1. San Joaquin River near Friant

The "San Joaquin River near Friant" gaging station (USGS station # 11-251000) is located at RM 265.5 and records streamflow data from the 1,676 mi² watershed above the gaging station. Until Friant Dam was completed, the gage recorded partially regulated streamflow from 1908 to 1943. Following completion of Friant Dam in 1944 and associated diversion canals in 1948, the gaging record after 1943 reflected much more regulated streamflow conditions. Because of the change in degree of streamflow regulation, the streamflow gaging record can be divided into separate pre- and post-dam series. The change in streamflow hydrology occurred over a 5-year period (1944-1948) as the dam and diversion became operational; therefore, the ACOE used 1948 as the end of the pre-Friant Dam period, while others use 1943 as the end of the pre-Friant Dam period.

The flood frequency analysis done in this report computes flood frequency for the gaging station using all historical gaging data at the USGS gage near Friant (pre- and post-dam). Flood magnitudes for recurrence intervals of 1.5, 5, 10, 25, and 50 years are summarized for both the pre-Friant Dam (moderately regulated) and post-Friant (regulated) periods of record. This analysis allowed a comparison of changes in flood frequency following the completion of Friant Dam (which can be linked to changes in fluvial process and channel form, as discussed in Chapter 3). The pre-Friant Dam analysis used data from 1908-1943, and the post-Friant Dam analysis used data from 1944-2000. Flood frequency analyses typically use annual instantaneous peak flow values in the computations; however, some of the early pre-Friant Dam data provided by the USGS is maximum daily average values rather than annual instantaneous peak values. No explanation was provided by USGS for not publishing annual instantaneous peak values. The maximum daily average values were nonetheless used in the flood frequency analysis, and using these values would slightly underestimate the pre-Friant Dam flood magnitude because the daily average flow values are slightly smaller than the annual instantaneous peak values.

The results of this analysis show a dramatic reduction in the flood flow regime as a result of the construction of Friant Dam and associated diversions. For example, the 1.5-year flood was reduced from 11,400 cfs to 400 cfs, and the 10-year flood was reduced from 32,400 cfs to 8,950 cfs (Figure 2-6). The smaller magnitude, higher frequency floods were much more severely impacted than were the large magnitude, less frequent floods, likely due to a relatively small storage capacity of Millerton Lake (Table 2-2). Additionally, when comparing the pre- and post-dam data, the pre-Friant Dam data is moderately regulated by small upstream dams, so the pre-Friant Dam data is a conservatively low flood magnitude estimate (i.e., actual unimpaired magnitude is probably larger). Lastly, the reduction in flood magnitude during the post-Friant Dam period is not necessarily entirely caused by reduced flow volume to the river downstream of Friant Dam. High flow releases tend to be 8,000 cfs or less due to channel capacity constraints downstream of Friant Dam (particularly in Reach 2) and ACOE flood control release limitations, and this constraint on flood management is observable on the larger number of flows in the 8,000 cfs range on Figure 2-6, Figure 2-7, and Figure 2-8.

The timing of annual instantaneous maximum floods on the San Joaquin River near Friant varied under both pre- and post-Friant Dam periods, although the patterns of magnitude and timing was different between the two periods (Figure 2-7). Prior to Friant Dam, annual instantaneous maximum floods occurred between mid-December and mid-June, indicating that early-winter rainstorms generated these peak flows some years, and by peak snowmelt runoff flows in other years. Figure 2-7 also illustrates that the earlier floods were larger magnitude than the later snowmelt flood peaks. These larger floods were generated from rainfall events, with the largest events generated from rain-on-snow events. The largest peak flood of record was 77,200 cfs (December 1937), although the 1862 flood was probably larger. The smallest annual peak flow was 3,380 cfs, most annual peak flows were greater than 5,000 cfs, and snowmelt peaks typically did not exceed 16,000 cfs (Figure 2-7).

The post-dam period has much lower flood magnitudes and the timing of these floods was spread out over a wider period of the water year. With the exception of the 1997 flood, which was estimated as an 80-year flood event (ACOE 1999), all post-dam peak flows were less than 16,000 cfs. Annual peak flows in the post-Friant Dam period occurred throughout the year because the natural periods of high flow (winter floods and spring snowmelt) are now completely captured by upstream dams and diversions, such that many of the peak flows occur during the summer when Friant Dam releases 200 cfs to 400 cfs for downstream riparian water rights holders.

The ACOE flood frequency curve for the Friant gaging station is presented in Figure 2-8. Although the ACOE did not perform a comparative analysis for the pre- and post-Friant Dam flood flow regime, their analysis shows that for the post-Friant Dam flow regime (based on a slightly shorter period of record than that used for Figure 2-6, from 1949-1997), the 1.5-year flood is approximately 220 cfs, and the 10-year flood flow is approximately 8,000 cfs (Figure 2-8) The ACOE prescribed controlled flood release limit at Friant is 8,000 cfs.

2.6.2.2. San Joaquin River at Gravelly Ford

The San Joaquin River near Gravelly Ford gaging station (CDEC station # “GRF”) is located at RM 229 and records streamflow data draining the 1,805 mi^2 watershed above the gaging station. The gaging period of record is 1987-present (Table 2-1); however, the ACOE analyzed flood frequency using data from 1949-1997. The ACOE does not describe their methods for expanding the measured data set back to 1949. Regardless, as with the San Joaquin River near Friant analysis, the flood frequency analysis at Gravelly Ford was performed as part of a post-flood assessment in response to the widespread flooding of 1997. The ACOE flood frequency curve is presented in Figure 2-9.

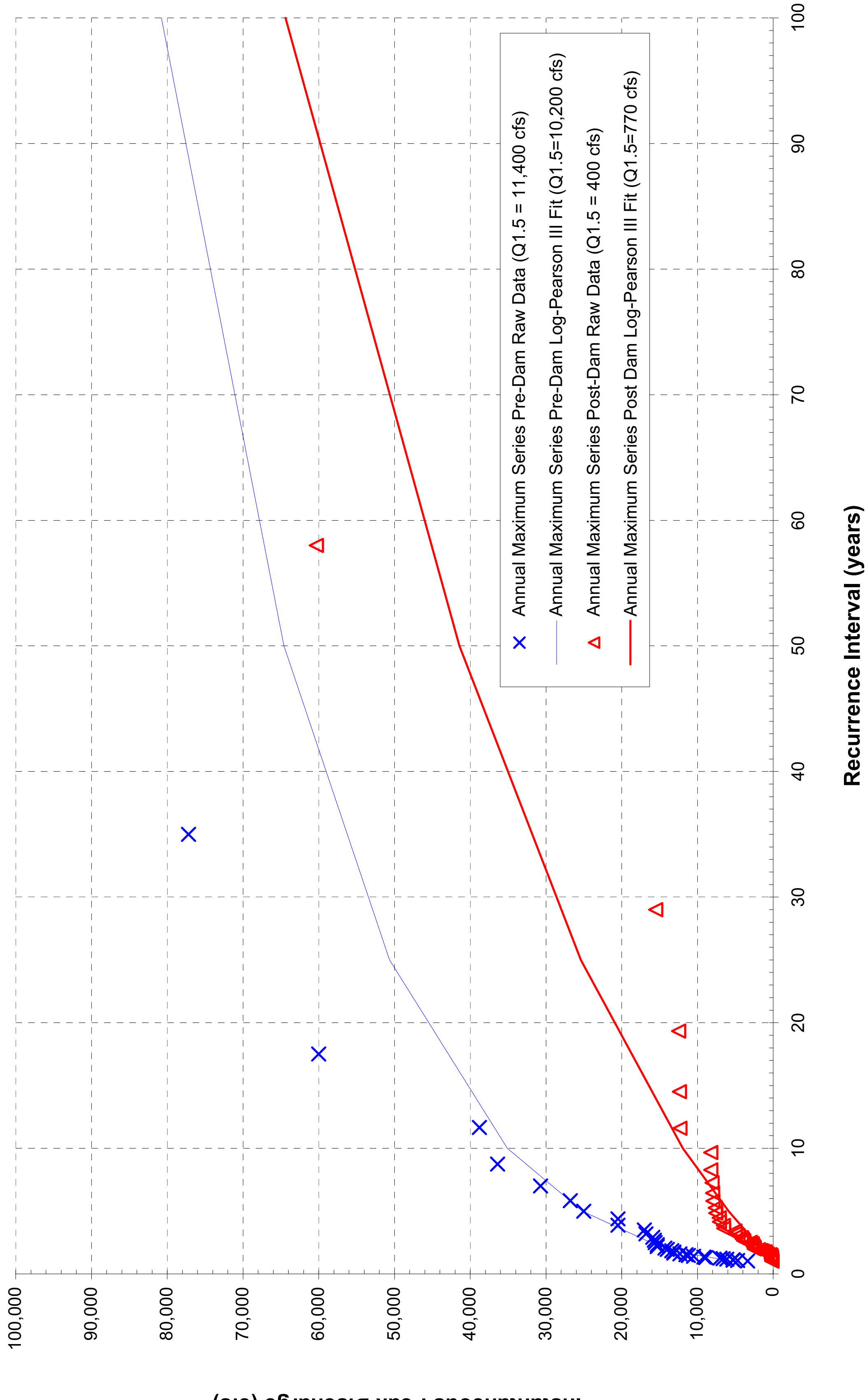

Figure 2-6. Flood frequency at the San Joaquin River below Friant Dam gaging station (# 11-251000) for pre- and post-Friant Dam (pre-dam 1908 – 1943; post-dam 1944 – 2000). Drainage area = 1,676 mi².

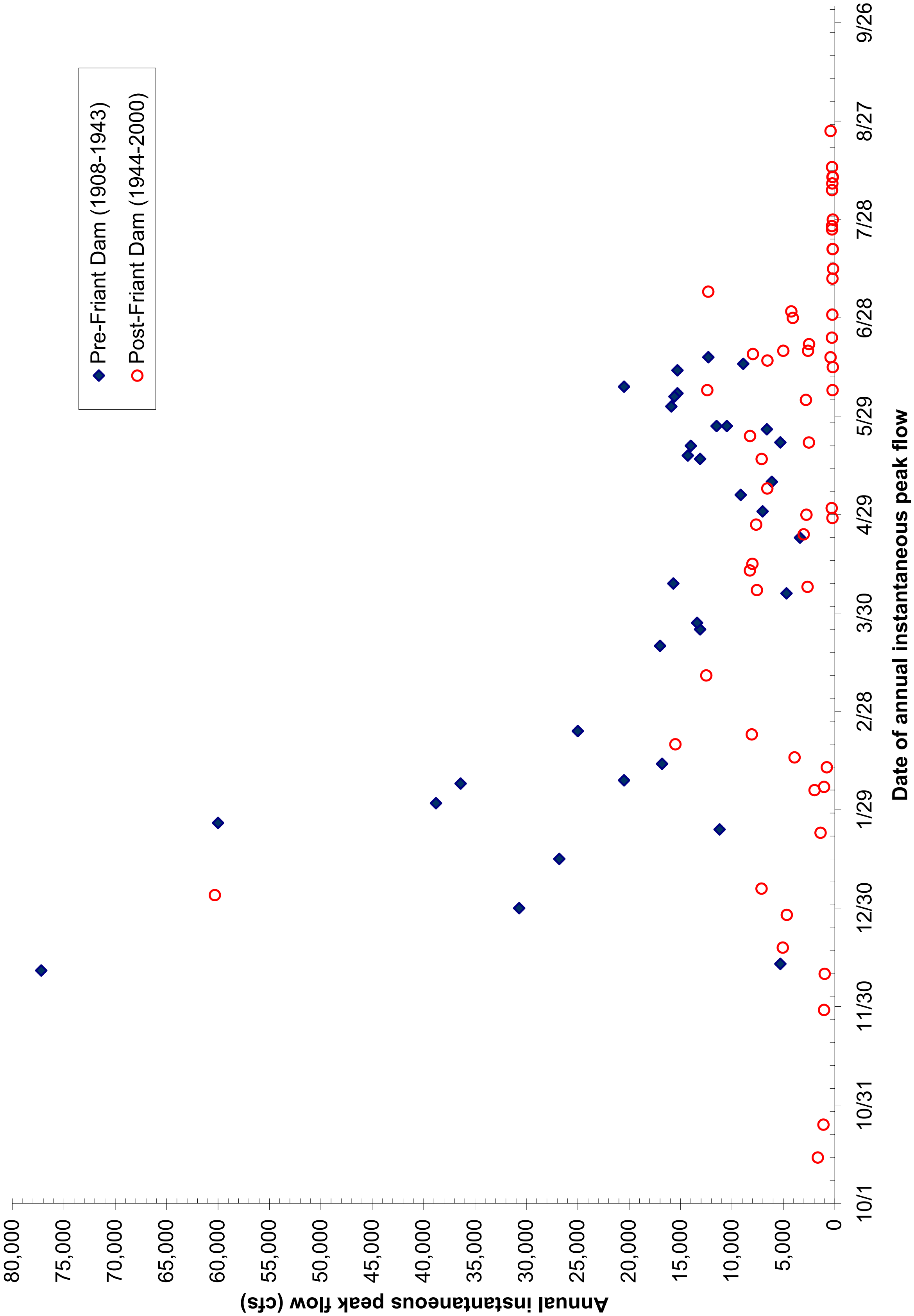

Figure 2-7. Temporal distribution of annual peak flows at the USGS gaging station near Friant (USGS # 11-251000) for pre- and post-Friant Dam records.

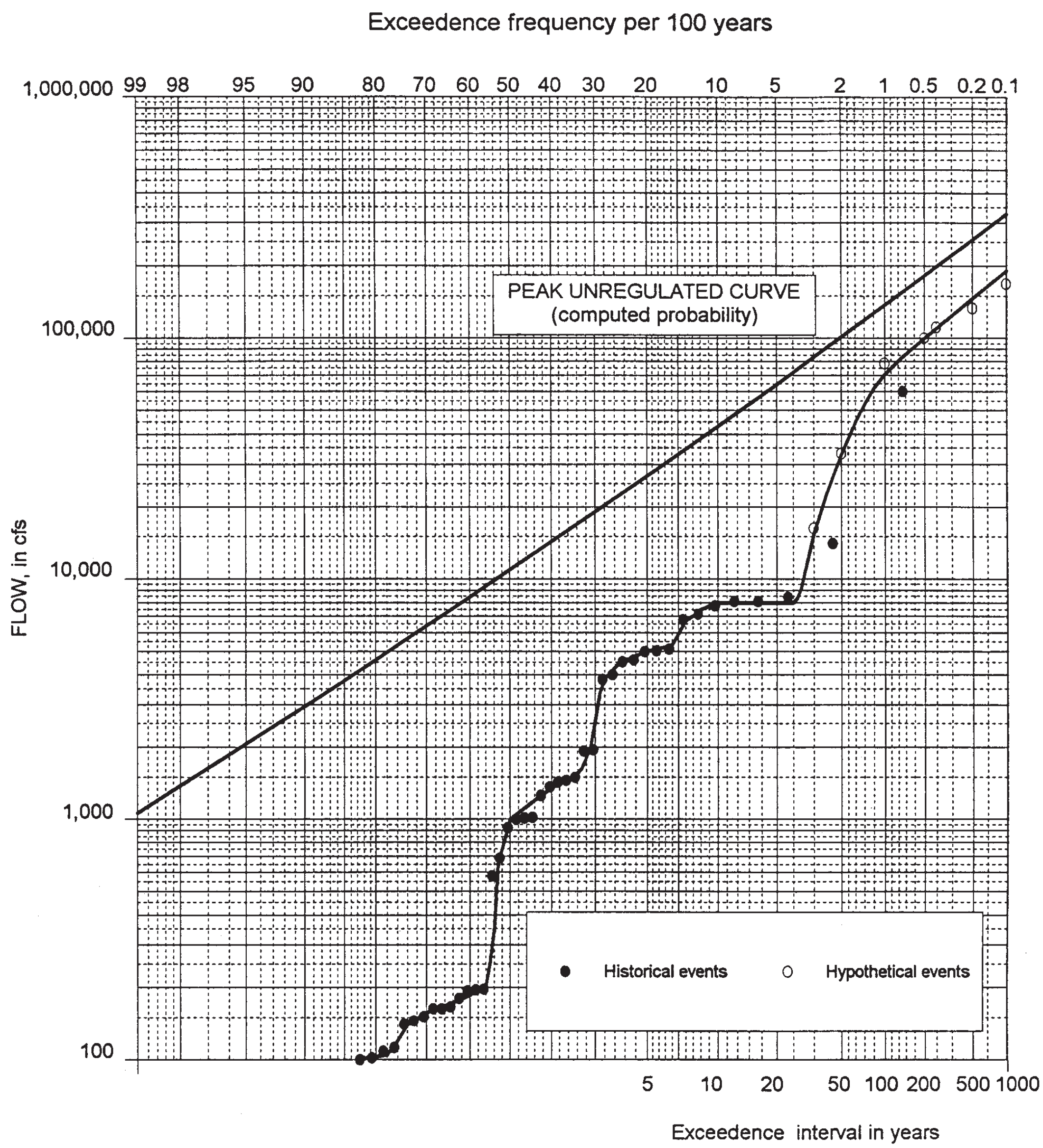

NOTES:

1. Median Plotting Positions
2. Drainage Area: 1,676 sq. mi.
3. 49 years of record (1949 to 1997)
4. 1997 event plotted as maximum in 94 years.

Prepared by TKP

SACRAMENTO-SAN JOAQUIN BASIN COMPREHENSIVE STUDY
SAN JOAQUIN RIVER BASIN, CALIFORNIA

PEAK RAIN FLOOD FREQUENCY CURVE
REGULATED CONDITION

SAN JOAQUIN RIVER AT FRIANT DAM

U.S. ARMY CORPS OF ENGINEERS
SACRAMENTO DISTRICT

Nov 98

PLATE 18

Figure 2-8. ACOE analysis of flood frequency at the San Joaquin River below Friant Dam gaging station (USGS # 11-251000), post-Friant Dam (1949 – 1997). Drainage area = 1,676 mi²

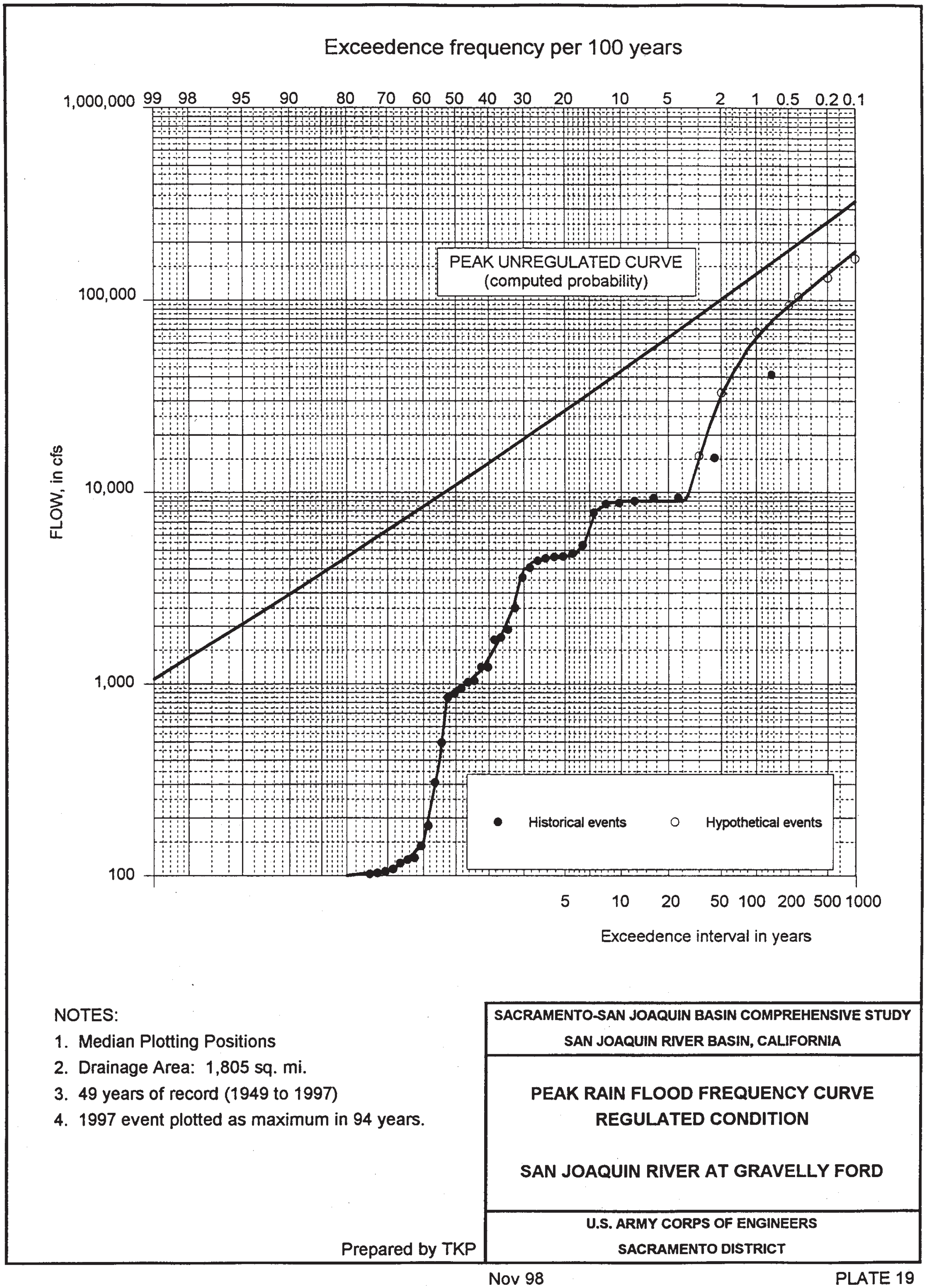

Figure 2-9: ACOE analysis of flood frequency at the San Joaquin River at Gravelly Ford gaging station (CDEC # GRF), post-Friant Dam (1949 – 1997). Drainage area = 1,805 mi²

2.6.2.3. San Joaquin River near Newman

The San Joaquin River near Newman gaging station (USGS station # 11-274000) is located at RM 118 and records streamflow data draining the 9,520 mi^2 watershed above the gaging station. At its location on the San Joaquin River, the gaging station is located just downstream of the confluence of the Merced River; therefore, streamflow records include considerable flow contribution by the Merced River, but loses some flow through the Merced River Slough. No attempt was made to subtract the Merced River flow data from the peak flood flow record.

The USGS gaging station near Newman recorded moderately regulated streamflow from 1914 to 1943. Following completion of Friant Dam and associated diversions, streamflow conditions changed. An additional change in hydrology measured at this station may have occurred in 1966 with the completion of New Exchequer Dam on the Merced River. The flood frequency curves for pre- and post-New Exchequer Dam were examined, and there were no significant differences between the two curves. Therefore, flood frequency was computed for the Newman gage by separating the annual peak flow record into two components (Figure 2-10): pre-Friant Dam (1914-1943) and post-Friant Dam (1944-2001). The ACOE analysis produced a rainfall flood frequency curve (Figure 2-11).

Because the computed flood frequency from the Newman gaging record does not solely capture San Joaquin River peak flood flow, the reduction in flood magnitude and frequency at the downstream project boundary is only partially due to Friant Dam and associated diversions. However, by examining the flood frequency curves, a reduction in flood magnitude and frequency is apparent. The post-Friant Dam curve shows a decrease in flood magnitude and frequency for the 1.5- and 2.3-year floods, but then shows a slight increase in flood magnitude and frequency for flood flows between a 5-year and 25-year recurrence, after which the pre-dam and post-dam data appear to converge. Based on this comparison, the flood frequency analysis at the Newman gaging station does not show a definitive trend in reduced magnitude and frequency of larger magnitude flood flows at the downstream end of the study area.

2.6.2.4. Cottonwood Creek near Friant

Cottonwood Creek is a tributary to the San Joaquin River, and joins the San Joaquin River at RM 265, just downstream of Friant Dam. The Cottonwood Creek gaging station was located approximately 0.5 miles upstream of the confluence with the San Joaquin River, and recorded streamflow data from the 35.6 mi^2 watershed above the gaging station. The short period of record (10 years) of USGS data limits the number of peak floods usable for conducting the flood frequency analysis; therefore, the flood frequency analysis for Cottonwood Creek did not extrapolate flood magnitudes for floods larger than the 10-year flood (Figure 2-12). Subsequent data collected by USBR was not used in the analysis.

2.6.2.5. Little Dry Creek near Friant

Similar to Cottonwood Creek, Little Dry Creek is a tributary to the San Joaquin River and joins the River at RM 260.4, approximately 5 miles downstream of Friant Dam. There were two gaging stations on Little Dry Creek, and the downstream-most gaging station was used in this analysis. The downstream-most gaging station was located approximately 4 miles upstream of the confluence with the San Joaquin River, and recorded streamflow data from the 57.9 mi^2 watershed above the gaging station. The period of record of USGS data for this gaging station was short (15 years), so the flood frequency analysis for Little Dry Creek did not extrapolate flood magnitudes for floods larger than the 10-year flood (Figure 2-13). Subsequent data collected by USBR was not used in the analysis.

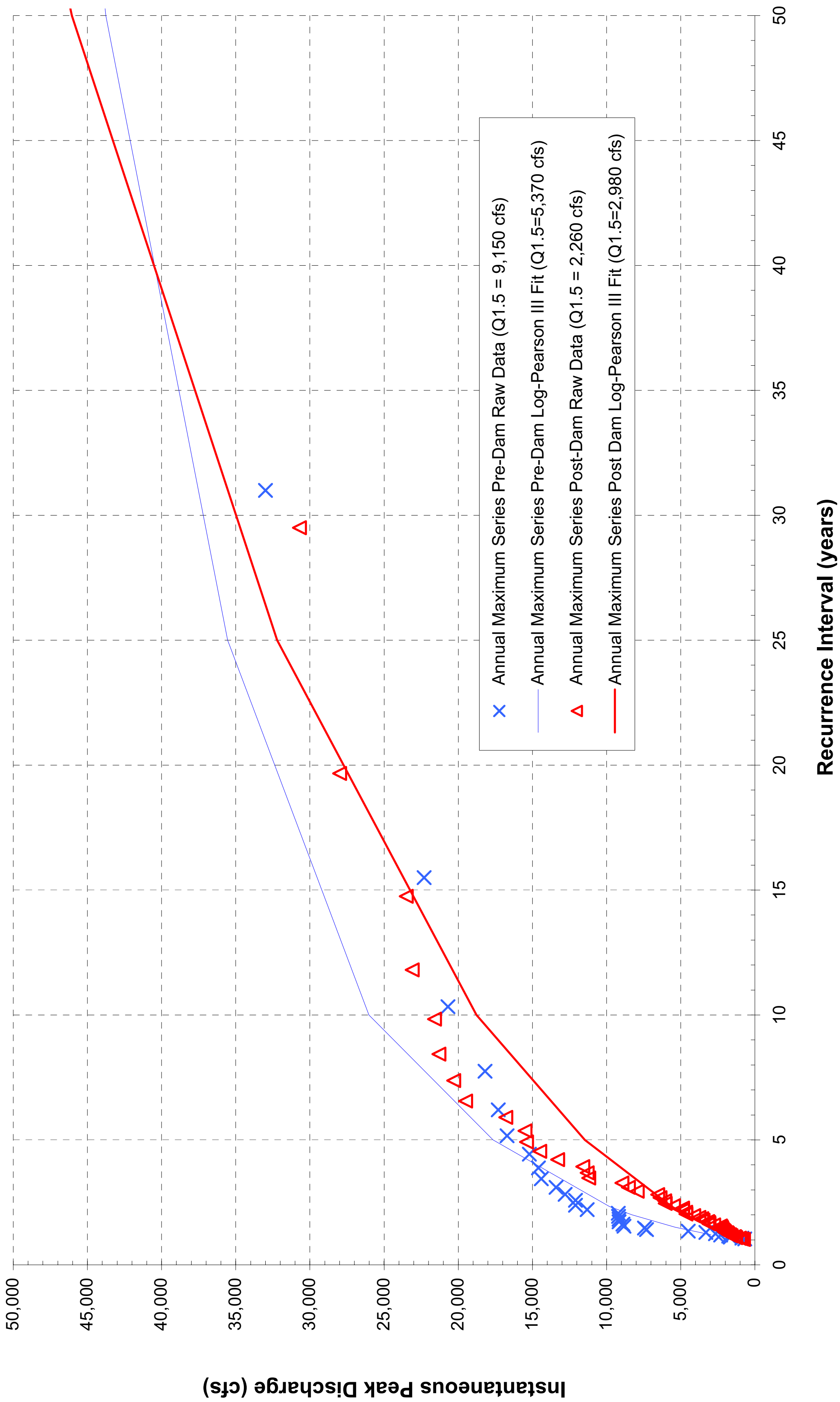

Figure 2-10. Flood frequency at the San Joaquin River near Newman gaging station (USGS # 11-274000) for pre- and post-Friant Dam (pre-dam 1914 – 1943; post-dam 1944 – 2001). Drainage area = 9,520 mi².

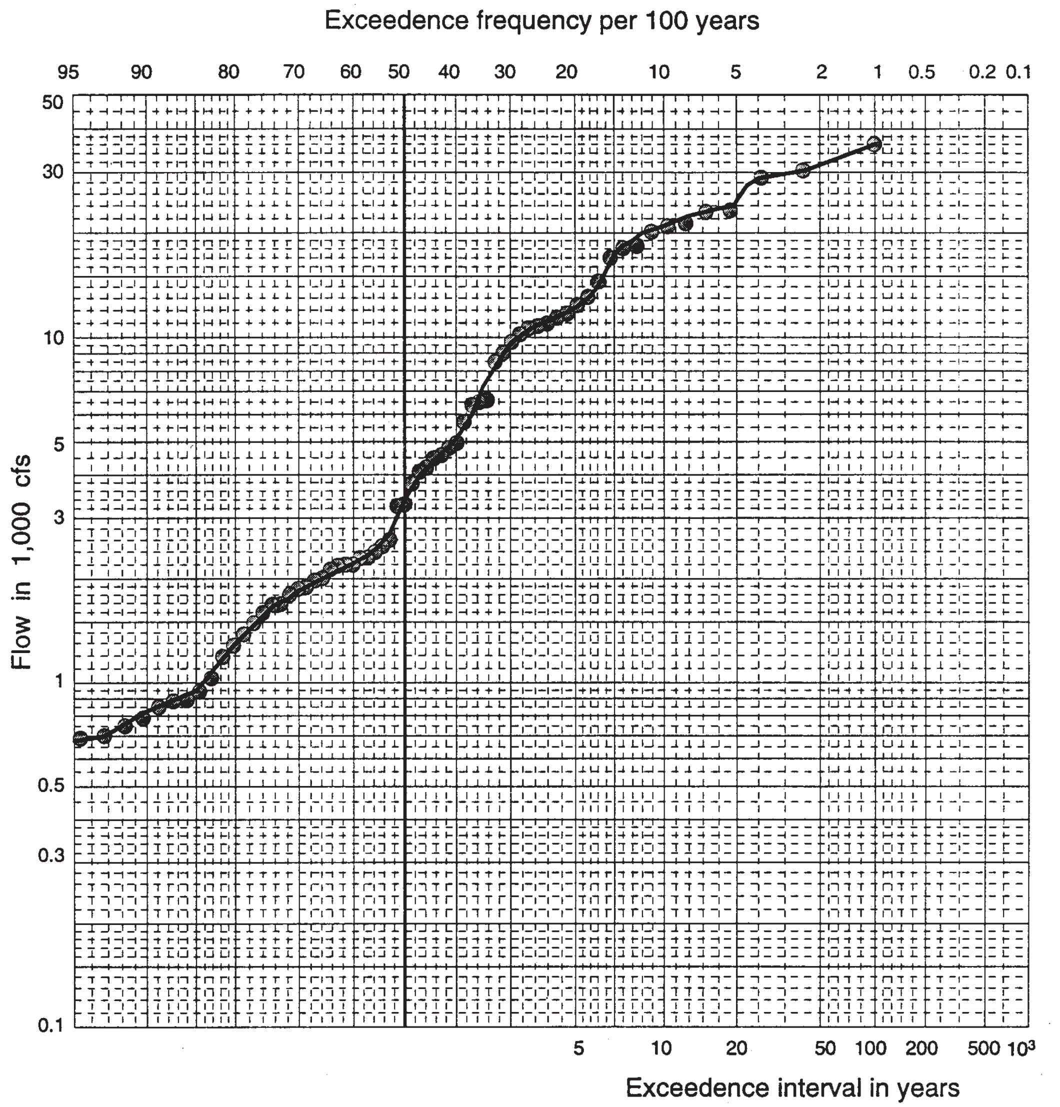

NOTES:

1. Drainage area is 9,520 sq. mi.
2. Median plotting positions based on 69 years of record (1930-1998)
3. Curve is graphically drawn.
4. Flows before 1975 are simulated.
5. Flows considered at latitude and may include flow out of channel.

Prepared by JAL

SACRAMENTO-SAN JOAQUIN BASIN COMPREHENSIVE STUDY
SAN JOAQUIN RIVER BASIN, CALIFORNIA

1-DAY RAIN FLOOD FLOW FREQUENCY CURVE
REGULATED CONDITION
SAN JOAQUIN RIVER NEAR NEWMAN

U.S. ARMY CORPS OF ENGINEERS
SACRAMENTO DISTRICT

Dec 98

PLATE 27

Figure 2-11. ACOE analysis of flood frequency at the San Joaquin River near Newman gaging station (USGS # 11-274000), post-Friant Dam (1949 – 1997). Drainage area = 9,520 mi^2.

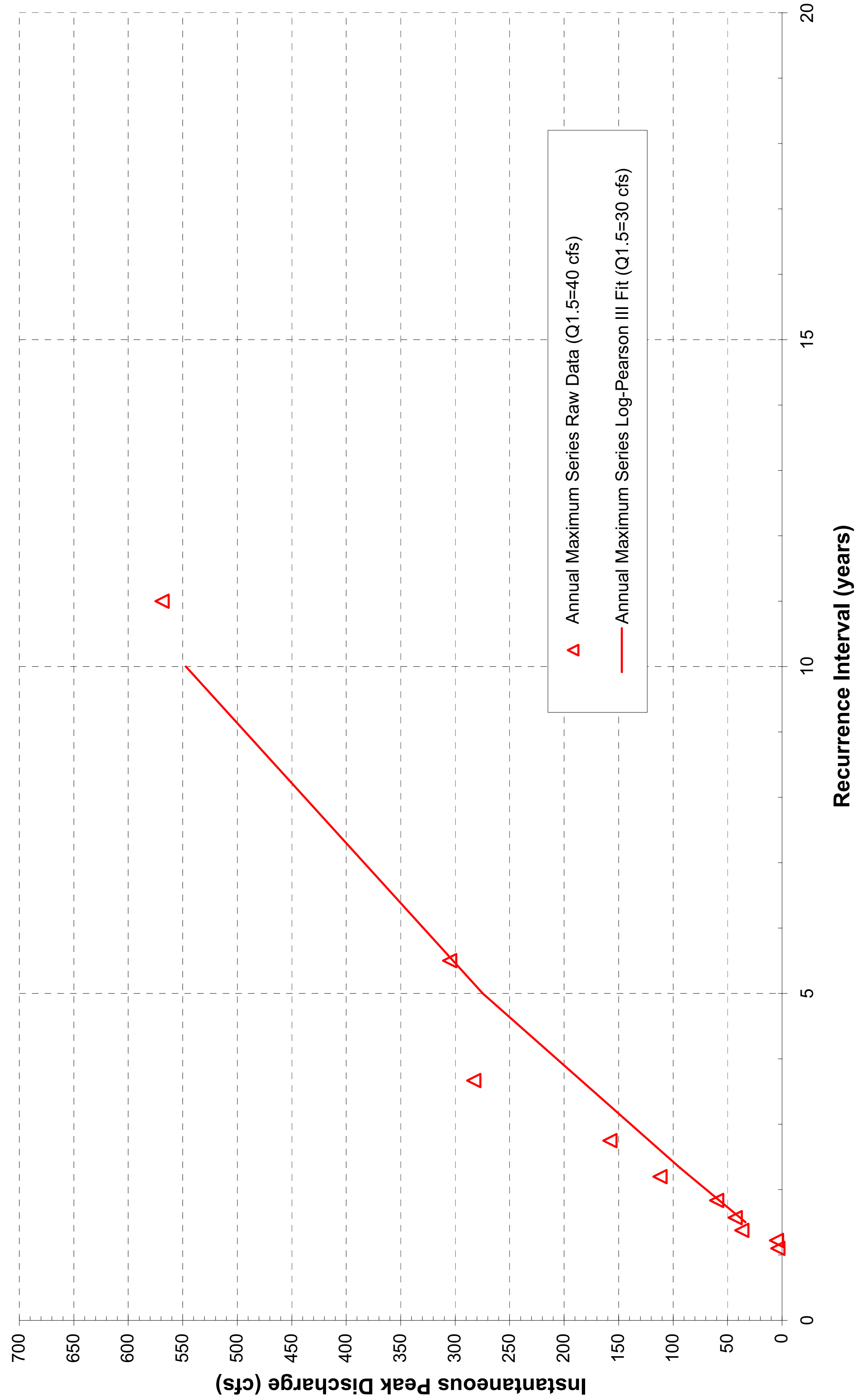

Figure 2-12. Flood frequency at the Cottonwood Creek near Friant gaging station (USGS # 11-250500), 1942 – 1951. Drainage area = 35.6 mi^2.

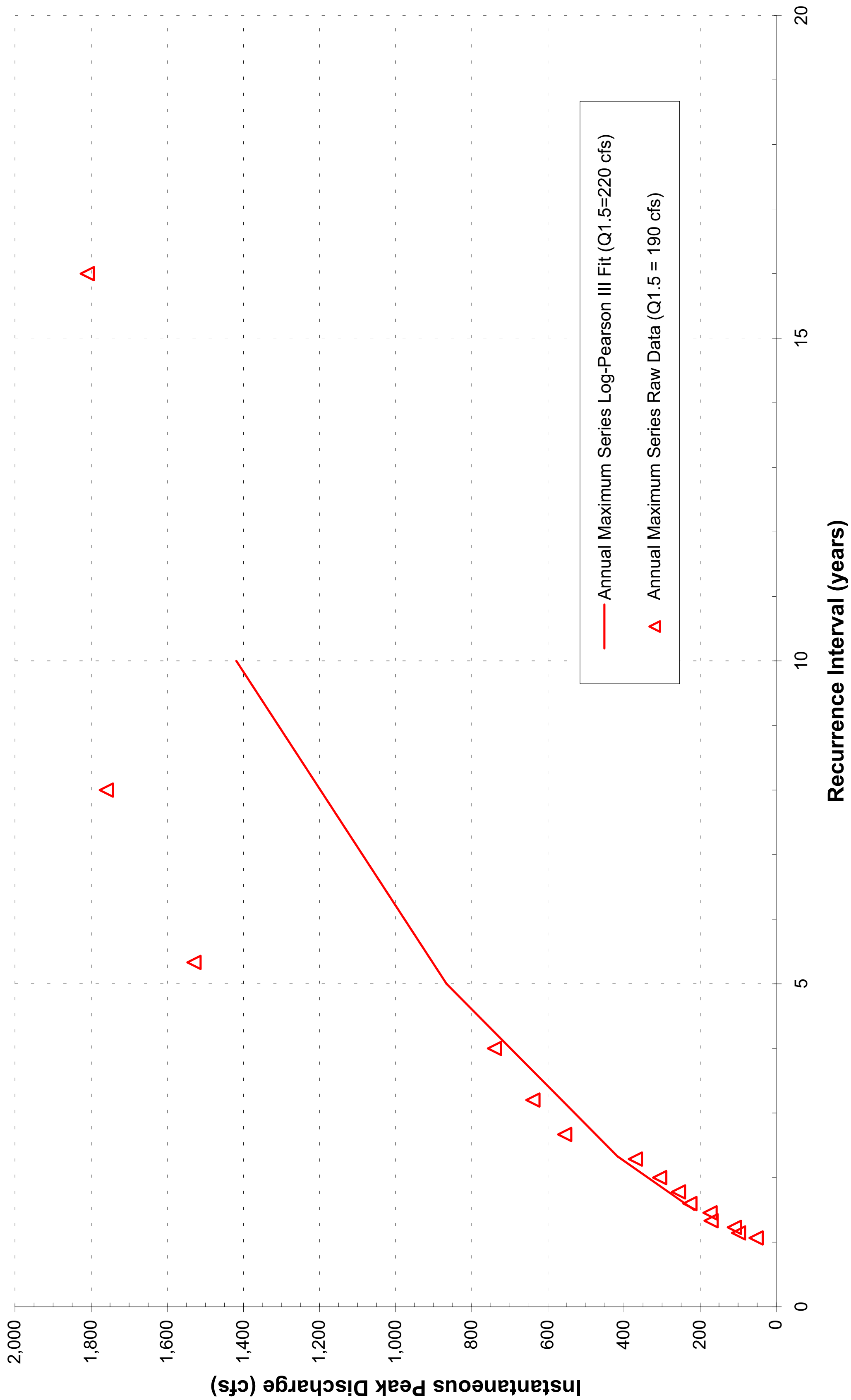

Figure 2-13. Flood frequency at the Little Dry Creek near Friant gaging station (USGS # 11-251500), 1942 – 1956. Drainage area = 57.9 mi².

2.6.2.6. James Bypass (Fresno Slough)

The James Bypass diverts flood flows from the Kings River (drains into the Tulare Lake basin south of the San Joaquin River) into the San Joaquin River at Mendota Pool (RM 205). During wetter water years, a considerable volume of flood flows are delivered to the San Joaquin River from the Kings River, where it is diverted at Mendota Pool or Sack Dam, and/or routed through the San Joaquin River flood management system. There are no records for annual instantaneous maximum flows for the period of record (the typical flow measure used in flood frequency analysis); therefore, annual maximum daily average values were used (Figure 2-14). Historical data is not available to quantify or estimate unimpaired flow contribution or seasonality to the San Joaquin River from the Kings River via Fresno Slough, but flow regulation on the Kings River must have significantly decreased the annual volume of flow contributed to the San Joaquin River. Review of recent flow data (1948-present) shows that flows are zero most of the year, with positive flows to the San Joaquin River primarily occurring during flood control releases on the Kings River. It is unknown how much (if any) unimpaired summer baseflows were contributed to the San Joaquin River from the Kings River, but historical accounts (e.g., Derby 1852) discuss Fresno Slough flow contributions over significant portions of the year (winter through the end of the snowmelt runoff season in August).

2.6.2.7. Rivers entering Eastside Bypass

The larger streams entering the San Joaquin River from the Sierra Nevada within the study area include the Fresno River, Chowchilla River, and Bear Creek. The ACOE (1999) developed flood frequency curves for the Fresno River below Hidden Dam (Figure 2-15), Chowchilla River below Buchanan Dam (Figure 2-16), Ash Slough below Chowchilla River (Figure 2-17), Berenda Slough below Chowchilla River (Figure 2-18), and the Eastside Bypass near El Nido (Figure 2-19). All these streams enter the Eastside Bypass system, and do not re-join the San Joaquin River until the Mariposa Bypass outlet (RM 148) or the outlet of the Eastside Bypass (RM 136).

2.6.3. Hydrograph Components

Larger rivers draining the Sierra Nevada have similar unimpaired runoff characteristics over the water years. While the specific timing and magnitude of these runoff events is variable, there are general trends that are broadly predictable in timing and magnitude. These “hydrograph components” include summer baseflows, fall baseflows, fall floods, winter floods, winter baseflows, spring snowmelt peak, and spring/summer snowmelt recession.

The high flow regime of the San Joaquin River is typical of other large Sierra Nevada rivers. There are two distinct periods of high flows: one in the fall/winter from rainfall and rain-on-snow storm events, and one in the spring and early summer during the snowmelt runoff period. The largest flows typically occurred during winter storms; the highest peak flows are produced when warm rains fall on a large snowpack, such as occurred in December-January 1997. The seasonal low flows typically occurred in late summer and fall, after snowmelt had been exhausted and before the onset of winter rains. There is considerable variation in precipitation (and therefore river flows) from year to year, but snowmelt reliably produced moderately high flows most years because of the San Joaquin River drains some of the highest elevation terrain in the Sierra Nevada. These unique unimpaired runoff characteristics of the San Joaquin River had significant implications to channel form and processes, as well as the life history and ecological connections among the biota that resided in the San Joaquin River corridor (see Section 2.6.4).

Typical unimpaired hydrograph components are described below, illustrated with a pre-Friant Dam hydrograph from the San Joaquin River at Friant (Figure 2-20).

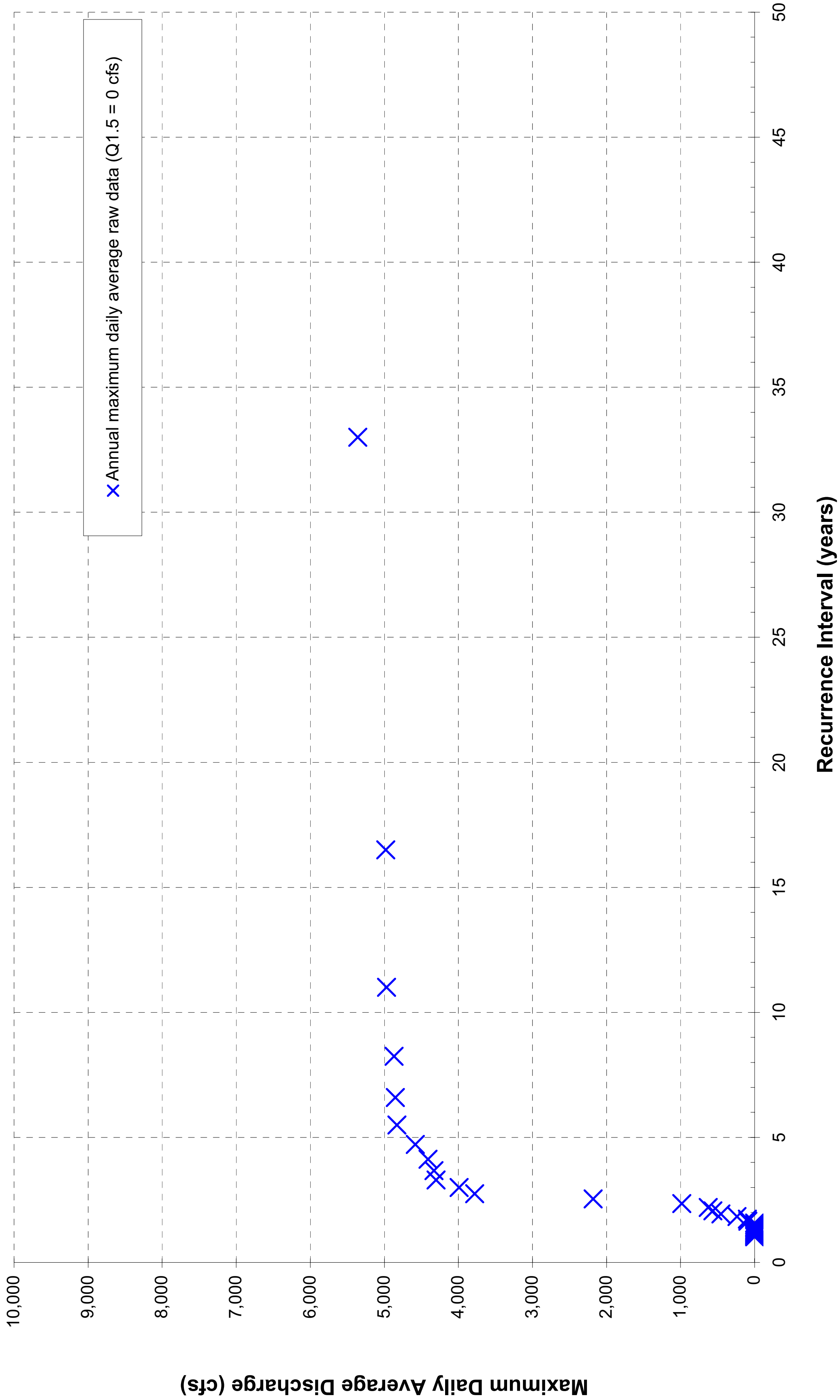

Figure 2-14. Flood frequency at the James Bypass (Fresno Slough) near San Joaquin CA gaging station (USGS # 11-253500), 1948-1954, 1974-2001. No annual instantaneous peak flows published, so flood frequency based on raw data of maximum daily average flows.

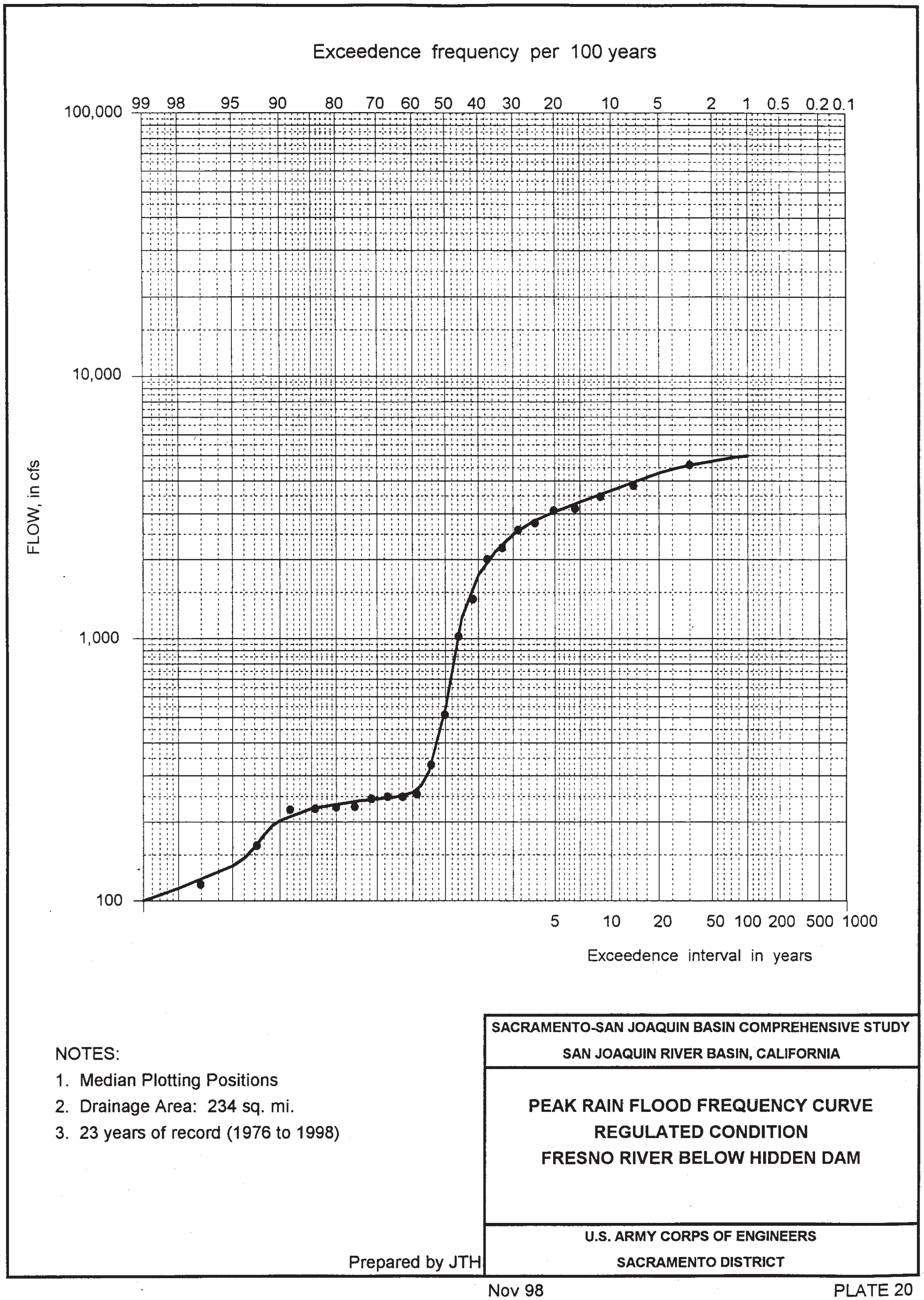

Figure 2-15. ACOE analysis of peak rain flood frequency at the Fresno River below Hidden Dam gaging station (USGS # 11-258000), post-dam (1976 – 1998). Drainage area = 234 mi^2.

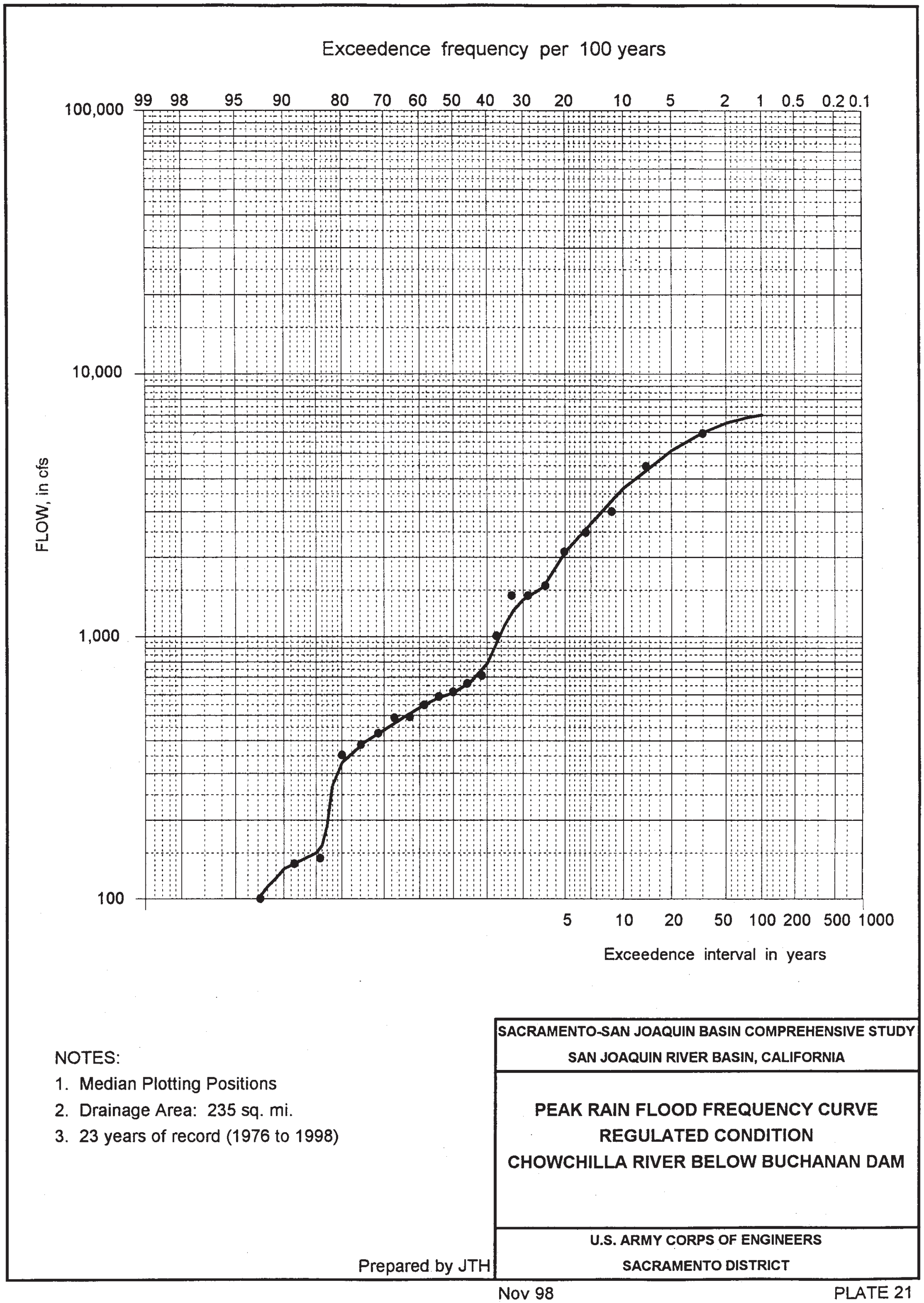

Figure 2-16. ACOE analysis of peak rain flood frequency at the Chowchilla River below Buchanan Dam gaging station (USGS # 11-259000), post-dam (1976 – 1998). Drainage area = 235 mi^2.

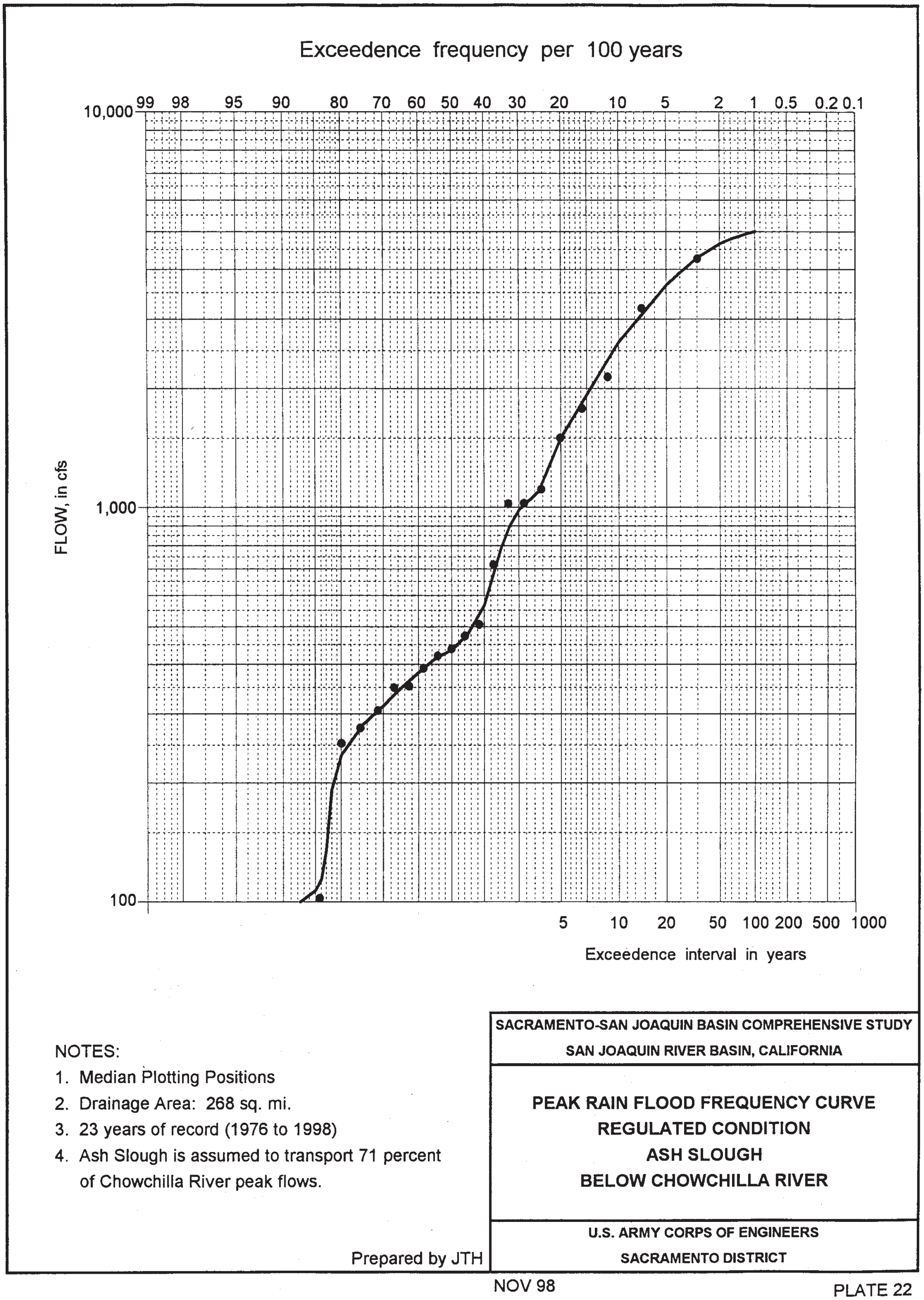

Figure 2-17. ACOE analysis of peak rain flood frequency at the Ash Slough below Chowchilla River, post-dam (1976 – 1998). Drainage area = 268 mi^2.

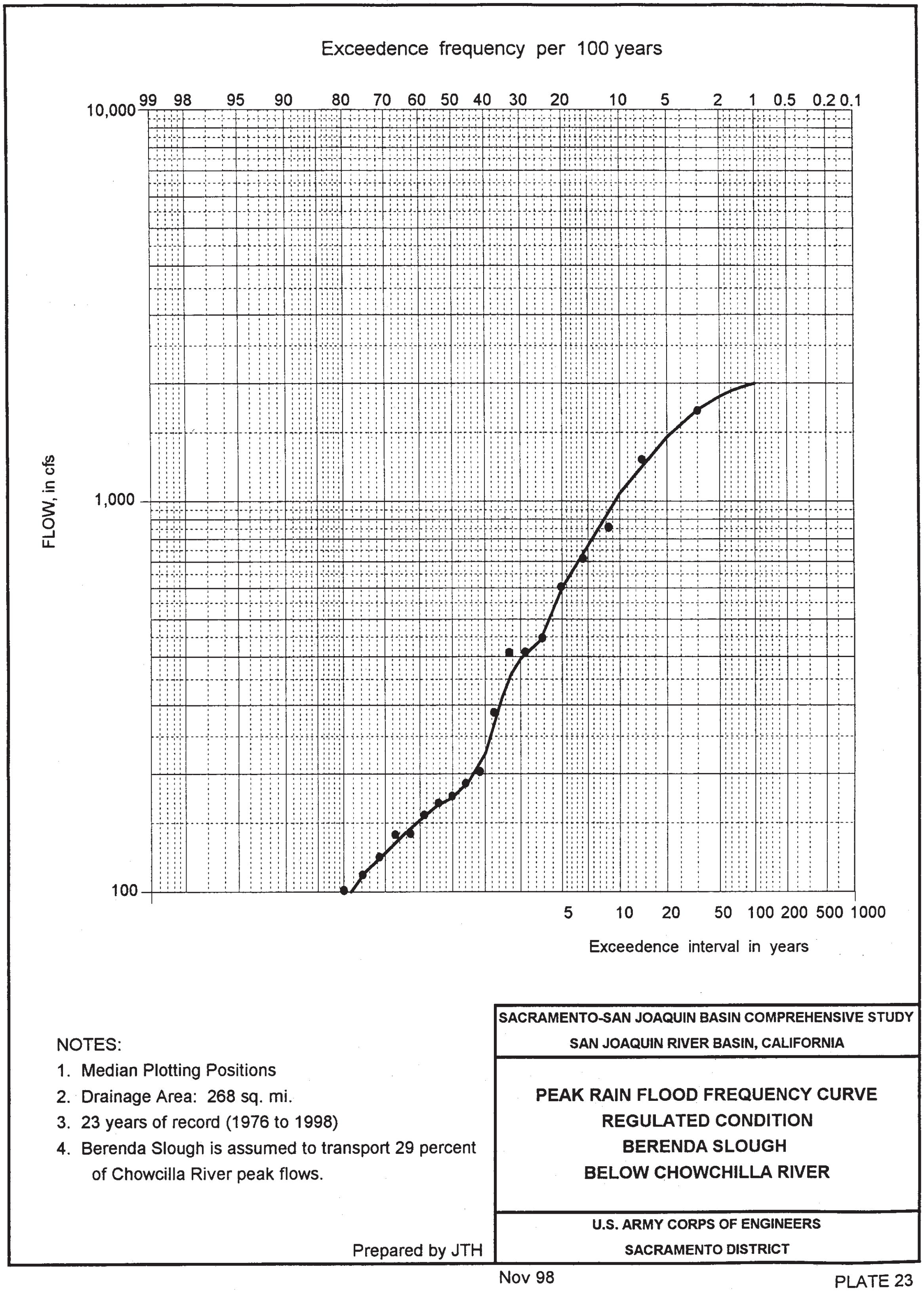

Figure 2-18. ACOE analysis of peak rain flood frequency at the Berenda Slough below Chowchilla River, post-dam (1976 – 1998). Drainage area = 268 mi^2.

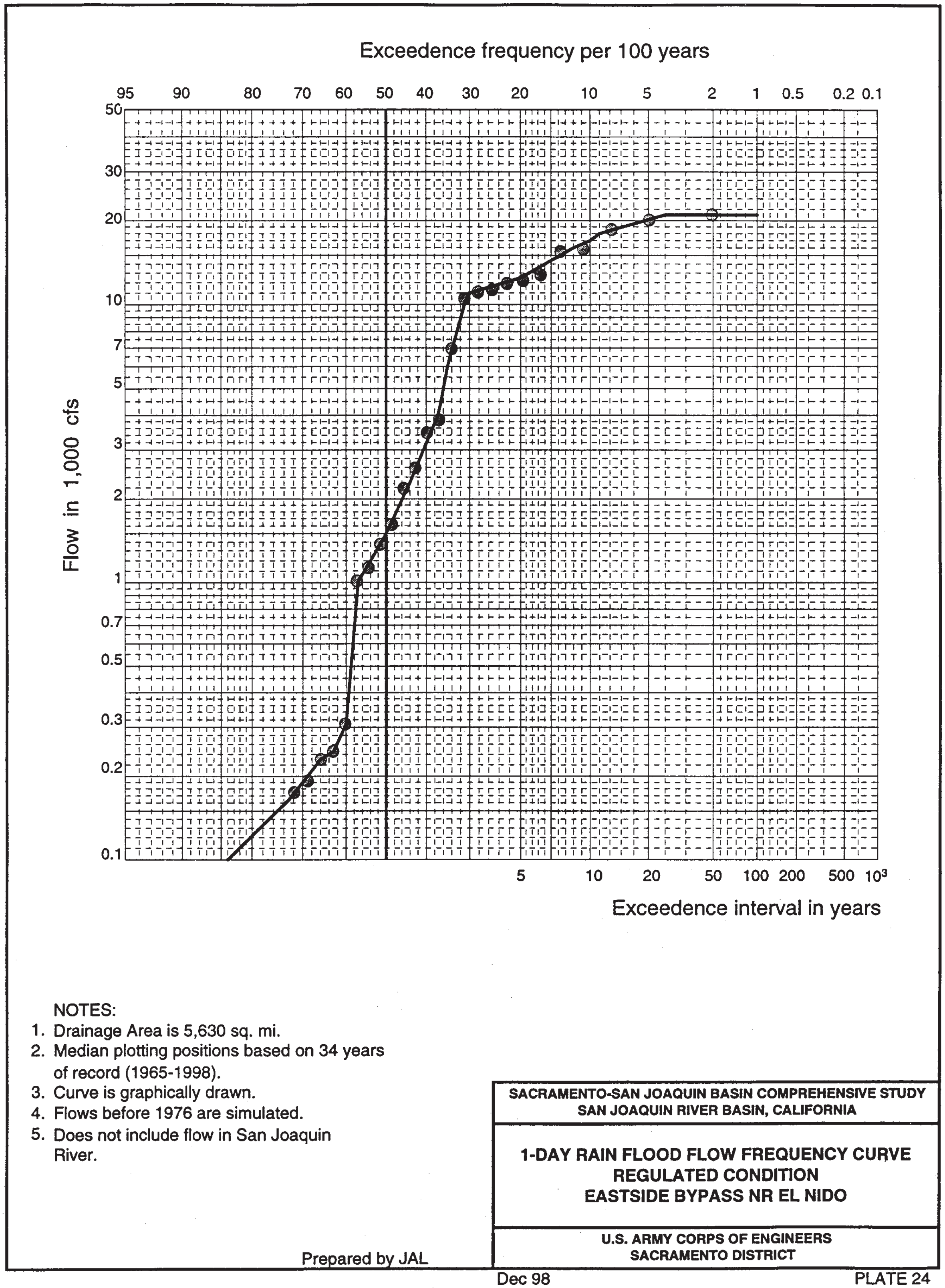

Figure 2-19. ACOE analysis of peak rain flood frequency at the Eastside Bypass near El Nido gaging station (CDEC # "ELN"), post-dam (1965 – 1998). Drainage area = 5,630 mi^2.

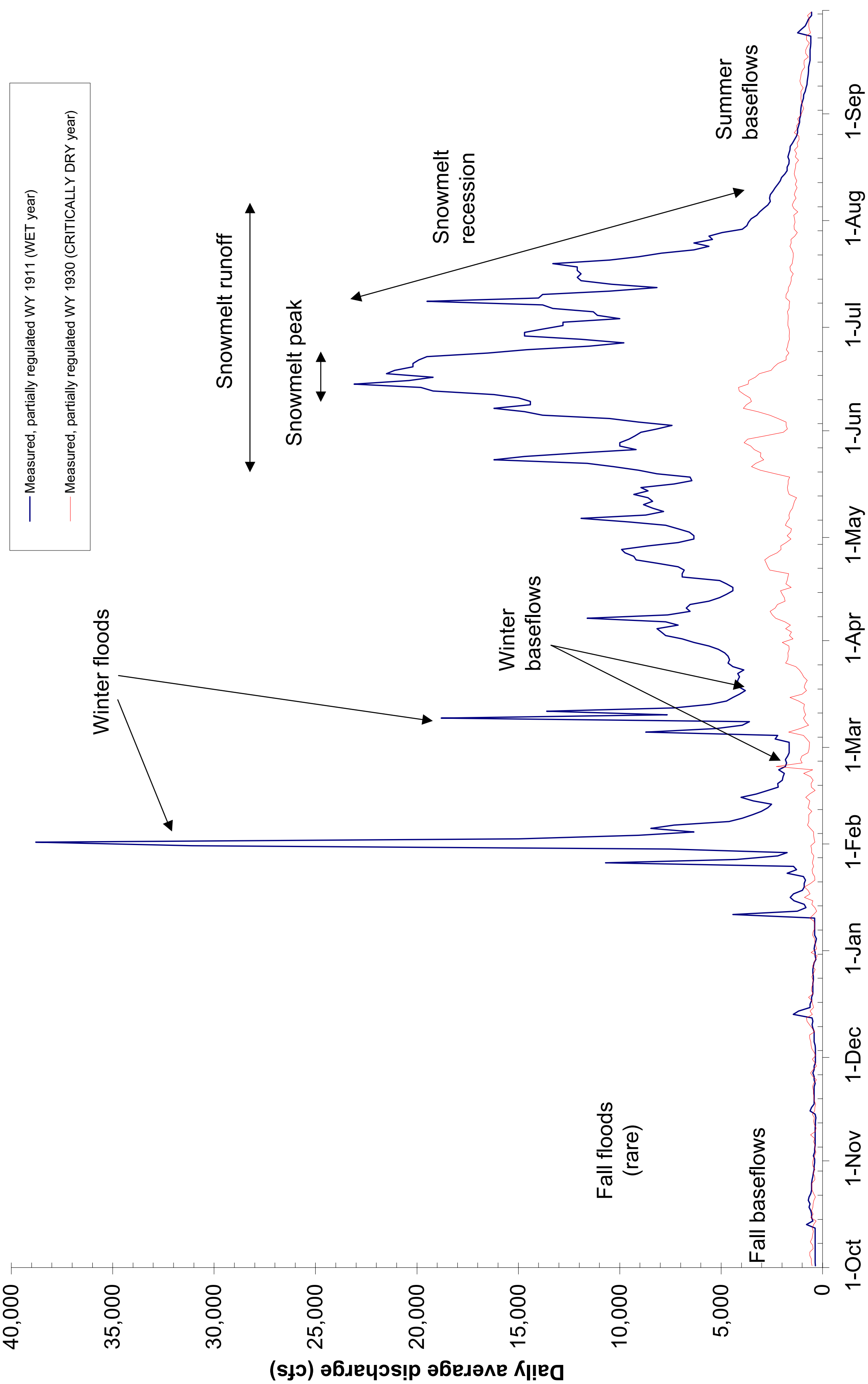

Figure 2-20. Illustration of hydrograph components of the San Joaquin River at Friant for an Extremely Wet water year (1911) and a Critically Dry water year (1930).

2.6.3.1. Summer-Fall Baseflow

Annual low flows occur after the snowmelt recession limb, and occur during the summer-fall baseflow hydrograph component (Figure 2-20). Summer-fall baseflows are derived from the slow drainage of water remaining in hillslopes, stored in riverbanks and floodplains along alluvial reaches (having been recharged by high winter floods), by springs in the Sierra Nevada mountains, and possibly also by artesian springs in the San Joaquin Valley (see Chapter 4). Summer-fall baseflows are neither the same throughout the summer-fall period, nor the same year after year. Summer-fall baseflows decline slowly such that changes in stage would typically not be noticeable to the casual observer on a daily basis, but may be noticeable on a weekly basis (e.g., Figure 2-20). Streams with substantial springs had much larger and more stable summer-fall baseflows, and the lower reaches of the San Joaquin River may have had substantial baseflow contributions from artesian springs and contribution from the shallow groundwater aquifer. Summer-fall baseflows occur from at least August through October (or until the first significant runoff-producing storm of the wet season). In wetter years such as 1911, the seasonal recession limb may continue well into the summer, while on a dry year (such as 1930), the spring snowmelt runoff may end by late-spring (Figure 2-20).

2.6.3.2. Winter Season Floods

Higher flood flows are produced by direct runoff from rainfall, especially when tropical storms drop rain at higher elevations in the watershed on a pre-existing snowpack (‘rain-on-snow’ floods). Peak flows from rainfall and rain-on-snow floods are typically sharply peaked, with rapid rising limbs and slightly slower but still rapidly falling recessional limbs (Figure 2-20). The ‘rain-on-snow’ events have been responsible for the largest historical floods, such as the 1862 flood and the recent flood of January 1997. Winter-spring peak flows tend to be larger for wetter years and smaller for drier years (Figure 2-20).

2.6.3.3. Winter Baseflows

Between winter-spring peak storm events, flow will tend to drop back to a baseflow level, but to a baseflow that is considerably higher than the summer-fall baseflow, and more variable in magnitude through the winter baseflow period (Figure 2-20). The degree to which baseflow recedes between winter storm runoff events depends on the time between storms, the magnitude of those storms, antecedent moisture conditions in the watershed, and watershed runoff characteristics. Wetter water years tend to have more winter storms, such that the baseflow periods between storm events are shorter than drier years (Figure 2-20).

2.6.3.4. Snowmelt Peak Flows

These were high flows occurring during spring and early summer as temperatures increased and the snowpack melted. With the potential exception of extreme drought years, the San Joaquin River had snowmelt peak flows. The USGS gaging station at Friant shows that peak flows for at least half of the years were generated by spring snowmelt runoff, as illustrated by the plot of annual peak discharge against day of the year prior to construction of Friant Dam (Figure 2-7). These were years that lacked a large, warm, runoff-producing winter storms that typically exceed snowmelt peak flows, especially when rain-on-snow events occurred.

Snowmelt runoff can be viewed as a seasonal high flow, driven by heating and melting of snow, with smaller peaks (reflecting warm periods) superimposed on a seasonal rise and fall, as illustrated by the example pre-Friant Dam hydrograph (Figure 2-20). The peaks typically have a moderate rise (over a few days) and less abrupt decline. Dates and length of peak snowmelt runoff would vary among years as a function of precipitation patterns, precipitation volumes, and runoff patterns, but also from year-to-year variation in that particular year's snowpack and the weather in the spring and early summer. In dry years, the (small) snowmelt peaks occurred earlier (typically May) and were shorter, in wet years the peaks were later (typically June) and longer. The snowmelt peak period often had multiple peaks fairly close in magnitude.

2.6.3.5. Snowmelt Recession Limb

The snowmelt recession limb in snowmelt stream is caused by a gradual depletion of melting snowpack. Under unimpaired conditions, this hydrograph component was typified by a gradual decline in flow in years without early summer rains or other abrupt changes in ambient air temperature. Snowmelt was important for slowing the recession of flows into the summer low flow season. In snowmelt-dominated streams (Figure 2-20), the snowmelt recession limb is not a constant decline, but contains frequent but small rises and falls due to changes in ambient air temperature and/or late-spring thunderstorms.

2.6.4. Geomorphic, Riparian, and Fishery Linkages to Hydrograph Components

As discussed earlier, hydrologists often describe the intra-annual flow regime using average values, such as mean monthly flows. However, most geomorphic and ecological processes are dependent upon flows on a much smaller time scale, such as days or hours. Plotting daily average flows for each water year generates the average annual hydrograph, and this daily time-step usually provides enough flow detail to relate to geomorphic and ecological processes (Appendix A). A hydrograph component analysis of the unimpaired annual hydrographs is very useful to describe intra-annual flow variability, and when overlain with the life-history of key biota, provides the foundation for hypotheses and conceptual models for (1) how these species evolved and adapted to best survive under the unimpaired flow regime, and (2) how changes to the unimpaired flow regime through watershed development (e.g., flow regulation, river engineering) have impacted these species.

2.6.4.1. Summer-Fall Baseflows

Although summer baseflows are not large enough to exceed geomorphic process thresholds, they are important for riparian and fishery purposes. Historically, summer baseflows provided year-round habitat for native fish assemblages in the watershed upstream of Friant Dam (Table 2-4). Historic water temperatures downstream of Friant Dam were likely too high to support year-round rearing of juvenile salmonids or adult spring-run Chinook salmon (see Chapter 6), with the exception of the potential occurrence of artesian springs that may have provided local cold-water refugia. However, during fall baseflows beginning mid to late October, historic ambient air temperatures and corresponding water temperatures cooled, allowing fall-run Chinook salmon to migrate upstream during these low flows. Unimpaired fall baseflows ranged between 200 cfs and 400 cfs, providing sufficient flows to allow adult migration. The unimpaired shallow groundwater table was assumed to be increasing flows in the San Joaquin River in most reaches (see Chapter 4), such that established riparian vegetation was supported by both baseflows in the river and the shallow groundwater table. Under current conditions, the overdrafted groundwater table makes future summer baseflows very important for maintaining the shallow groundwater table and associated riparian vegetation.

2.6.4.2. Fall and Winter Floods

Fall and winter floods are nearly all rainfall or rain-on-snow generated events. While fall baseflows likely provided adequate passage flows for upstream adult Chinook salmon migration, the first fall storms may have improved passage by increasing water depths, lowering water temperatures, and providing a physiological queue for adult salmon to begin their upstream migration (Table 2-4). Perhaps the most important function of the fall and winter flood events was geomorphic work along the floodway. These floods were larger magnitude and thus initiated larger scale geomorphic processes (channel migration, channel avulsion, bar creation, bed scour, floodplain creation) than other hydrograph components (Table 2-4). Habitat was created and maintained by these floods. Riparian vegetation benefited by these floods as geomorphic surfaces and seedbeds were created (fine sediment deposited on floodplains, scour channels created on floodplains, meander cutoff, and oxbow creation).

2.6.4.3. Winter Baseflows

Between winter storms, flow tends to recede back to a baseflow level, but one that is considerably higher than the late summer-fall baseflow, and one that varies more day-to-day compared to summer-fall baseflows. Slow draining of the shallow groundwater table largely supports this baseflow, and because it is always higher magnitude than summer baseflows, it is important for allowing upstream migration of winter-run steelhead and juvenile rearing for all salmonid species (Table 2-4). Because of the low magnitude of winter baseflows, sand transport would have been the only geomorphic processes potentially provided by winter baseflows.

2.6.4.4. Snowmelt Runoff Peak

The timing of the snowmelt runoff peak coincided with important life history stages of several key species, and the longer duration of these flows compared to fall and winter floods provided important functions to several species. Spring-run and fall-run Chinook salmon smolts tended to outmigrate during this time; the increasing flows likely provided a behavioral queue for smolt outmigration, and the large magnitude of cold snowmelt runoff likely provided adequate water temperatures for successful outmigration in most years. The snowmelt peak in wetter years provided long-duration periods of overbank flow, which provided high quality rearing habitat for juvenile salmonids and other native species within the "deep-bodied fishes assemblage" (e.g., delta smelt, splittail per Moyle 2002) that inhabit aquatic habitats along the valley floor. The snowmelt runoff peak was often large enough to initiate some larger scale geomorphic processes (e.g., bed mobility, channel migration), while in drier years, the smaller snowmelt peak may only have transported sand (Table 2-4). The timing of the snowmelt runoff peak often corresponded to the peak of key riparian species seed distribution (e.g., Fremont cottonwood, black willow), such that the snowmelt runoff peak facilitated seed germination and seedling growth. During wetter years with larger peak flows, riparian vegetation also benefited by overbank flows, fine sediment deposition on floodplains, weed removal on floodplains, and seedbed creation.

Table 2-4. General hypothesized relationships between hydrograph components and ecosystem processes for the San Joaquin River.

Hydrograph component	Geomorphic-hydrologic processes	Riparian processes	Salmonid life-history processes
Summer-fall baseflows		Encourages late seeding riparian vegetation initiation and establishment within bankfull channel	Water temperature for over-summering salmonid juveniles and spring-run Chinook salmon adults, immigration for fall-run Chinook salmon adults
Fall and winter floods	Wetter years: channel avulsion, significant channel migration, bed scour and deposition, bed mobility, floodplain scour, floodplain inundation, fine sediment deposition on floodplains, large woody debris recruitment Normal years: Some channel migration, minor bed scour, bed mobility, floodplain inundation and fine sediment deposition	Wetter years: mature riparian removal within bankfull channel and portions of floodplain, scour of seedlings within bankfull channel, seedbed creation on floodplains for new cohort initiation, microtopography from floodplain scour and fine sediment deposition Normal years: scour of seedlings within bankfull channel, some fine sediment deposition on floodplains	Wetter years: partial loss of salmon cohort due to redd scour or entombment from deposition, improve spawning gravel quality by scouring/redepositing bed and transporting fine sediment, mortality by flushing fry and juveniles, mortality by stranding fry and juveniles on floodplains, reduce growth during periods of high turbidity, reduce predation during periods of high turbidity, creation and maintenance of high quality aquatic habitat Normal years: improve spawning gravel quality by mobilizing bed and transporting fine sediment, low mortality by flushing fry and juveniles, low mortality by stranding fry and juveniles on floodplains, reduce growth during periods of high turbidity, reduce predation during periods of high turbidity, maintenance of high quality aquatic habitat
Winter baseflows	Fine sediment transport		Increase habitat area in natural channel morphology, migration flows for winter-run steelhead
Snowmelt peak	Wetter years: bed mobility, long duration floodplain inundation, moderate channel migration, groundwater recharge Normal years: bed mobility, short duration floodplain inundation	Wetter years: riparian seedling scour within bankfull channel, riparian seedling initiation on floodplains, discourages riparian seedling initiation within bankfull channel Normal years: periodic riparian seedling initiation on floodplains	Wetter years: Increase juvenile salmonid growth rates by long-term floodplain inundation, increase stranding by inundating floodplains, stimulate smolt outmigration, reduce predation mortality by reducing smolt density and increasing turbidity Normal years: Increase juvenile growth rates by short-term floodplain inundation, increase stranding by short-term floodplain inundation, stimulate outmigration, reduce predation mortality by reducing smolt density and increasing turbidity Drier years: Increase smolt outmigration predation mortality by increasing density and reducing turbidity
Snowmelt recession	Gradual decrease in water stage, maintain floodplain soil moisture	Wetter years: Allow riparian seedling establishment on floodplains Normal and drier years: Discourages riparian seedling establishment on floodplains by desiccating them, encourage seedling establishment within bankfull channel	Wetter years: Increase smolt outmigration success by reducing water temperatures and extending outmigration period Normal years: Increase smolt outmigration success by reducing water temperatures and extending outmigration period Drier years: Increase smolt outmigration mortality by increasing water temperatures and shortening outmigration period

2.6.4.5. Snowmelt Recession Limb

As the water stage falls during the recession limb, it leaves behind moist, bare, mineral surfaces on point bars and other channel and floodplain surfaces on which seedlings of riparian plants can potentially establish (depending on timing of the recession limb relative to timing and mode of seed dispersal for different species). The rate of stage decline during this recession limb is also an important hydrologic variable, because if the water table in the gravel bar drops faster than the seedlings can extend their roots downward, they will not survive the summer and fall. This effect has been documented for cottonwoods in the Rocky Mountain region (e.g., Mahoney and Rood 1998). Presumably, similar controls exist along the San Joaquin River. Fall-run Chinook salmon smolts outmigrate during this period, while adult spring-run Chinook immigrate during this period.

2.6.5. Significance of Inter-Annual Flow Variations

The volume and pattern of runoff from the San Joaquin River varies widely between years (Figure 2-5); segregating annual hydrographs by water year classes is a useful tool to identify trends between years. Assessing this inter-annual variability can develop initial hypotheses for important ecosystem processes. For example, comparing annual water yield with recruitment success of Fremont cottonwood and narrow-leaf willow may illustrate that the cottonwood is more successful during wet years, and the narrow-leaf willow is more successful during drought years. From this casual observation, we can then change temporal scales by developing more focused hypotheses on what parts of wet or dry years cause this to occur. This example is expanded a bit below, discussing the role of wetter and drier water years to geomorphic processes, cottonwood regeneration and survival, and Chinook salmon life-history (Table 2-5).

2.6.5.1. Wetter Water Years

Wetter water years tend to have larger floods, larger snowmelt runoff peaks, later snowmelt peaks, longer snowmelt recession, and higher baseflows. Because of these higher flood flows, the larger scales of geomorphic work (channel avulsion, large sediment fluxes, etc.) tend to occur during wetter years. Cottonwood recruitment may also tend to occur during wetter water years because (1) high flood flows clear a space on floodplains for seeds to land and germinate, and (2) the long duration snowmelt hydrograph keeps the substrate wet where the seeds germinate and grow, thus enabling establishment and maturation. By overlaying cottonwood seed phenology over annual hydrographs, we find that cottonwoods tend to disperse their seeds during the snowmelt recession limb, and because wetter years have larger snowmelt runoff flows, the cottonwood seedlings tend to initiate on floodplains rather than in the low flow channel (because the low flow channel is underwater during seed dispersal, germination cannot occur there). Lastly, wetter water years may also tend to provide longer and colder flows during the Chinook salmon smolt outmigration period, increasing their outmigration success and overall productivity.

2.6.5.2. Drier Water Years

Drier water years tend to have smaller floods, smaller snowmelt runoff peaks, earlier snowmelt runoff peaks, shorter snowmelt recession, and smaller baseflows. Typically, the drier the water year, the less geomorphic work is accomplished by flows during that year. Flows during some dry years are insufficient to accomplish any significant geomorphic work. Riparian seedlings (particularly narrow-leaf willow) may tend to initiate along the summer baseflow channel margins because flows are lower during their seed dispersal period. These seedlings would normally be scoured away by the first high flows of a wetter year. However, sequences of drier water years may allow these seedlings and those

Table 2-5. Hypothesized relationships between water year classes and ecosystem processes for gravel-bed streams. Only three water year classes chosen to better illustrate the differences between water years.

Water year	**Hydrologic processes**	**Geomorphic processes**	**Ecological processes**
Extremely Wet	Large winter floods (much larger than bankfull), large snowmelt runoff peak (larger than bankfull), long duration snowmelt runoff that occurs later in season (June), higher summer and winter baseflows, lower water temperatures	Channel avulsion, channel migration, high bedload transport rates, bed scour, floodplain scour, prolonged floodplain inundation, large amount of fine sediment deposition on floodplains, new alluvial deposits formed	Scours seedlings along low flow channel margin, mature riparian vegetation removal, woody debris recruitment, recruit successful cottonwood cohort, greater migrational access to upstream habitat, salmonid redd scour/burial, high juvenile salmonid growth rates on floodplains, low salmonid outmigration mortality
Normal	Moderate winter floods (near or exceeds bankfull), moderate snowmelt runoff peak (smaller than bankfull), moderate summer and winter baseflows	Initiate channel migration, initiate bedload transport, short-term floodplain inundation, small amount of fine sediment deposition, alluvial deposits mobilized	Scours seedlings along low flow channel margin, minor woody debris recruitment, moderate salmonid migrational access to upstream habitat, low salmonid outmigration mortality
Critically Dry	Small winter floods (much below bankfull), minor snowmelt runoff peak, short duration snowmelt runoff that occurs early in season (April), higher water temperatures	No channel migration, some sand transported as bedload, no gravel transport, alluvial deposits not mobilized	Riparian vegetation initiates lower in channel, no riparian scour along channel margin, low salmonid migrational access to upstream habitat, moderate water temperature induced stress and mortality to salmonids, moderate salmonid outmigration mortality

of other more invasive species to mature, leading to riparian encroachment if a large flood does not soon follow to remove the encroaching vegetation.

In dry years, the (small) snowmelt peaks occurred earlier (typically May) and were shorter; in wet years the peaks were later (typically June) and longer. Many young salmon smolts would migrate seaward during these snowmelt flows, taking advantage of the strong downstream currents, cold temperatures, and turbidity (which made them less visible to predators). Similarly, spring-run Chinook salmon and other species migrated upstream as adults during this time period, taking advantage of predictable high flows to navigate shallow sections and otherwise difficult passage conditions. The impact of drier water years on Chinook salmon production may be variable; lower flood flows during egg incubation periods would reduce mortality caused by bed scour; however, lower flows during smolt outmigration increase temperature stress and predation as the smolts migrate down the San Joaquin River to the delta.

2.6.6. Hydrograph Component Analysis

The hydrograph component analysis focused on two USGS gages along the San Joaquin River corridor with lengthy periods of record available prior to, and after, construction of Friant Dam – the San Joaquin River below Friant (USGS 11-251000), and the San Joaquin River near Newman (USGS 11-274000) (Table 2-6). The Friant gage is ideally located at the upstream end of the study reach. Unimpaired daily average flows for the Friant gage is estimated (computed unimpaired) for the 1896-1951period from a model developed by former ACOE hydrologist Huxley Madeheim, using flow data from the Kings River at Piedra (USGS 11-222000); from water years 1952 to 1999 the unimpaired flows are computed by the USBR using actual flow data from the San Joaquin River and adjusting it for upstream storage changes and diversions. It is important to note that reservoir storage began upstream of Friant Dam in 1910, such that flow data measured prior to Friant Dam at the San Joaquin River at Friant gaging station does not represent unimpaired conditions, but rather minor impairment conditions (Table 2-2). This is one of several reasons why the hydrograph component analysis uses computed unimpaired flow data at Friant rather than USGS gaging data. Post-dam flow data for the San Joaquin River at Friant used actual flow data from the USGS gage for the period 1950 to 2000.

The San Joaquin River near Newman gage is located below the confluence with the Merced River, and includes a portion of the runoff from the Merced River, as well as contributions from the Fresno River, Chowchilla River, and other small streams that join the San Joaquin River between Friant and Newman. Computed unimpaired flow data were not available at the Newman gage, so the actual flow data from 1914-1942 were used (a period which is about 8% drier than the long term (1910-2000) average runoff at Friant). Selection of this data assumes that significant regulation by Friant Dam (and associated diversion canals) began in 1950, whereas minor impairments prior to completion Friant Dam in 1942 were not considered as significant. Flow regulation by prior to Friant Dam was most significant during the summer baseflow period, when riparian diversions into canals caused the most proportional reduction in flows in the San Joaquin River. The regulated period of record used data from the Newman gage for 1967-2001, which included regulation by both Friant Dam and New Exchequer Dam on the Merced River.

The San Joaquin River at Fremont Ford gaging station would have been a more ideal location at the downstream end of the study reach (above the Merced River confluence), but the period of record (1938-1989) was inadequate for the pre- and post-Friant Dam comparison. Additional USGS data were available for the San Joaquin River at Dos Palos (1941-1954), El Nido (1940-1949), and Mendota (1940-1954), but these data were not extensive enough for analysis of hydrograph components.

Table 2-6. Summary of selected streamflow gaging stations used for Hydrograph Component Analysis.

Gaging station name and USGS or CDEC I.D. (from Table 2-1)	Period of record	Drainage Area (mi^2)	Average annual water yield (AF)
San Joaquin River below Friant, CA. USGS: 11-251000	1896-1999 (modeled unimpaired)	1,676	1,828,000
San Joaquin River below Friant, CA. USGS: 11-251000	1950-2000 (post-Friant Dam)		538,000
San Joaquin River near Newman, CA. USGS: 11-274000	1914-1942 (pre-Friant Dam)	9,520	1,866,000
San Joaquin River near Newman, CA. USGS: 11-274000	1967-2001 (post-Friant Dam, post-New Exchequer Dam)		1,537,000

2.6.6.1. Methods

Our hydrograph component analysis for the two gaging stations listed in Table 2-6 used the following procedure:

- The unimpaired annual water yield (runoff volume in acre-feet) was computed for each water year between 1896 and 1999, then plotted as a cumulative distribution curve by ranking the annual yield (Figure 2-5).
- The cumulative distribution curve was then divided symmetrically into five equally weighted classes separated by annual exceedance probabilities (p) of 0.80, 0.60, 0.40, and 0.20, and the five water year classes were named “Extremely Wet,” “Wet,” “Normal,” “Dry,” and “Critically Dry,” respectively. This classification system addresses the range of variability in the annual water yield and provides an equal probability for each class that a given water year will fall into that category (equally distributed around the mean), which in turn allows for simpler interpretation of comparisons between water year types.
- Based on the computed unimpaired water yield at the Friant gage, the annual water yields for both pre-and post-Friant Dam periods were grouped into the five water year classes. For example, if water year 1965 computed unimpaired runoff at Friant was classified as a “Wet” year, then the regulated runoff was also classified as a “Wet” water year. Then, to highlight the true annual flow variability, a single representative annual hydrograph for that water year class was overlaid on the average annual hydrograph for that water year class.
- Based on the patterns exhibited by the annual hydrographs and the range of their occurrence, the following hydrograph components were delineated (Figure 2-20):
- Fall Baseflows, October 1 – December 20
- Fall Floods, October 1 – December 20
- Winter Baseflows, December 21 – March 20
- Winter Floods, December 21 – March 20
- Snowmelt Floods, March 21 – June 21
- Snowmelt Recession, variable based on peak snowmelt flood
- Summer Baseflows, July 15 – September 30

After each hydrograph component was assigned a period of occurrence, all water years for each water year type were grouped, and statistical parameters (e.g., median, maxima, minima) were computed for each hydrograph component. This analysis was performed for the unimpaired and regulated periods of record for the two gaging stations listed in Table 2-6, to allow for a comparison of how each hydrograph component was affected as a result of streamflow regulation. The dates for each component were chosen to provide a discrete period for analyses that are comparable for each gaging record and water year, but do not necessarily capture all the variability in the duration of the component.

The results of the Hydrograph Component Analysis for the San Joaquin River at Friant gage are summarized in Table 2-7 (computed unimpaired) and Table 2-8 (Post-Friant Dam), and for the San Joaquin River near Newman gage in Table 2-9 (Pre-Friant Dam) and Table 2-10 (Post-Friant Dam and Post New Exchequer Dam). Following the summary tables, we include all the hydrologic information we used for the Hydrograph Component Analysis at each gage, including (1) table of annual water yields, exceedance probability, and water year classification, (2) bar chart of annual water yield, and (3) frequency distribution of annual water yield, (4) average and representative hydrographs, and (5) annual hydrograph for each year of record used in the analyses. The following sections discuss the results of our Hydrograph Component Analysis for each gaging record. The summary is not meant to report all the hydrograph components for each of the periods of record analyzed, nor to provide comparisons among the different rivers, but is instead intended to summarize the salient components and the major changes that have occurred at each location.

2.6.6.2. San Joaquin River below Friant

The San Joaquin River below Friant gaging record was analyzed for the period 1896-1999, and separated into an unimpaired record (1896-1999) and a post-dam regulated period (1950–2000). Based on analyzing water yield between the two data sets, the average annual water yield was reduced from 1,812,000 acre-ft to 528,000 acre-ft, a 71% reduction in yield. More than half the regulated runoff years analyzed had annual yield less than 125,000 acre-ft, which is approximately 7% of the average unimpaired water yield. The following discussion highlights several key differences between the modeled unimpaired hydrograph components and the regulated post-Friant Dam components. In addition to the hydrograph component summary in Tables 2-7 and 2-8, Figures 2-21 through 2-25 illustrate (1) the average annual hydrograph for a given water year class, (2) an example representative unimpaired hydrograph for that given water year class, and (3) the corresponding representative regulated hydrograph for that given water year class.

2.6.6.2.1. Summer, Fall, and Winter Baseflows

- Unimpaired summer baseflows generally varied as a function of the duration of the snowmelt recession and the water year type (i.e., the wetter the year and consequently the longer the snowmelt recession, the higher were the subsequent summer baseflows). Median summer baseflows ranged from approximately 200 cfs in Critically Dry years, to above 1,000 cfs during Extremely Wet years. During Extremely Wet years the snowmelt hydrograph descending limb extended nearly to the end of August, and remained above 1,000 cfs in August for nearly all Extremely Wet years. The September baseflows during Extremely Wet years typically remained above 500 cfs. Under regulated conditions, summer/fall baseflows have been reduced to the minimum flow releases required to meet downstream water deliveries. Median summer baseflows ranged from 135-245 cfs. Minimum summer baseflows generally remained above 75 cfs, during dryer water year types; maximum summer baseflows approached flows typical of unimpaired conditions, suggesting Friant dam has less effect on summer flow releases during wetter water year types because of its relatively smaller storage capacity.

Table 2-7. Summary of Hydrograph Components for the San Joaquin River near Friant for unimpaired conditions (USBR and modeled unimpaired flows from Hux Madeheim) for water years 1896-1999.

	WATER YEAR TYPE					
Hydrograph Component	***Extremely Wet***	***Wet***	***Normal***	***Dry***	***Critically Dry***	***All Water Years***
Probabilty of Exceedence	*20%*	*40%*	*60%*	*80%*	*100%*	
Number of Water Years	20	21	21	21	21	104
Average Daily Flow (cfs)	4,597 cfs	3,022 cfs	2,307 cfs	1,635 cfs	1,063 cfs	2,505 cfs
Average Annual Yield (af)	3,328,190 ac-ft	2,187,744 ac-ft	1,670,032 ac-ft	1,183,424 ac-ft	769,731 ac-ft	1,812,000 ac-ft
Maximum Annual Yield (af)	4,641,537 ac-ft	2,672,303 ac-ft	1,936,172 ac-ft	1,321,069 ac-ft	949,591 ac-ft	2,304,134 ac-ft
Minimum Annual Yield (af)	2,755,032 ac-ft	1,945,119 ac-ft	1,326,827 ac-ft	1,026,184 ac-ft	361,178 ac-ft	1,482,868 ac-ft
Fall Baseflows (Oct 1 - Dec 20)						
Median	380 cfs	318 cfs	432 cfs	295 cfs	274 cfs	340 cfs
Minimum	115 cfs	114 cfs	194 cfs	97 cfs	100 cfs	124 cfs
Maximum	1,705 cfs	1,547 cfs	895 cfs	666 cfs	610 cfs	1,085 cfs
Fall Floods (Oct 1 - Dec 20)						
Median Peak Magnitude	2,118 cfs	2,368 cfs	2,066 cfs	1,315 cfs	909 cfs	2,066 cfs
Maximum	45,728 cfs	19,677 cfs	42,352 cfs	11,734 cfs	8,294 cfs	45,728 cfs
Winter Baseflows (Dec 21 - Mar 20)						
Median	1,712 cfs	875 cfs	564 cfs	450 cfs	310 cfs	782 cfs
Minimum	989 cfs	160 cfs	200 cfs	250 cfs	154 cfs	350 cfs
Maximum	3,202 cfs	1,975 cfs	1,512 cfs	867 cfs	627 cfs	1,637 cfs
Winter Floods (Dec 21 - Mar 20)						
Average Peak Magnitude	31,256 cfs	15,560 cfs	9,719 cfs	6,655 cfs	3,797 cfs	13,397 cfs
Median Peak Magnitude	28,345 cfs	12,822 cfs	8,489 cfs	5,734 cfs	3,735 cfs	11,825 cfs
Minimum	11,248 cfs	6,407 cfs	3,548 cfs	2,078 cfs	1,486 cfs	4,953 cfs
Maximum	77,467 cfs	40,982 cfs	23,908 cfs	27,292 cfs	7,928 cfs	35,515 cfs
Snowmelt Floods (Mar 21 - June 21)						
Average Peak Magnitude	18,925 cfs	15,361 cfs	12,162 cfs	9,640 cfs	5,942 cfs	12,406 cfs
Median Peak Magnitude	19,275 cfs	14,467 cfs	11,740 cfs	9,641 cfs	5,742 cfs	12,173 cfs
Minimum	11,645 cfs	10,512 cfs	8,583 cfs	6,635 cfs	3,549 cfs	8,185 cfs
Maximum	25,316 cfs	32,217 cfs	16,941 cfs	13,986 cfs	10,092 cfs	19,711 cfs
Snowmelt Recession						
Median Date of Peak	31-May	23-May	27-May	19-May	12-May	22-May
Earliest Peak	28-Apr	26-Apr	6-May	25-Apr	22-Apr	27-Apr
Latest Peak	21-Jun	30-Jun	13-Jun	15-Jun	16-Jun	19-Jun
Summer Baseflows (July 15 - Sep 30)						
Baseflow Median	1,013 cfs	583 cfs	389 cfs	284 cfs	212 cfs	496 cfs
Minimum	453 cfs	302 cfs	200 cfs	133 cfs	114 cfs	241 cfs
Maximum	2,105 cfs	1,049 cfs	582 cfs	664 cfs	584 cfs	997 cfs

Daily Average Discharge	=	2,505 cfs
Total Annual Runoff	=	1,812,000 ac-ft

Annual Maximum Flood Frequency		***Unimpaired***	***Regulated***
$Q_{1.5}$	=	10,227 cfs	850 cfs
Q_{5}	=	26,195 cfs	6,749 cfs
Q_{10}	=	36,758 cfs	13,644 cfs
Q_{25}	=	53,000 cfs	28,727 cfs

Table 2-8. Summary of Hydrograph Components for the San Joaquin River near Friant for post-Friant regulated conditions (USGS data) for water years 1950-2000.

	WATER YEAR TYPE					
Hydrograph Component	**Extremely Wet**	**Wet**	**Normal**	**Dry**	**Critically Dry**	**All Water Years**
Probabilty of Exceedence	20%	40%	60%	80%	100%	
Number of Water Years	10	10	10	10	11	51
Average Daily Flow (cfs)	2,345 cfs	950 cfs	208 cfs	121 cfs	88 cfs	730 cfs
Average Annual Yield (af)	1,697,624 ac-ft	687,662 ac-ft	150,839 ac-ft	87,888 ac-ft	63,570 ac-ft	528,224 ac-ft
Maximum Annual Yield (af)	3,174,569 ac-ft	1,180,140 ac-ft	262,264 ac-ft	99,816 ac-ft	75,116 ac-ft	3,174,569 ac-ft
Minimum Annual Yield (af)	1,187,252 ac-ft	285,118 ac-ft	104,426 ac-ft	79,474 ac-ft	48,424 ac-ft	48,424 ac-ft
Fall Baseflows (Oct 1 - Dec 20)						
Median	117 cfs	105 cfs	127 cfs	81 cfs	62 cfs	105 cfs
Minimum	52 cfs	71 cfs	54 cfs	44 cfs	36 cfs	36 cfs
Maximum	480 cfs	1,050 cfs	495 cfs	125 cfs	87 cfs	1,050 cfs
Fall Floods (Oct 1 - Dec 20)						
Median Peak Magnitude	299 cfs	196 cfs	194 cfs	126 cfs	93 cfs	194 cfs
Maximum	5,020 cfs	3,130 cfs	1,020 cfs	693 cfs	120 cfs	5,020 cfs
Winter Baseflows (Dec 21 - Mar 20)						
Median	1,095 cfs	65 cfs	86 cfs	54 cfs	36 cfs	65 cfs
Minimum	49 cfs	52 cfs	56 cfs	26 cfs	24 cfs	24 cfs
Maximum	5,720 cfs	110 cfs	173 cfs	71 cfs	61 cfs	5,720 cfs
Winter Floods (Dec 21 - Mar 20)						
Average Peak Magnitude	10,313 cfs	5,777 cfs	684 cfs	361 cfs	165 cfs	3,460 cfs
Median Peak Magnitude	7,985 cfs	4,900 cfs	711 cfs	172 cfs	117 cfs	711 cfs
Minimum	4,030 cfs	936 cfs	146 cfs	106 cfs	66 cfs	66 cfs
Maximum	36,800 cfs	14,900 cfs	1,380 cfs	1,950 cfs	580 cfs	36,800 cfs
Snowmelt Floods (Mar 21 - June 21)						
Average Peak Magnitude	7,320 cfs	4,212 cfs	888 cfs	418 cfs	183 cfs	2,604 cfs
Median Peak Magnitude	7,960 cfs	3,890 cfs	583 cfs	229 cfs	171 cfs	583 cfs
Minimum	291 cfs	168 cfs	198 cfs	121 cfs	136 cfs	121 cfs
Maximum	12,400 cfs	8,080 cfs	2,370 cfs	2,110 cfs	217 cfs	12,400 cfs
Snowmelt Recession						
Median Date of Peak	8-Jun	8-May	18-Jun	5-Jul	10-Jul	15-Jun
Earliest Peak	26-Apr	21-Apr	20-May	1-May	25-Apr	30-Apr
Latest Peak	12-Jul	4-Jul	15-Aug	11-Aug	17-Aug	30-Jul
Summer Baseflows (July 15 - Sep 30)						
Baseflow Median	245 cfs	148 cfs	175 cfs	162 cfs	135 cfs	162 cfs
Minimum	76 cfs	86 cfs	107 cfs	82 cfs	90 cfs	76 cfs
Maximum	2,090 cfs	1,750 cfs	267 cfs	201 cfs	144 cfs	2,090 cfs

Daily Average Discharge	=	730 cfs	
Total Annual Runoff	=	528,224 ac-ft	
Annual Maximum Flood Frequency		***Unimpaired***	***Regulated***
$Q_{1.5}$	=	10,187 cfs	771 cfs
Q_5	=	25,177 cfs	5,885 cfs
Q_{10}	=	35,111 cfs	11,922 cfs
Q_{25}	=	50,650 cfs	25,379 cfs

Table 2-9. Summary of Hydrograph Components for the San Joaquin River near Newman for unimpaired conditions (USGS data) for water years 1912-1942.

	WATER YEAR TYPE					
Hydrograph Component Probabilty of Exceedence	**Extremely Wet** 20%	**Wet** 40%	**Normal** 60%	**Dry** 80%	**Critically Dry** 100%	**All Water Years**
Number of Water Years	6	6	6	6	6	
Average Daily Flow (cfs)	5,920	3,243	2,233	1,114	377	2,577
Average Annual Yield (af)	4,285,758	2,347,746	1,616,433	806,555	273,157	1,868,153
Maximum Annual Yield (af)	6,257,161	2,759,183	1,780,792	1,108,268	390,522	
Minimum Annual Yield (af)	2,929,807	1,959,896	1,361,260	453,271	141,808	
Fall Baseflows (Oct 1 - Dec 20)						
Median	204	275	143	300	187	222
Minimum	86	120	81	103	60	90
Maximum	450	484	1,030	955	458	675
Fall Floods (Oct 1 - Dec 20)						
Median Peak Magnitude	940	1,155	966	1,275	300	927
Maximum	4,840	6,000	3,700	1,910	870	3,464
Winter Baseflows (Dec 21 - Mar 20)						
Median	2,850	1,325	1,480	713	421	1,358
Minimum	735	540	222	305	231	407
Maximum	3,970	1,910	3,120	1,180	970	2,230
Winter Floods (Dec 21 - Mar 20)						
Average Peak Magnitude	19,577	11,740	7,837	4,125	1,138	8,883
Median Peak Magnitude	19,450	12,000	8,050	3,505	838	8,769
Minimum	8,260	7,140	3,660	2,240	560	4,372
Maximum	33,000	14,600	13,400	6,520	2,240	13,952
Snowmelt Floods (Mar 21 - June 21)						
Average Peak Magnitude	16,583	12,133	9,190	5,252	1,328	8,897
Median Peak Magnitude	15,600	11,750	8,985	5,540	675	8,510
Minimum	12,000	8,600	7,200	1,570	227	5,919
Maximum	25,200	15,200	12,600	8,900	4,280	13,236
Snowmelt Recession						
Median Date of Peak	5-Jun	29-May	24-May	8-May	6-May	20-May
Earliest Peak	21-Mar	4-Apr	21-Mar	31-Mar	22-Mar	26-Mar
Latest Peak	17-Jun	21-Jun	13-Jun	21-Jun	3-Jun	15-Jun
Summer Baseflows (July 15 - Sep 30)						
Baseflow Median	720	352	251	214	105	328
Minimum	353	260	84	92	23	162
Maximum	1,045	450	467	315	200	495

Daily Average Discharge	2,577
Total Annual Runoff	1,868,153

Table 2-10 Summary of Hydrograph Components for the San Joaquin River near Newman for post-Friant and post-New Exchequer regulated conditions (USGS data) for water years 1967-2001.

Hydrograph Component	WATER YEAR TYPE					
	Extremely Wet	Wet	Normal	Dry	Critically Dry	Average
Probabilty of Exceedence	20%	40%	60%	80%	100%	
Number of Water Years	7	7	7	7	7	
Average Daily Flow (cfs)	5,898	2,504	1,144	656	415	2,124
Average Annual Yield (af)	4,270,314	1,813,004	827,999	474,705	300,744	1,537,365
Maximum Annual Yield (af)	8,413,250	2,390,894	925,537	568,721	395,665	
Minimum Annual Yield (af)	2,470,020	955,928	577,676	413,343	182,221	
Fall Baseflows (Oct 1 - Dec 20)						
Median	630	1,110	901	767	414	764
Minimum	83	266	308	523	270	290
Maximum	2,930	5,700	1,370	875	574	2,290
Fall Floods (Oct 1 - Dec 20)						
Median Peak Magnitude	1,050	2,370	1,510	1,550	691	1,434
Maximum	11,600	10,100	2,360	2,130	996	5,437
Winter Baseflows (Dec 21 - Mar 20)						
Median	570	984	887	791	520	750
Minimum	293	438	532	626	208	419
Maximum	9,050	2,040	1,190	864	683	2,765
Winter Floods (Dec 21 - Mar 20)						
Average Peak Magnitude	24,300	9,793	5,221	1,821	1,189	8,465
Median Peak Magnitude	23,300	6,570	4,630	1,840	1,010	7,470
Minimum	13,100	3,650	1,380	850	661	3,928
Maximum	36,000	23,000	10,900	2,740	2,310	14,990
Snowmelt Floods (Mar 21 - June 21)						
Average Peak Magnitude	15,016	9,534	2,950	1,236	946	5,936
Median Peak Magnitude	15,500	6,190	3,280	1,070	875	5,383
Minimum	2,210	1,180	1,330	747	299	1,153
Maximum	24,900	20,200	3,720	2,180	2,010	10,602
Snowmelt Recession						
Median Date of Peak	28-Mar	23-Mar	29-Mar	12-Apr	28-Mar	30-Mar
Earliest Peak	21-Mar	21-Mar	21-Mar	21-Mar	21-Mar	21-Mar
Latest Peak	11-Jun	27-Apr	25-Apr	9-May	30-May	14-May
Summer Baseflows (July 15 - Sep 30)						
Baseflow Median	1,165	657	508	365	264	592
Minimum	410	360	415	251	50	297
Maximum	3,440	1,160	908	517	415	1,288

Daily Average Discharge	2,124
Total Annual Runoff	1,537,365

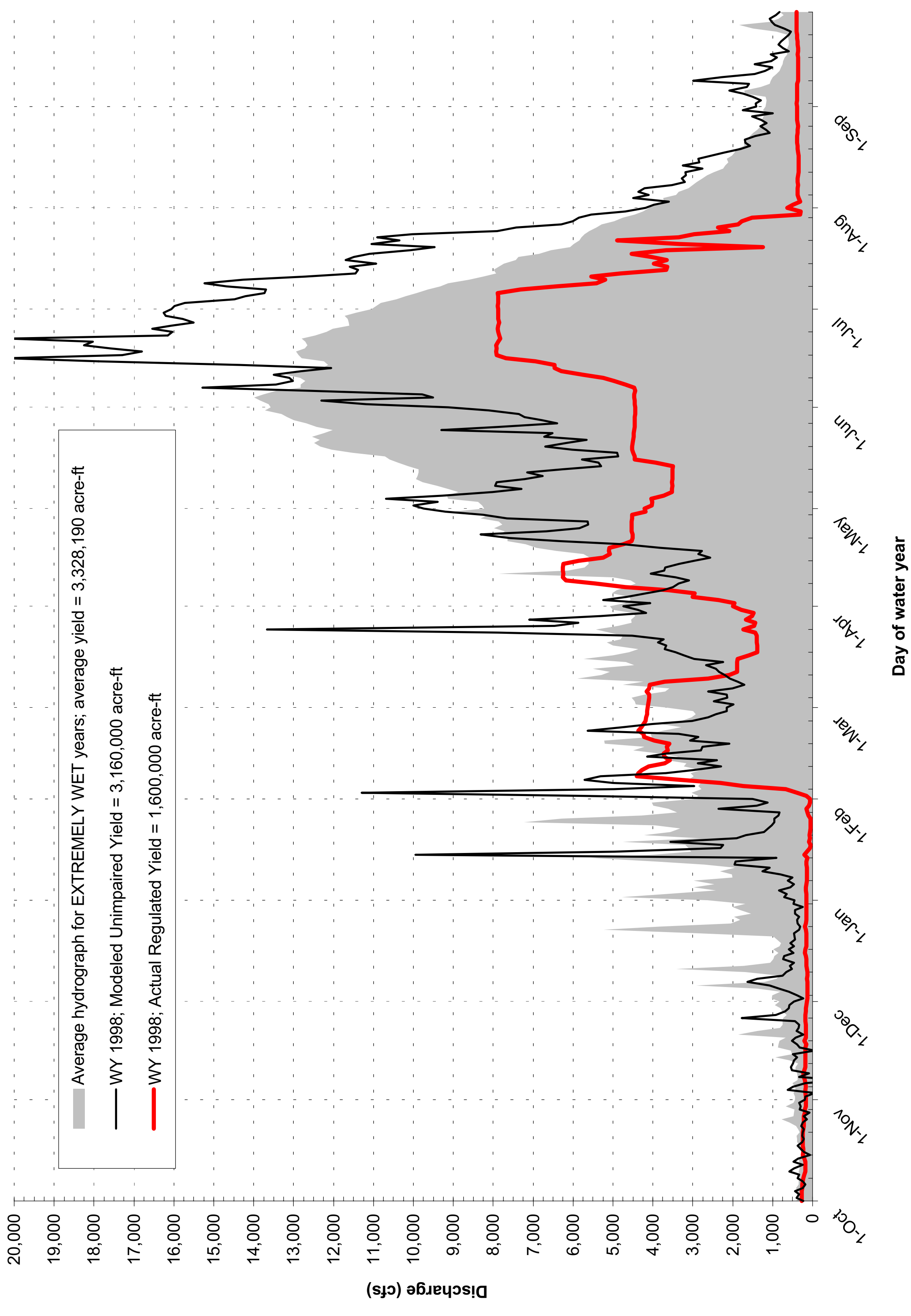

Figure 2-21. Average annual unimpaired hydrograph for an Extremely Wet water year at the San Joaquin River at Friant gaging station. A representative Extremely Wet water year hydrograph (1998) for unimpaired and post-Friant Dam conditions is included.

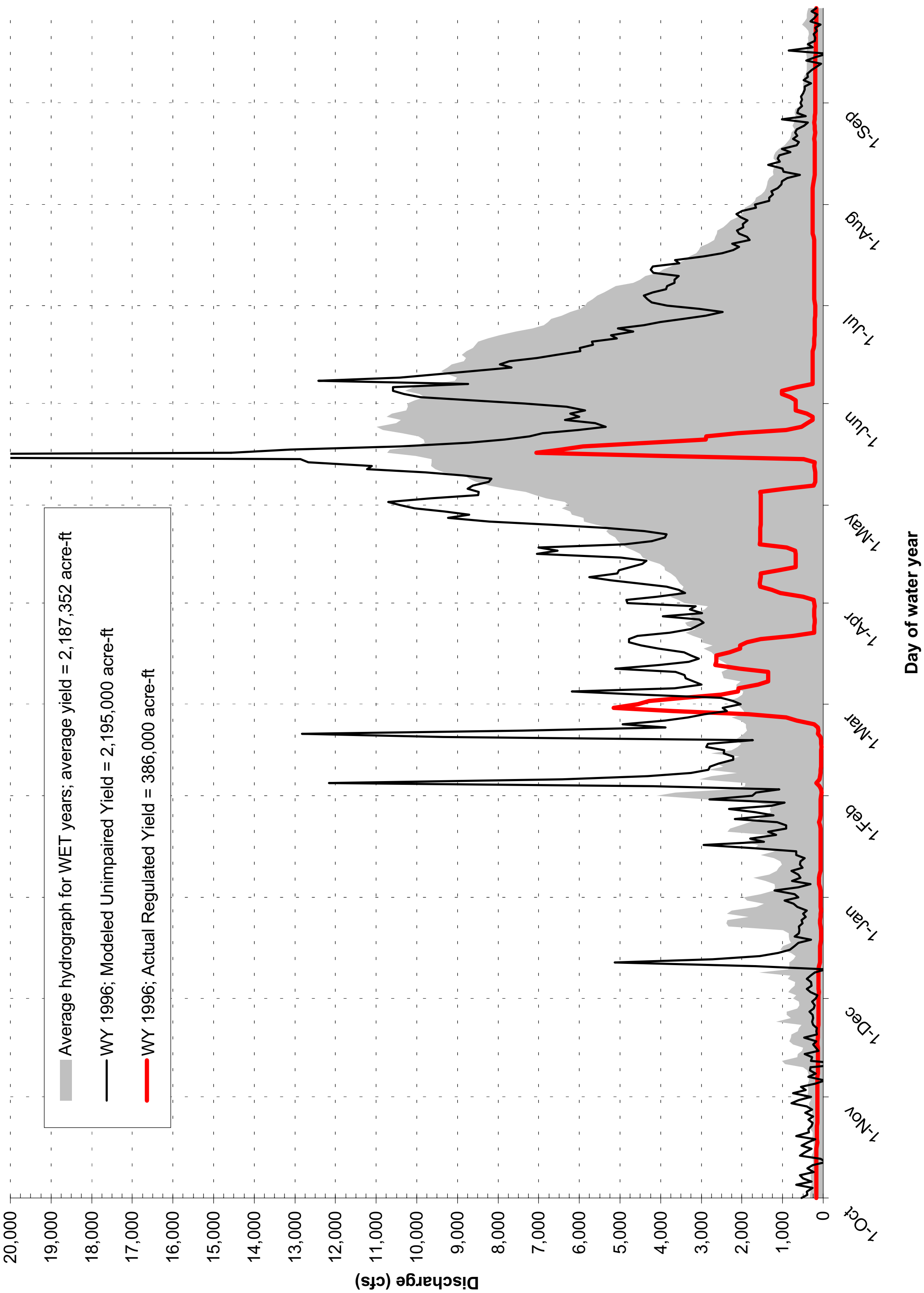

Figure 2-22. Average annual unimpaired hydrograph for a Wet water year at the San Joaquin River at Friant gaging station. A representative Wet water year hydrograph (1996) for unimpaired and post-Friant Dam conditions is included.

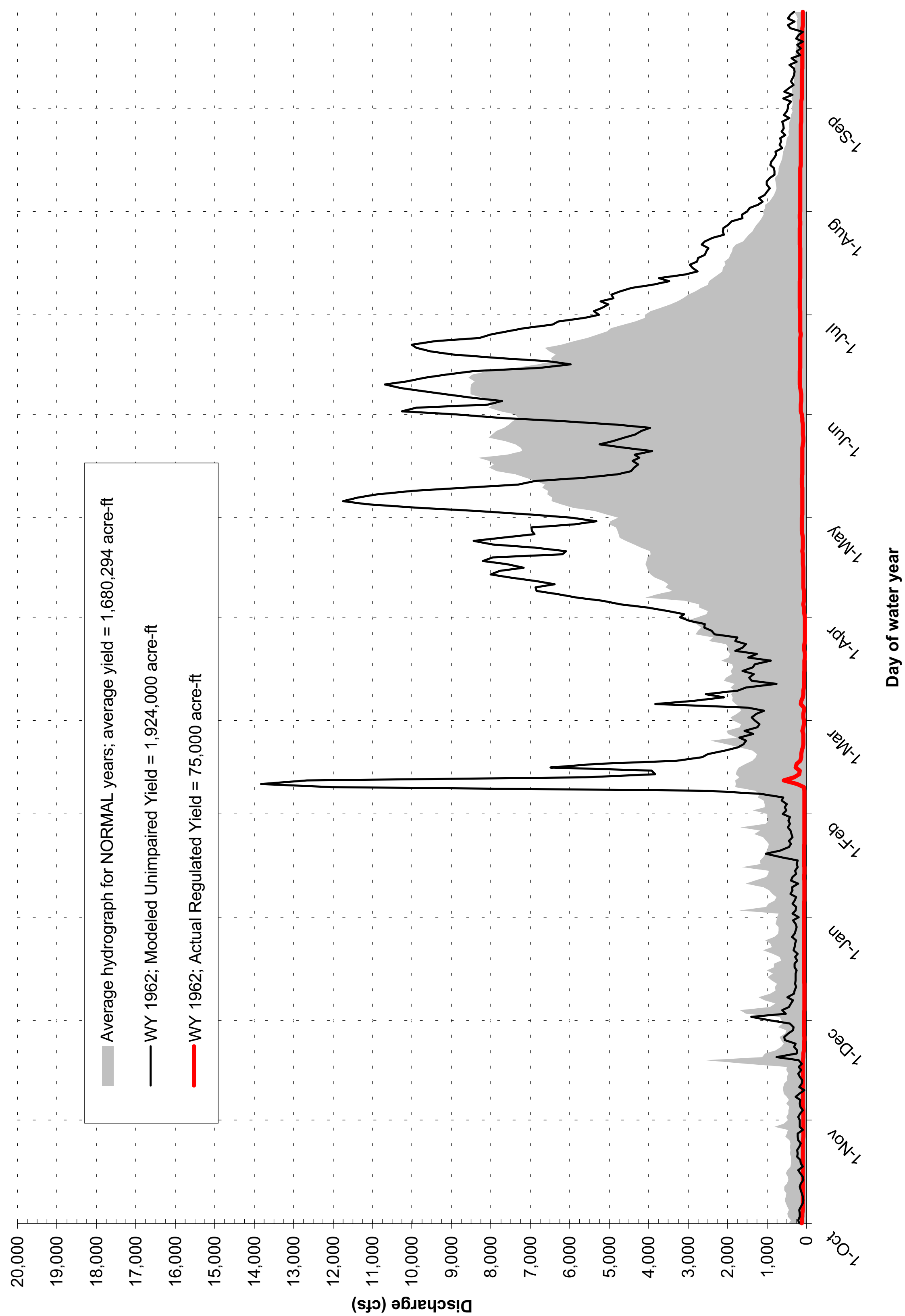

Figure 2-23. Average annual unimpaired hydrograph for a Normal water year at the San Joaquin River at Friant gaging station. A representative Normal water year hydrograph (1962) for unimpaired and post-Friant Dam conditions is included.

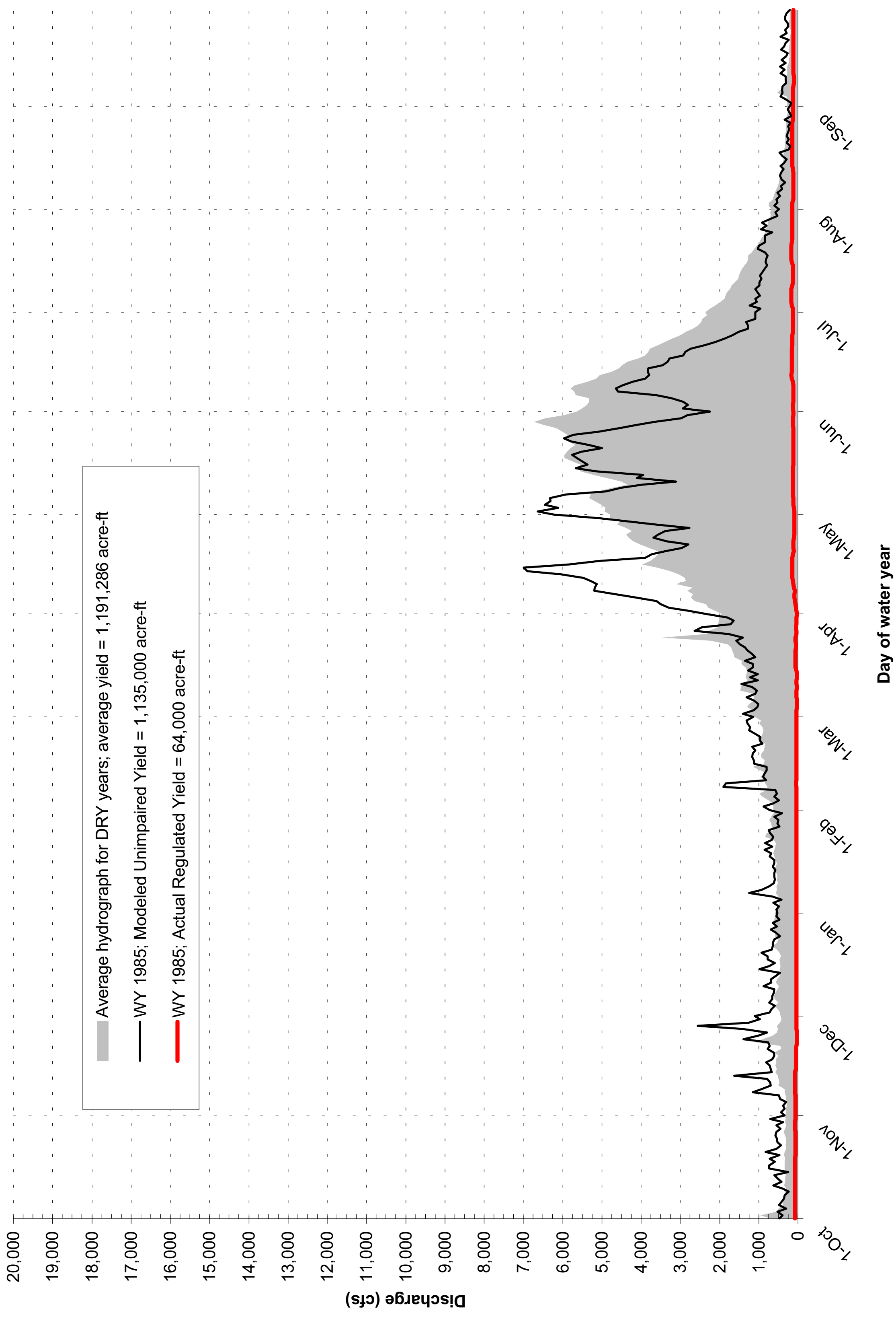

Figure 2-24. Average annual unimpaired hydrograph for a Dry water year at the San Joaquin River at Friant gaging station. A representative Dry water year hydrograph (1985) for unimpaired and post-Friant Dam conditions is included.

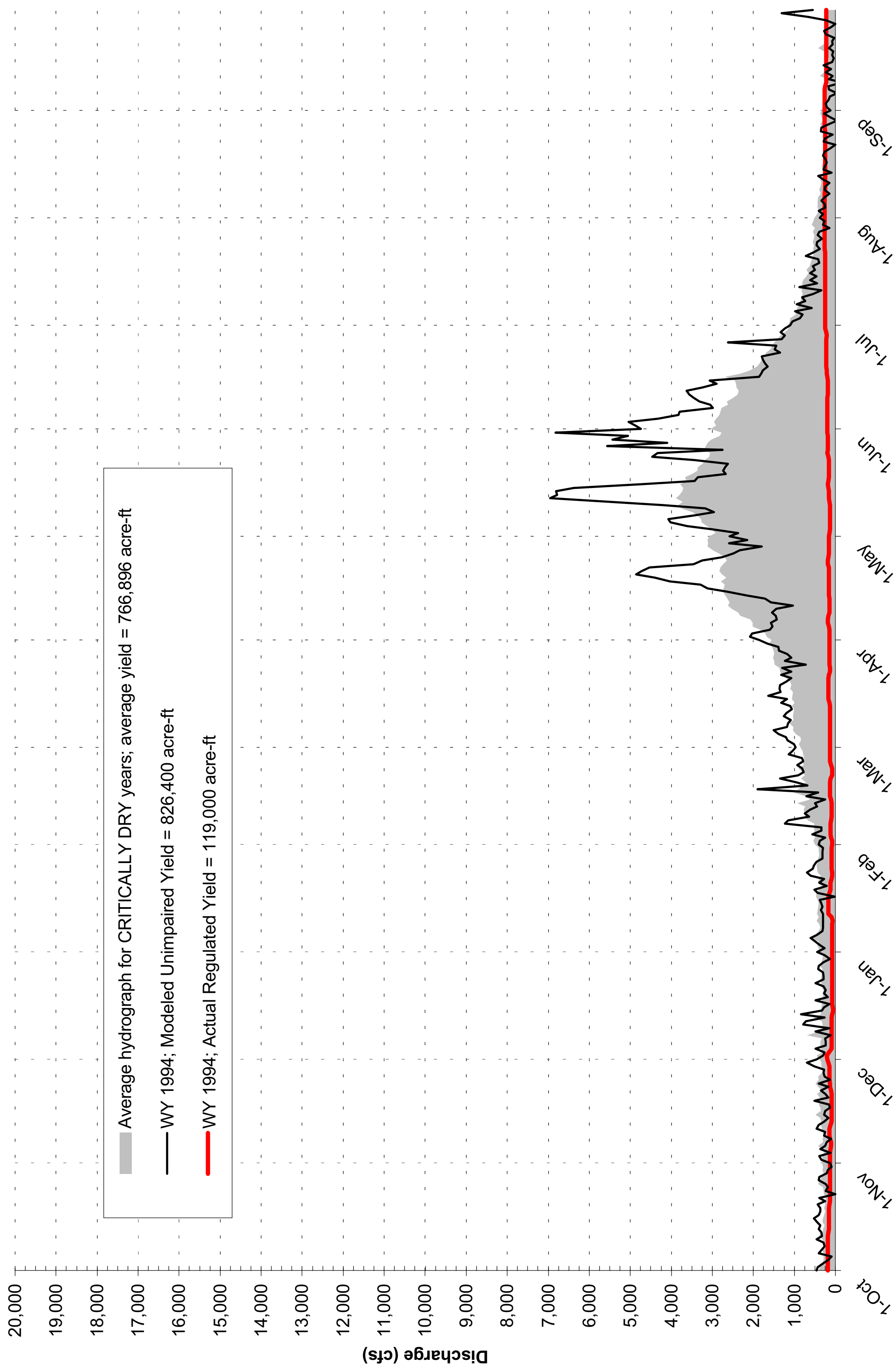

Figure 2-25. Average annual unimpaired hydrograph for a Critically Dry water year at the San Joaquin River at Friant gaging station. A representative Critically Dry water year hydrograph (1994) for unimpaired and post-Friant Dam conditions is included.

- Unimpaired fall baseflows also varied as a function of the water year type, and ranged from 274-380 cfs in Critically Dry and Extremely Wet years, respectively. Wet and Extremely Wet year fall baseflows occasionally exceeded 1,000 cfs, whereas minimum fall baseflows were often as low as 100 cfs. Under regulated conditions, fall baseflows have been reduced to the minimum flow releases required to meet downstream water deliveries, until the irrigation season ended and fall baseflow releases were reduced to increase reservoir storage. Median summer/fall baseflows ranged from 36-71 cfs during Critically Dry and Wet years, respectively. The flow release requirements for irrigation water delivery appear to have sustained higher summer baseflows than fall baseflows. Occasionally, Wet and Extremely Wet fall baseflow maxima exceeded 4,000 cfs, which likely resulted from flow releases to vacate flood storage space in Millerton Reservoir during wet water year conditions.
- Median winter baseflows ranged from 310-1,700 cfs under unimpaired conditions, and were reduced significantly more than summer/fall baseflows by regulation from Friant Dam. Median winter baseflows under regulated conditions were less than 300 cfs more than 80% of the days, but were conversely extremely high during Extremely Wet water years, with median flows exceeding 5,000 cfs. Critically Dry year minima frequently reached as low as 33 cfs. The larger winter flow releases were also likely due to the small flood storage space available in Millerton Reservoir and the consequent need to spill large volumes of water during wet winters.
- Two distinct periods of record – from April 1974 to November 1978 (1,332 days), and from April 1986 to October 1993 (2,350 days) – were particularly dry. Compared to the unimpaired winter baseflow daily average flow of approximately 2,500 cfs, these two periods reported daily average flows of 100 cfs and 125 cfs, respectively, with maximum flows for these entire periods of only 236 and 313 cfs, respectively.

2.6.6.2.2. Fall and Winter Floods

- Fall rainstorms and the consequent floods they caused were generally the first floods of the runoff season, and were thus generally smaller in magnitude than floods occurring between December and March. Median unimpaired fall floods ranged from 900-2,300 cfs during Critically Dry and Wet years respectively. These early-season fall storms were essentially eliminated in Critically Dry, Dry, and Normal water year types, and appear to have been largely unaffected in Wet and Extremely Wet years. The largest floods of record generally occurred earlier in December to March when early cold snowstorms were followed by warm tropical rains that resulted in a rain-on-snow flood event. This scenario occurred most recently during the January 1997 flood (ACOE 1999). In the unimpaired period of record, the flood of record occurred on December 11, 1937, and was thus categorized as a Fall Storm. The maximum daily average discharge of this flood was 45,000 cfs, with an instantaneous peak discharge of 77,200 cfs and recurrence interval of 32 years.
- Most other flood events were categorized as winter floods. The hydrograph component analysis evaluates the daily average maxima, whereas the flood frequency analysis (Section 2.6.2) evaluates the annual instantaneous maxima. Median daily average unimpaired winter storms ranged from 3,700-28,000 cfs during Critically Dry and Extremely Wet years, respectively. Under regulated conditions, winter floods were eliminated during Critically Dry, Dry, and Normal water year types, and were reduced to 4,000-10,000 cfs during Wet and Extremely Wet water year types. Several winter floods during the unimpaired period of record exceeded 30,000 cfs, but only one winter flood exceeded 15,000 cfs since construction of Friant Dam: the flood of January 1997 with measured instantaneous peak discharge below Friant of 60,300 cfs. The unimpaired peak magnitude of this flood, measured as peak hourly inflow into Millerton Lake, was 95,000 cfs (ACOE 1999).

2.6.6.2.3. Snowmelt Peak and Recession Limb

- The snowmelt hydrograph component contains the largest portion of the total annual runoff, and is consequently affected most severely by regulation. Under unimpaired conditions, the median snowmelt floods ranged from 5,700-19,000 cfs, during Critically Dry and Extremely Wet water years, respectively. These snowmelt peaks had a duration lasting up to several weeks, and corresponding recession limbs lasted several months. The recession limb lasted through August in most years, and lasted into September in wetter years. Several unimpaired snowmelt flood peaks exceeded 20,000 cfs as a daily average maximum. The minimum unimpaired snowmelt flood magnitude during Critically Dry years still exceeded 3,500 cfs.
- The snowmelt hydrograph component was virtually eliminated in all water year types. Computation of the median spring peak runoff showed that the peak flow for Normal, Dry, and Critically Dry water year types did not exceed 800 cfs, which is not truly a flood peak, but is merely a sustained baseflow throughout the snowmelt period. Wet and Extremely Wet years had substantially reduced snowmelt floods ranging from 1,700-5,000 cfs, respectively.

2.6.6.3. San Joaquin River near Newman

The gaging station on the San Joaquin River near Newman records the volume of flow from the San Joaquin River, a portion of the Merced River, and other tributary inflows such as Cottonwood Creek, the Fresno River, Fresno Slough, the Kings River, and the Chowchilla River. Prior to construction of Friant Dam, streamflow regulation occurred on many of these tributaries, and as such, flows recorded near Newman for the period of record prior to Friant Dam are considered "partially regulated." In addition, natural hydrologic processes, such as groundwater accretion, storage of floodwaters on floodplains, contributions of shallow groundwater to surface flow, and anthropogenic processes resulting from irrigation diversion and return flows, all cumulatively affect flows measured at the Newman gage. Therefore, comparison of hydrograph components between the Friant and Newman gaging stations are somewhat obscured. Based on analyzing water yield at the Newman gage before and after Friant Dam was constructed, the average annual water yield was reduced from 1,868,153 acre-ft to 1,537,365 acre-ft, an 18% reduction in yield. This reduction includes effects of New Exchequer Dam on the Merced River, Friant Dam, and other diversions, as well as irrigation water imported to the basin from the Delta-Mendota canal. In addition to the hydrograph component summary in Table 2-8 and Table 2-9, Figure 2-26 through Figure 2-30 illustrate (1) the average annual hydrograph for a given water year class, (2) an example representative unimpaired hydrograph for that given water year class, and (3) the corresponding representative regulated hydrograph for that given water year class. The following section summarizes the important hydrograph components as measured at the Newman gage.

2.6.6.3.1. Summer, Fall, and Winter Baseflows

- Median summer baseflows near Newman ranged from 105-720 cfs during the pre-Friant period, with minimum summer baseflows occasionally falling below 100 cfs. The highest summer baseflows at Newman (pre-Friant) infrequently exceeded 1,000 cfs. During the post-Friant period, median summer baseflows have actually increased, and now range from 264-1,165 cfs. The maximum baseflows during this period are also higher, ranging as high as 4,000 cfs during Extremely Wet years, and up to 1,600 cfs during Critically Dry years.

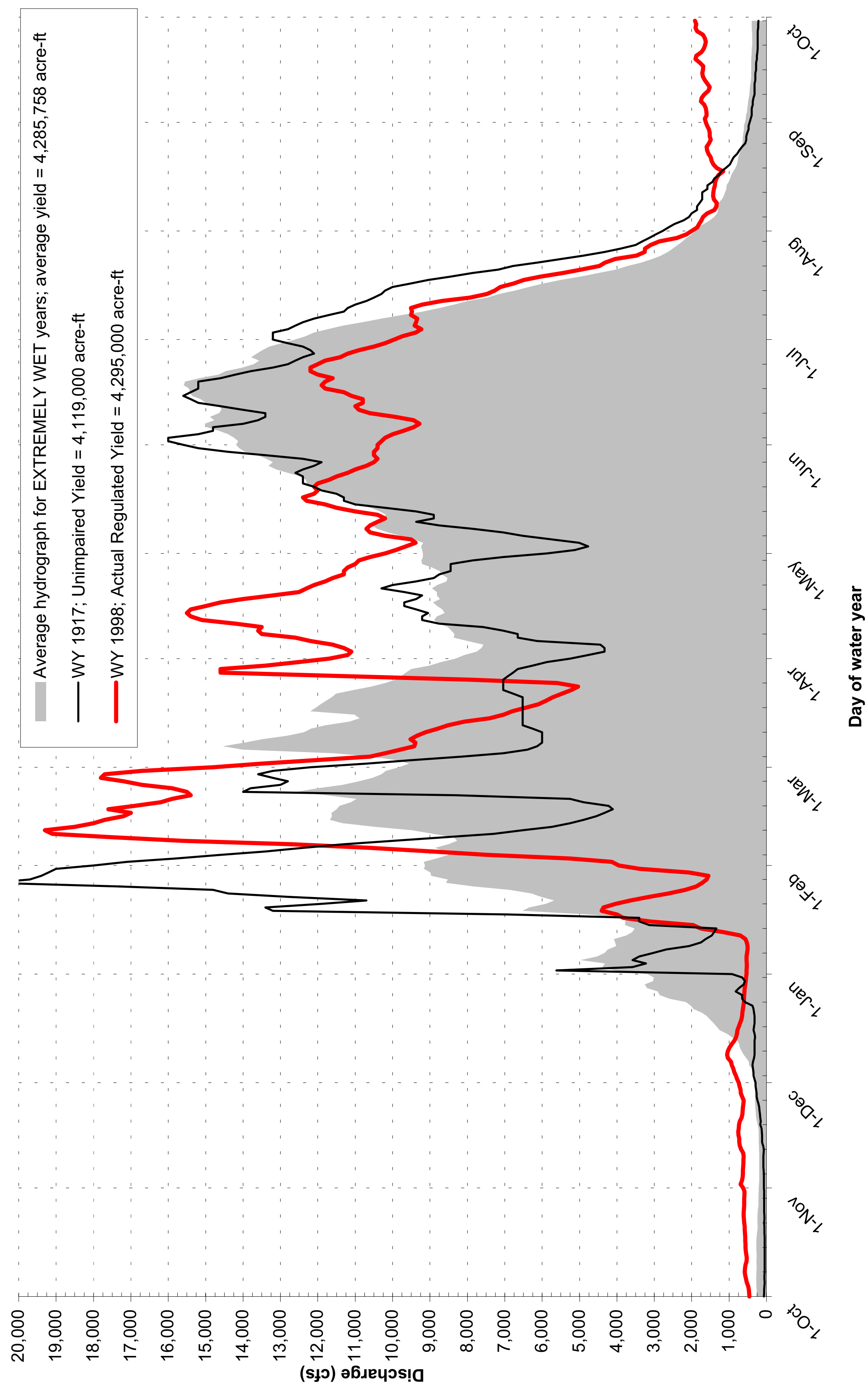

Figure 2-26. Average annual unimpaired hydrograph for an Extremely Wet water year at the San Joaquin River at Newman gaging station. Representative Extremely Wet water year hydrographs for Pre-Friant Dam (1917) and post-Friant Dam (1998) conditions are included.

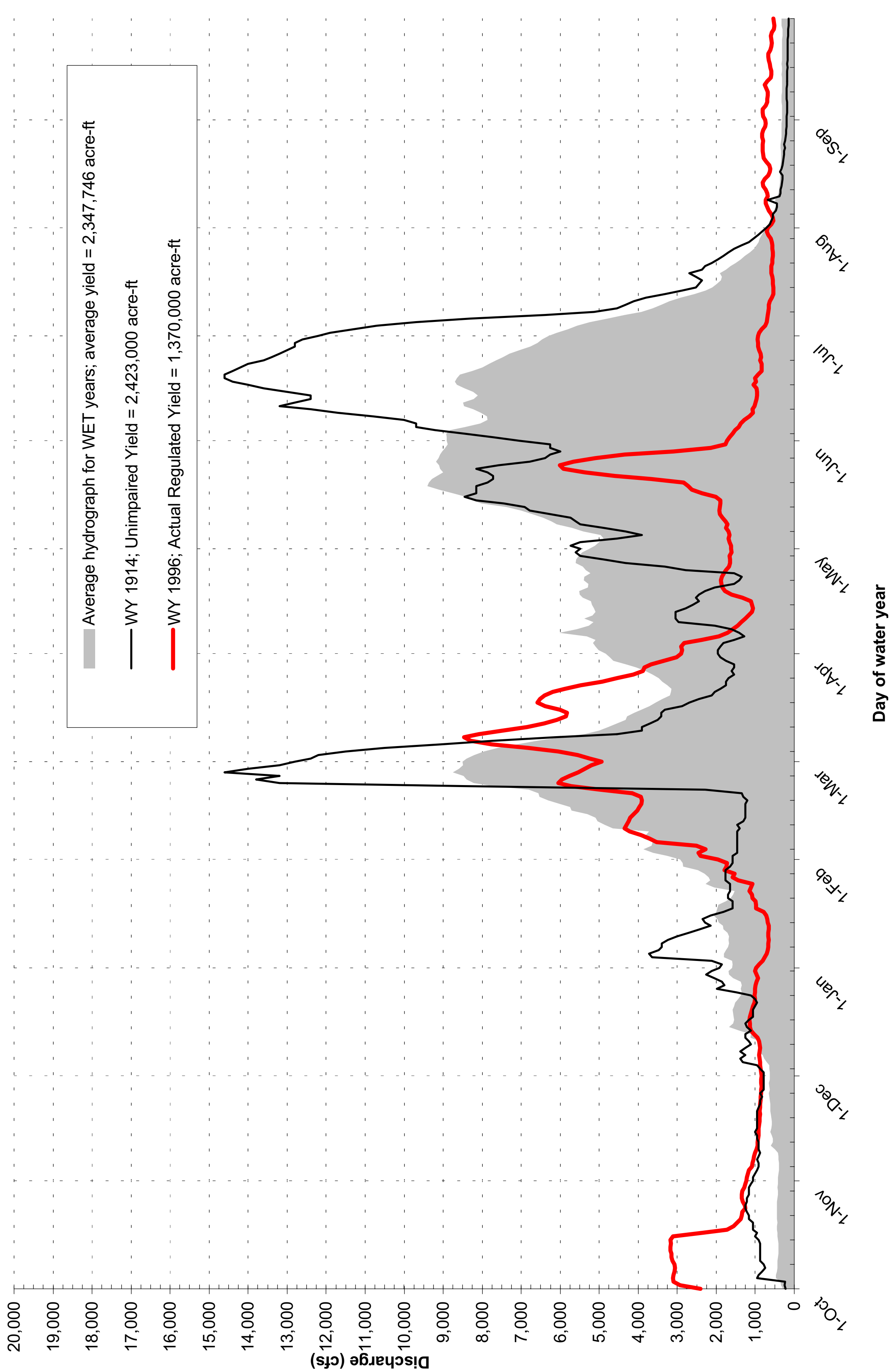

Figure 2-27. Average annual unimpaired hydrograph for a Wet water year at the San Joaquin River at Newman gaging station. Representative Wet water year hydrographs for Pre-Friant Dam (1914) and post-Friant Dam (1996) conditions are included.

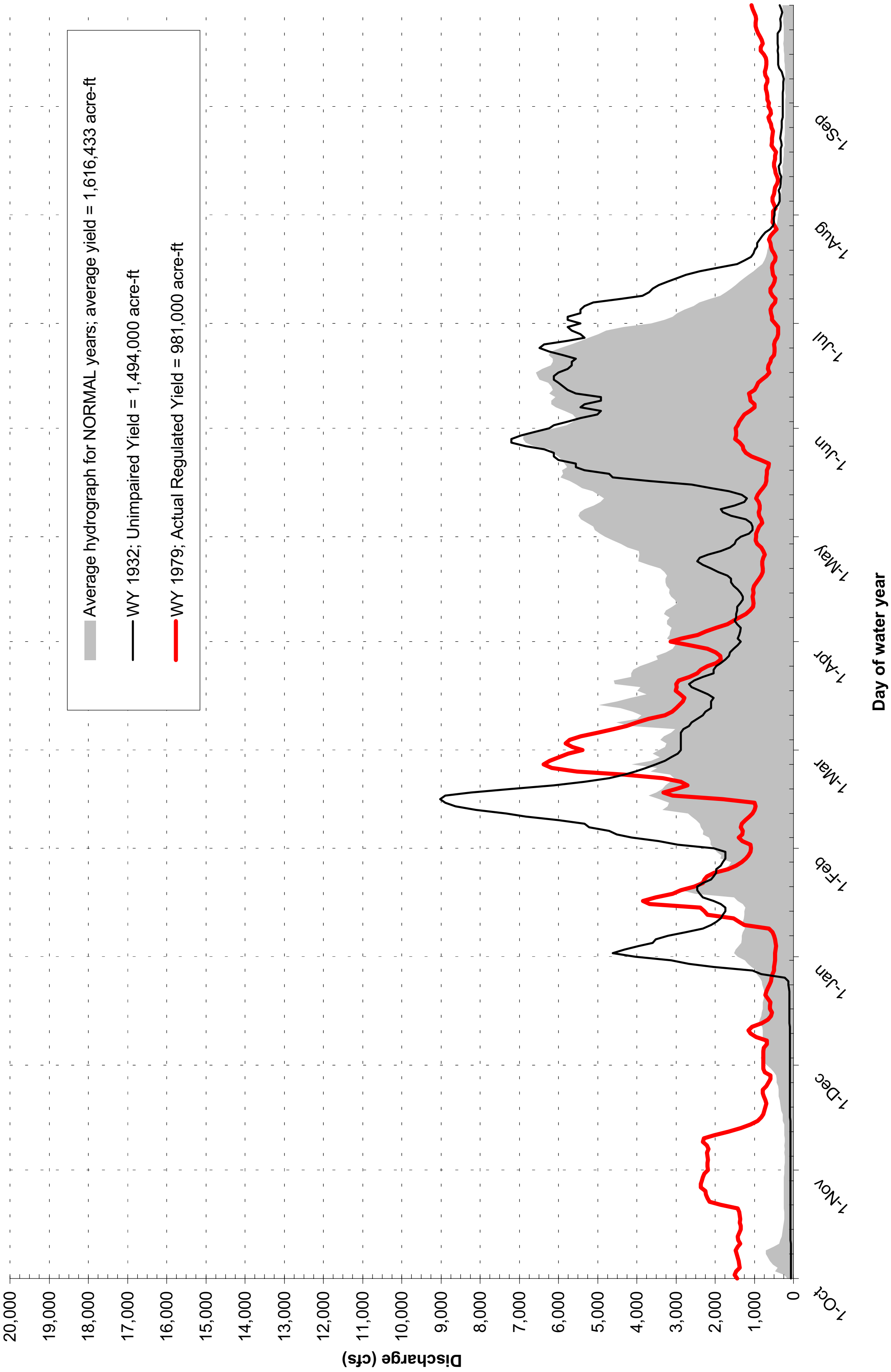

Figure 2-28. Average annual unimpaired hydrograph for a Normal water year at the San Joaquin River at Newman gaging station. Representative Normal water year hydrographs for Pre-Friant Dam (1932) and post-Friant Dam (1979) conditions are included.

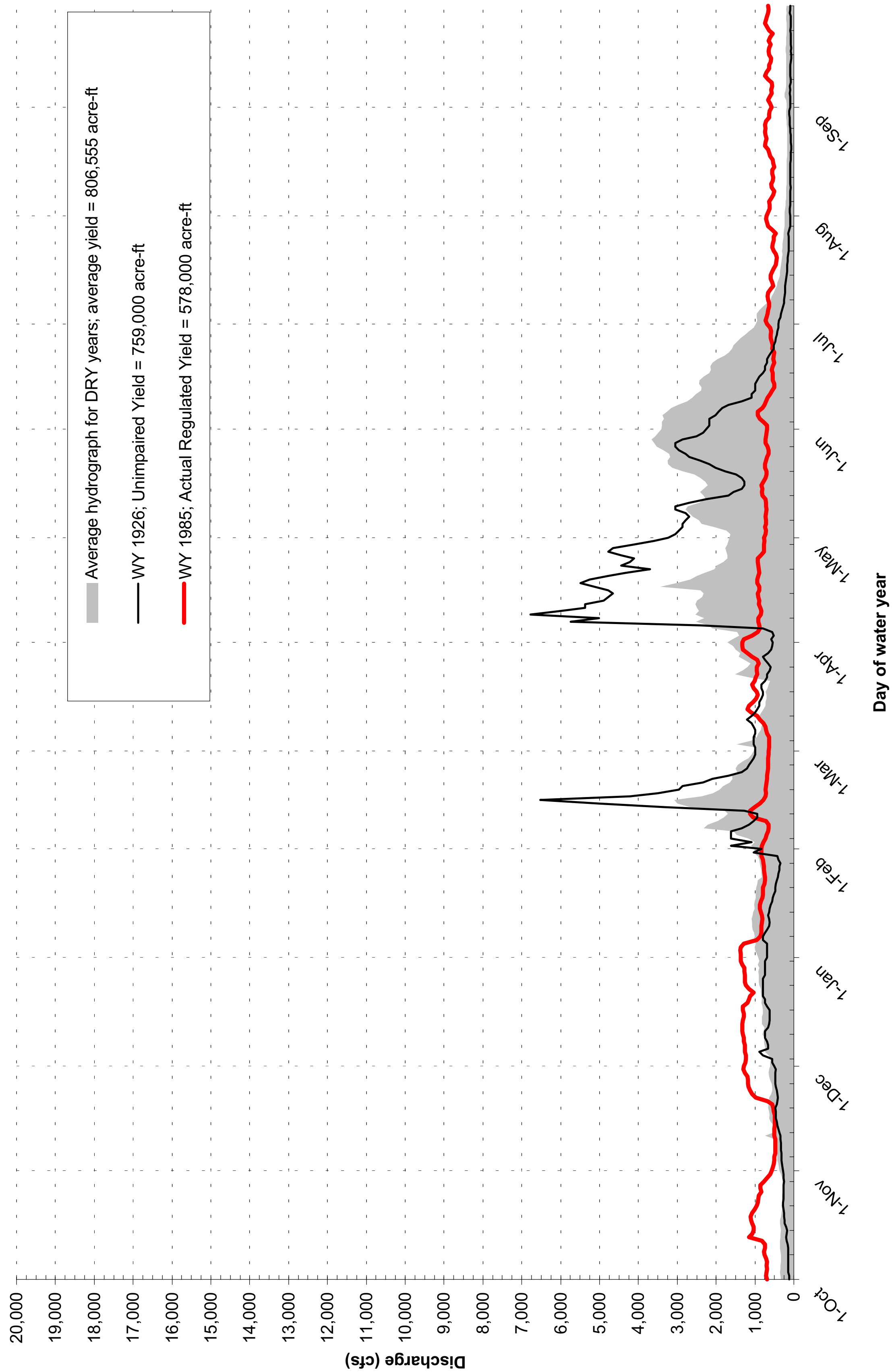

Figure 2-29. Average annual unimpaired hydrograph for a Dry water year at the San Joaquin River at Newman gaging station. Representative Dry water year hydrographs for Pre-Friant Dam (1926) and post-Friant Dam (1985) conditions are included.

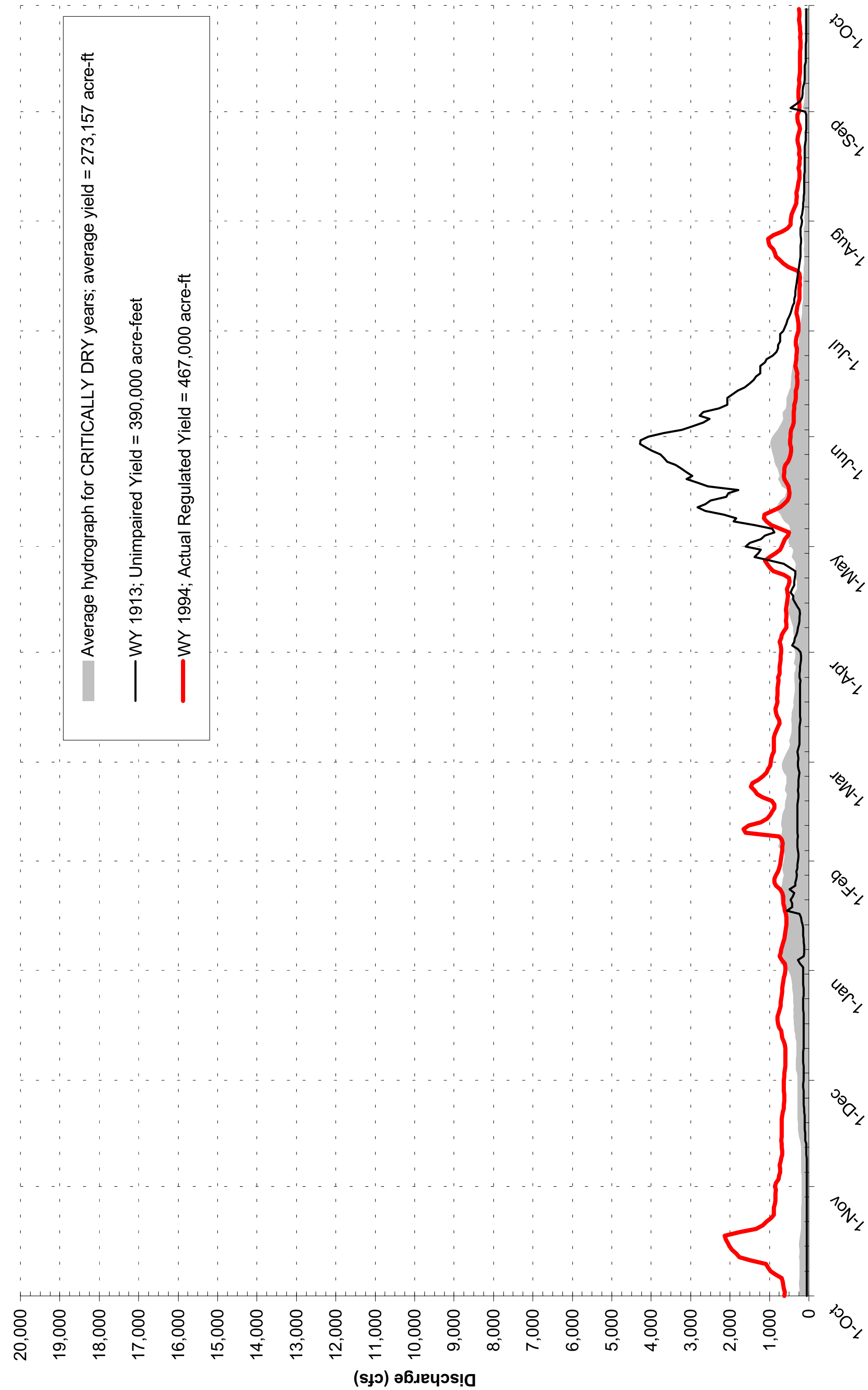

Figure 2-30. Average annual unimpaired hydrograph for a Critically Dry water year at the San Joaquin River at Newman gaging station. Representative Critically Dry water year hydrographs for Pre-Friant Dam (1913) and post-Friant Dam (1994) conditions are included.

- Median (pre-Friant) fall baseflows near Newman generally had a very narrow range during the pre-Friant period, ranging between 143-300 cfs. The maximum fall baseflows occasionally ranged as high as 1,000 cfs. Under regulated conditions, median fall baseflows also increased and ranged from 414-1,110 cfs. This increase is likely attributed to irrigation return flows from water imported via the Delta-Mendota Canal.
- Pre-Friant median winter baseflows were an order of magnitude larger than the summer/ fall baseflows. The median winter baseflow for Extremely Wet years was 2,850 cfs, with a maximum baseflow of 3,970 cfs. Critically Dry and Dry median pre-Friant winter baseflows were 421 cfs and 713 cfs, respectively. Under regulated conditions (post-Friant Dam and post-New Exchequer Dam), both the magnitude and the range of winter baseflows were reduced, and ranged from 520-980 cfs during Critically Dry and Wet years, respectively. The primary cause of this reduction in winter baseflows was Friant Dam operation; however, a large but unknown cause was also likely the reduced flow contribution from the Kings River via Fresno Slough.

2.6.6.3.2. Fall and Winter Floods

- The fall flood hydrograph component appears to have been much less significant at the Newman gage than at Friant due to the vast flood storage in Reaches 2-5 attenuating peak flows moving downstream along the San Joaquin River. Pre-Friant streamflow regulation could also have reduced the magnitude of fall floods. The pre-Friant fall floods (peak daily average flow magnitude) ranged from 300-1,200 cfs, but did not appear to increase with wetter water years. Pre-Friant fall peak magnitudes increased slightly, ranging from 690-2,300 cfs, and again not increasing with wetter water years.
- Considering the location of the Newman gage below the Merced River confluence, winter storms were much smaller in magnitude than might be expected, compared to unimpaired peak magnitudes recorded at the Friant gage. Again, this factor is likely attributable to flood peak attenuation as floodwaters inundated floodplains and filled wetlands along the valley bottom, then were slowly released back into the channel. This effect reduced the overall magnitude of flood events, but increased the duration of winter floods. Daily average unimpaired winter floods ranged from 1,100-19,000 cfs during Critically Dry and Extremely Wet years, respectively, with the maximum daily average peak reaching 33,000 cfs in water year 1938.
- Regulation by Friant Dam and New Exchequer Dam appears to have had little effect in reducing winter flood magnitudes at the Newman gaging station. Median winter floods near Newman ranged from 1,100-24,000 cfs under regulated conditions. The flood of January 1997 reached 38,000 cfs near Newman, which is estimated to be approximately the 100-year flood (ACOE 1999). Flood flow contribution from the Kings River via Fresno Slough still occurs for winter storm events under present-day conditions (although probably reduced in magnitude by Pine Flat Dam), as opposed to the winter baseflow hydrograph component where significant flow reductions were likely significantly caused by reductions in Kings River contribution.
- A comparison of annual hydrographs for Friant and Newman indicates that antecedent conditions were an important factor determining the magnitude and duration of floods near Newman. Early winter floods appear to have been more readily absorbed by low-land floodplains and wetlands, and these early flood peaks near Newman were strongly dampened. Later in winter, however, relatively smaller peak magnitudes at Friant produced sustained-duration and higher peak floods near Newman as the downstream flood storage capacity of floodplains and wetlands was more readily exceeded.

2.6.6.3.3. Snowmelt Hydrograph

- Snowmelt floods near Newman varied widely under pre-Friant conditions, ranging from small floods of 1,300 cfs during Critically Dry years up to 16,500 cfs under Extremely Wet conditions. The maximum flood under unimpaired conditions was 25,000 cfs (WY 1938). The drought years of 1929-31 and 1934 did not have measurable snowmelt floods, and may have been more significantly influenced by instream diversions.
- Under regulated conditions, median snowmelt floods did not change appreciably during Extremely Wet and Wet water years (15,000-9,000 cfs, respectively), but were reduced considerably more during Normal to Critically Dry water years (3,000-900 cfs, respectively). The water year 1983 snowmelt flood of 24,900 cfs (daily average flow) was the largest snowmelt flood during the post-Friant Dam and post-New Exchequer Dam period.

2.6.7. Representative Annual Hydrographs

Tributary streams downstream of Friant Dam play an important role in delivering water to the mainstem San Joaquin River channel, particularly during storm runoff periods when flow releases from Friant Dam are minimal. Two tributaries, Cottonwood Creek and Little Dry Creek, are located in the immediate downstream reach below Friant Dam (see Figure 2-2 and Figure 2-3). These two tributaries are unregulated (with the exception of small watering ponds for livestock), so their natural flow pattern is more variable than the regulated release from Friant Dam. As such, the flow contribution from these tributaries can contribute peak flows during winter rainfall generated storms. The following discussion focuses on (1) Cottonwood Creek and Little Dry Creek, highlighting their relationships to mainstem San Joaquin River flows in the upper portion of the project reach; and (2) mainstem San Joaquin River gages to illustrate longitudinal gradient in hydrographs for the mainstem San Joaquin River. Representative hydrographs for the Friant gaging station (RM 266) and the Newman gaging station (RM 119) are not discussed in this section because they were discussed in the hydrograph component section, and all hydrographs for these two gaging stations over the entire period of record are included in Appendix A. Representative hydrographs for the Friant gaging station and Fremont Ford gaging station (RM 125) are provided to assess flood pulse lag time and potential changes in flood routing due to levees and other floodway manipulations.

2.6.7.1. Cottonwood Creek near Friant

Streamflow on Cottonwood Creek (drainage area = 35.6 mi^2) was recorded by the USGS from water year 1942 to water year 1951; the USBR has monitored the station since 1951. Although the USGS period of record does not provide enough pre-Friant information to perform a comprehensive hydrograph component analysis, the variability of water year types that can be classified as ranging from Extremely Wet to Critically Dry within this time provides an example of Cottonwood Creek's hydrology. For the measured period of record, we plotted all annual hydrographs (see Appendix A) and selected three that represent Extremely Wet, Normal, and Critically Dry water year types (1942, 1947, and 1948, respectively). These hydrographs illustrate the variability of streamflow hydrology in Cottonwood Creek, such as the timing and magnitude of flows delivered to the mainstem San Joaquin River during each of these water year types (Figure 2-31). Cottonwood Creek is dry most of the year, such that fish species that require year-round flow (e.g., steelhead) could not survive in most years without supplemental flows. Cottonwood Creek is extremely flashy in response to rainfall events, increasing from low flow to over 100 cfs in a short period of time (hours to a few days), with receding flows decreasing more gradually, but still dropping down to low baseflows in a matter of days. This pattern is characteristic of all rainfall dominated small streams draining the Sierra Nevada foothills.

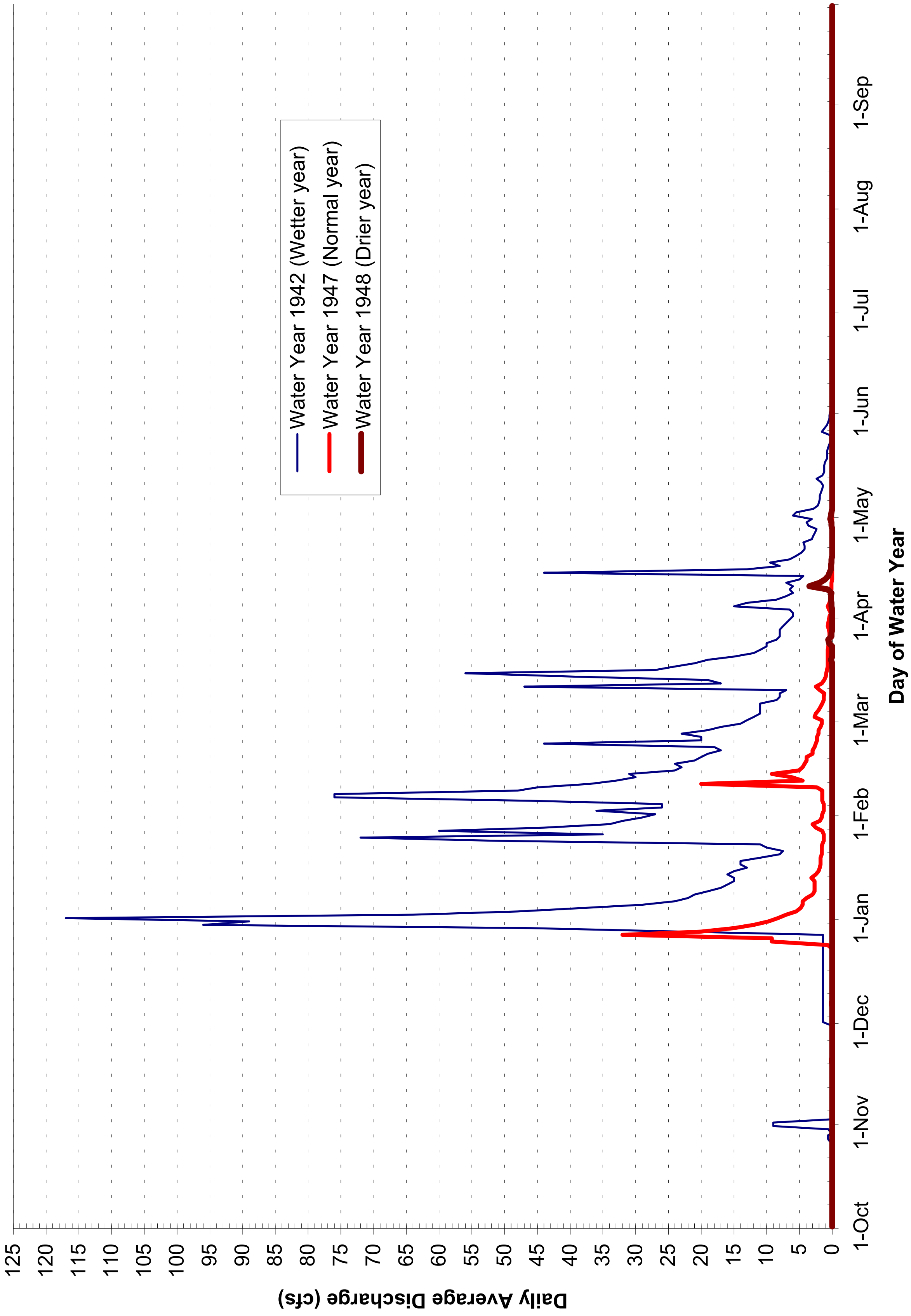

Figure 2-31. Cottonwood Creek near Friant, CA, annual hydrographs for Extremely Wet (1942), Normal (1947), and Critically Dry (1948) water year types.

2.6.7.2. Little Dry Creek near Friant

Streamflow on Little Dry Creek (drainage area = 57.9 mi^2) was recorded by the USGS from water year 1942 to water year 1956; the USBR has monitored the station since 1956. Similar to Cottonwood Creek, the USGS streamflow record is relatively short and does not provide enough information to perform a comprehensive hydrograph component analysis. However, the variability of water year types that can be classified as ranging from Extremely Wet to Critically Dry within this time provides an example of Little Dry Creek's hydrology. As with Cottonwood Creek, we plotted all annual hydrographs for the 1942-1956 period of record, and then selected three that represent Extremely Wet, Normal, and Critically Dry water year types (1942, 1944, and 1948, respectively). These hydrographs illustrate the variability of streamflow hydrology in Little Dry Creek, such as the timing and magnitude of flows delivered to the mainstem San Joaquin River during each of these water year types (Figure 2-32).

Because of its proximity to the Cottonwood Creek gage, we would expect the Little Dry Creek water year classifications that span the same time period (1942-1951) to match those for Cottonwood Creek. These gages are located so close to each other that they experience the same climatic events responsible for their runoff; therefore, the water year classifications should be similar. However, only three years classify as the same water year type for both records. The primary cause for this difference is likely that the short period of record for both gages captures less variability in flows than would otherwise be captured with a longer record. More specifically, the Cottonwood Creek record is 10 years, and the Little Dry Creek record is 15 years. The longer record for Little Dry Creek captures greater variability (thereby biasing its comparison with Cottonwood Creek) but is too short to accurately portray actual runoff conditions in the watershed. Other factors that may account for the difference between the gage can be attributed to the physical (geomorphic) differences between watersheds, such as drainage area size and aspect.

The larger drainage area of Little Dry Creek result in larger peak flows (up to 1,250 cfs in 1956) compared to Cottonwood Creek, but the pattern of long periods of low to zero flow still occurs. The lower portions of Little Dry Creek would be inhospitable to fish species requiring a year-round flow without supplemental flows, but the basin is large enough that upstream reaches have perennial flow based on field observations in August 2002 (B. Trush, pers. comm.).

2.6.7.3. Friant to Fremont Ford Hydrographs

Two methods were used to examine high flow routing relationships between Friant and downstream locations (1) empirical method comparing daily average hydrographs between the San Joaquin River at Friant gaging station (RM 266) and the San Joaquin River at Fremont Ford (RM 125) gaging station, and (2) high flow routing modeling. The flow magnitude and travel time of peak flows at Friant Dam and Fremont Ford was analyzed to determine the changes in flow peak attenuation and travel time caused by Friant Dam and the flood control system downstream of Friant Dam. The periods of record for the two gages that overlapped (water years 1938-43; 1950-71) were used, and each annual hydrograph was examined for discrete high flow events at Friant Dam that produced a subsequent high flow peak at Fremont Ford. The dates and magnitudes of these peaks were compiled for each of the gages, then plotted to determine the relationship between upstream and downstream peak flow magnitudes and timing. Because the travel distance between the two gages was so large (140 miles), daily average hydrographs provided adequate resolution to assess changes in flow magnitude and travel time, thus hourly flow data was not necessary. For the pre-Friant Dam period with moderately-regulated hydrographs, paired high flow peaks between the two gaging stations were more common, and 20 data points were identified. During the post-Friant record, the effects of regulation severely altered the shape of almost all peak hydrographs, and only six discrete peak

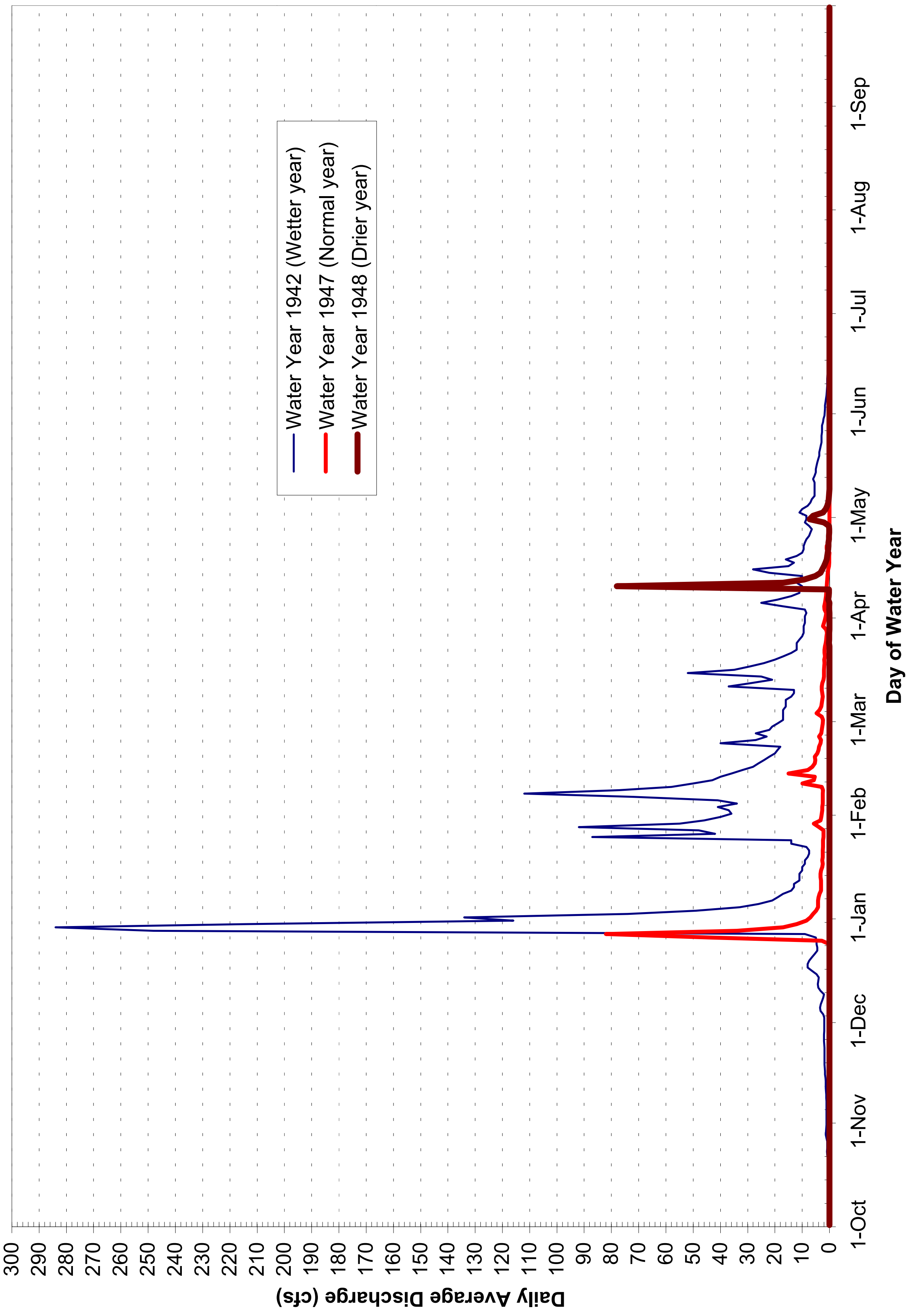

Figure 2-32. Little Dry Creek near Friant, CA, annual hydrographs for Extremely Wet (1942), Normal (1947), and Critically Dry (1948) water year types.

events from 26 water years contained a distinct connection upon which magnitude and travel time differences could be compared. Both the Pre-Friant Dam hydrographs are shown on Figure 2-33 and post-Friant hydrographs shown in Figure 2-34.

During unregulated conditions, there appears to have been an upper limit in peak discharge at the San Joaquin River at Fremont Ford gaging station, relatively independent of discharge from Friant Dam (Figure 2-35). Peak discharges ranging from 5,000 cfs to 20,000 cfs at Friant consistently produced peak flows up to, but rarely exceeding 5,500 cfs at Fremont Ford. The ratio of Friant to Fremont Ford discharge was 2.8. The range of flood peak magnitudes occurring in the post-Friant Dam period was much lower than the pre-dam period, ranging up to only a 7,980 cfs peak at the Friant gage. During the post-dam period, the peak discharge data points were clustered within the pre-Friant Dam data (Figure 2-35), but the ratio of Friant to Fremont Ford discharge was closer to one (1.4). The USGS water resources records state that for the Fremont Ford gaging station, "during periods of high flow, water bypasses this station through Mud Slough." This undefined high flow bypass is likely a leading cause of the approximate 5,500 cfs cap at the Fremont Ford gage, but because Mud Slough was not gaged during this period, the degree of flow bypass (and flow threshold for beginning to bypass) cannot be determined.

The travel time for floods from Friant Dam to Fremont Ford was relatively consistent under the pre-Friant Dam period, ranging from 6-10 days, with a median (and mean) of 7 days. One outlier was identified from water year 1938, in which a December 11, 1937 flood peak of 45,700 cfs at Friant Dam caused only a 3,500 cfs peak at Fremont Ford (Figure 2-36). Overlaying more recent travel times under the post-Friant Dam period suggest that the travel time is slightly less, ranging from 1-8 days, with a median of 5 days. This slight decrease is not conclusive due to the small number (8) of high flow peaks compared.

The hypothesis being evaluated in this travel time assessment is that the increased confinement along the lower San Joaquin River between the two gaging stations has reduced travel time of flood peaks and reduced the amount of flood peak attenuation provided by the large-scale flood basins that were historically flooded. Unfortunately, the small number of data points available for the post-Friant Dam evaluation is too small (eight high flow peaks) to make any definitive conclusions about changes in travel time or flood magnitude. Other sources of variability that hampered this comparison include the following:

- in the pre-Friant Dam period, there may have been several other tributaries (e.g., Fresno River) that contributed to flood peaks at Fremont Ford, increasing the difference in magnitude and travel time between Friant and Fremont Ford (i.e., making the data more random, and less dependent upon overbank flood storage).
- in the post-Friant Dam period, most or all of these other tributaries are now regulated by a large storage dam, so there is a better relationship between the Friant and Fremont Ford peak magnitudes (and shorter travel time).

2.7. FLOW ROUTING

This section provides broad flow routing processes under historical and existing conditions between Friant Dam and the Merced River confluence. There are two primary components of flow routing: baseflows and flood flows. The descriptions of baseflow routing are based on historical accounts and maps from early explorers, aerial photographs, and gaging stations. The descriptions of flood flow routing are based on historical accounts and maps from early explorers, aerial photographs, gaging stations, and modeling.

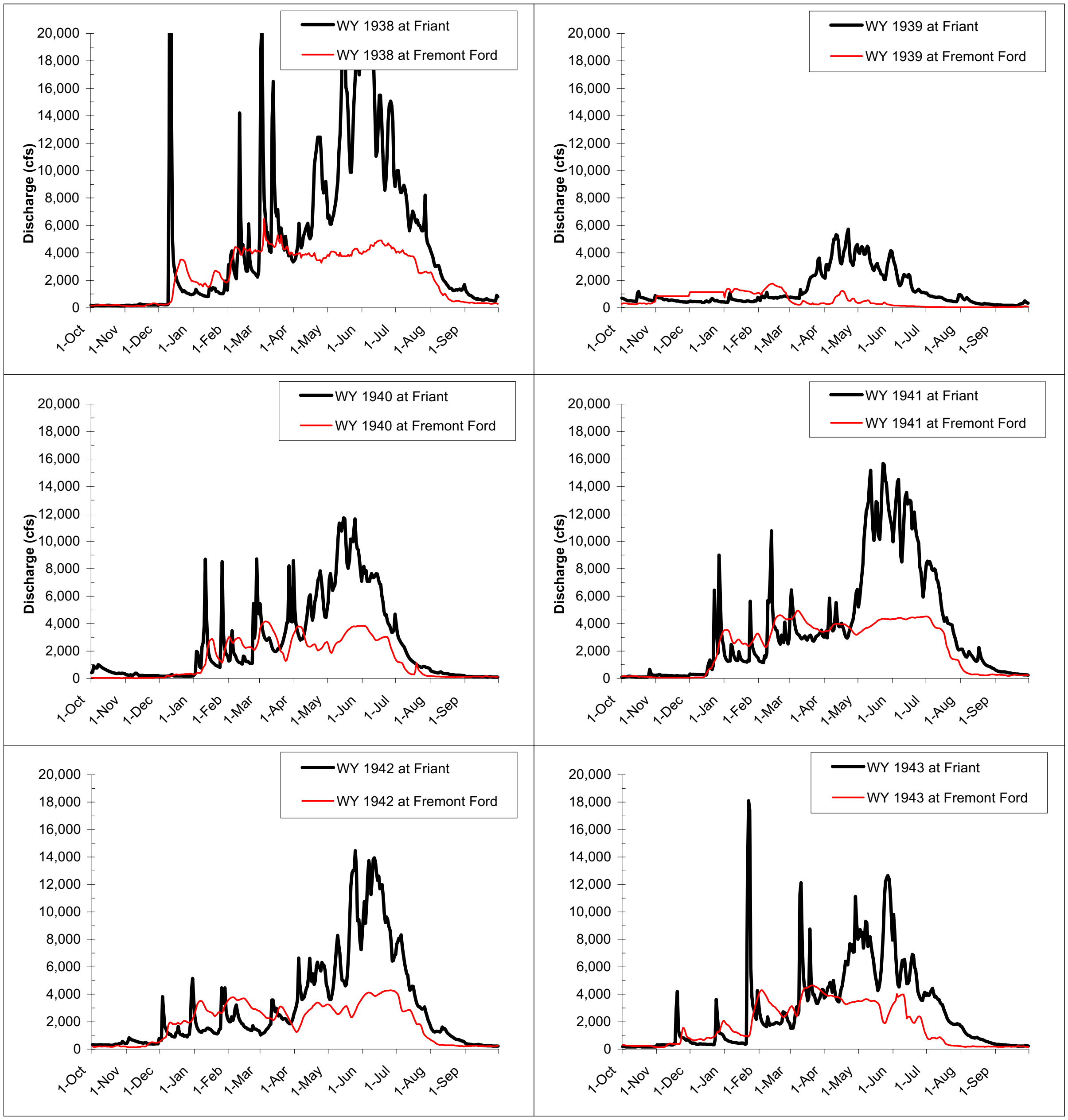

Figure 2-33. Overlay of annual hydrographs at the San Joaquin River at Friant gaging station and San Joaquin River at Fremont Ford gaging station (1938-1943), showing pre-Friant Dam peak flow magnitude and travel time for specific high flow events.

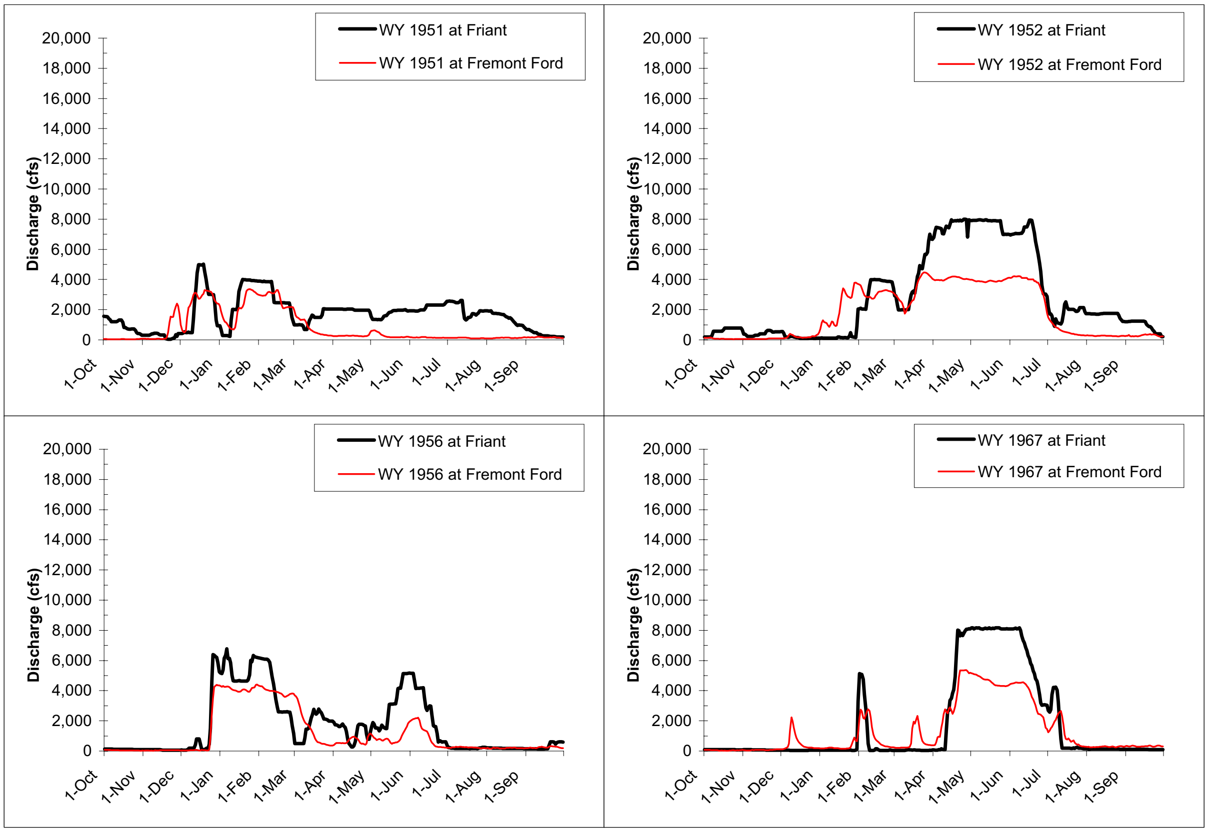

Figure 2-34. Overlay of annual hydrographs at the San Joaquin River at Friant gaging station and San Joaquin River at Fremont Ford gaging station (1951, 1952, 1956, 1967), showing post-Friant Dam peak flow magnitude and travel time for specific high flow events.

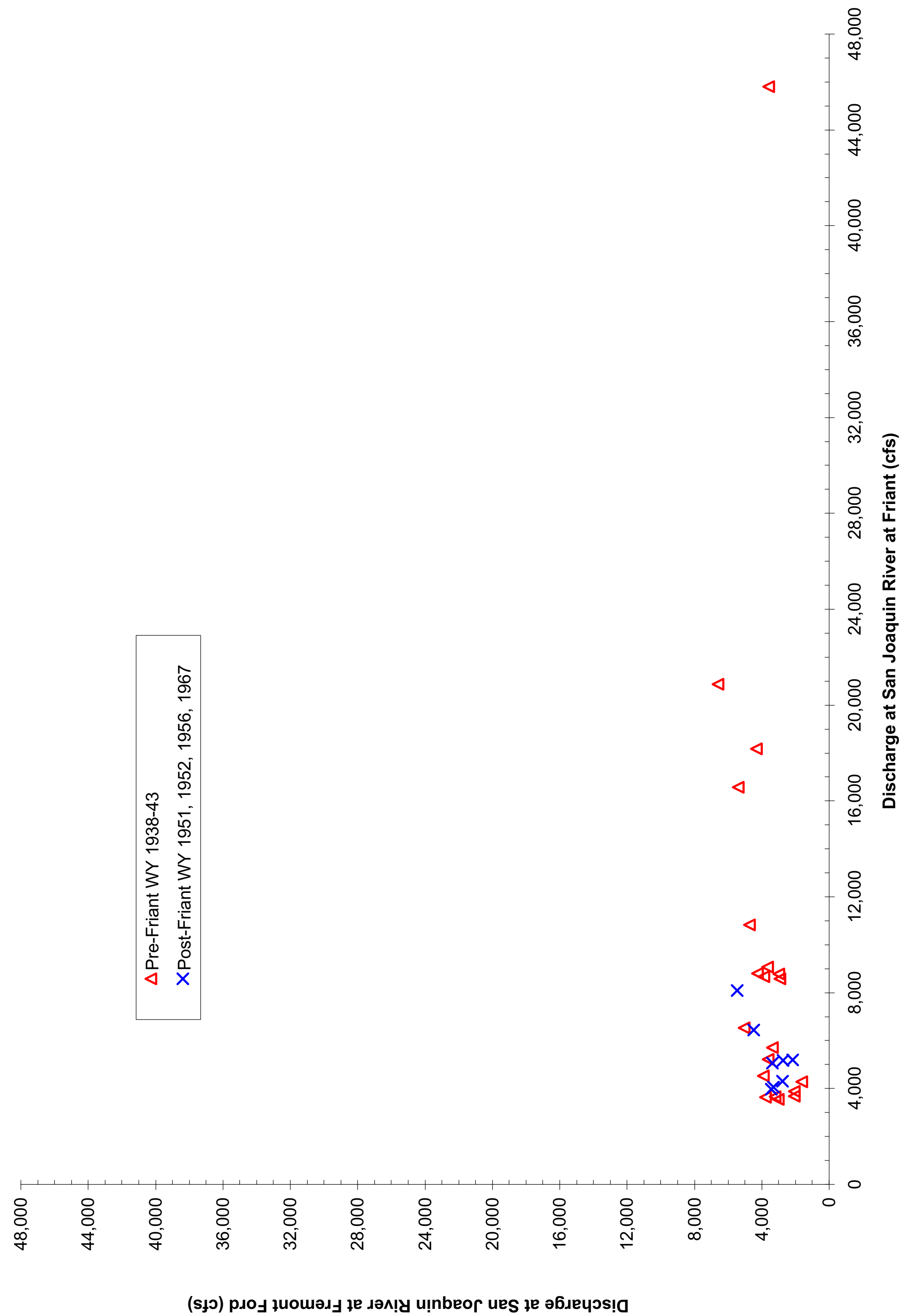

Figure 2-35. Comparison of flood magnitude between the San Joaquin River at Friant gaging station and San Joaquin River at Fremont Ford gaging station under pre-and post-Friant Dam periods. Hydrographs in Figures 2-33 and 2-34 are used.

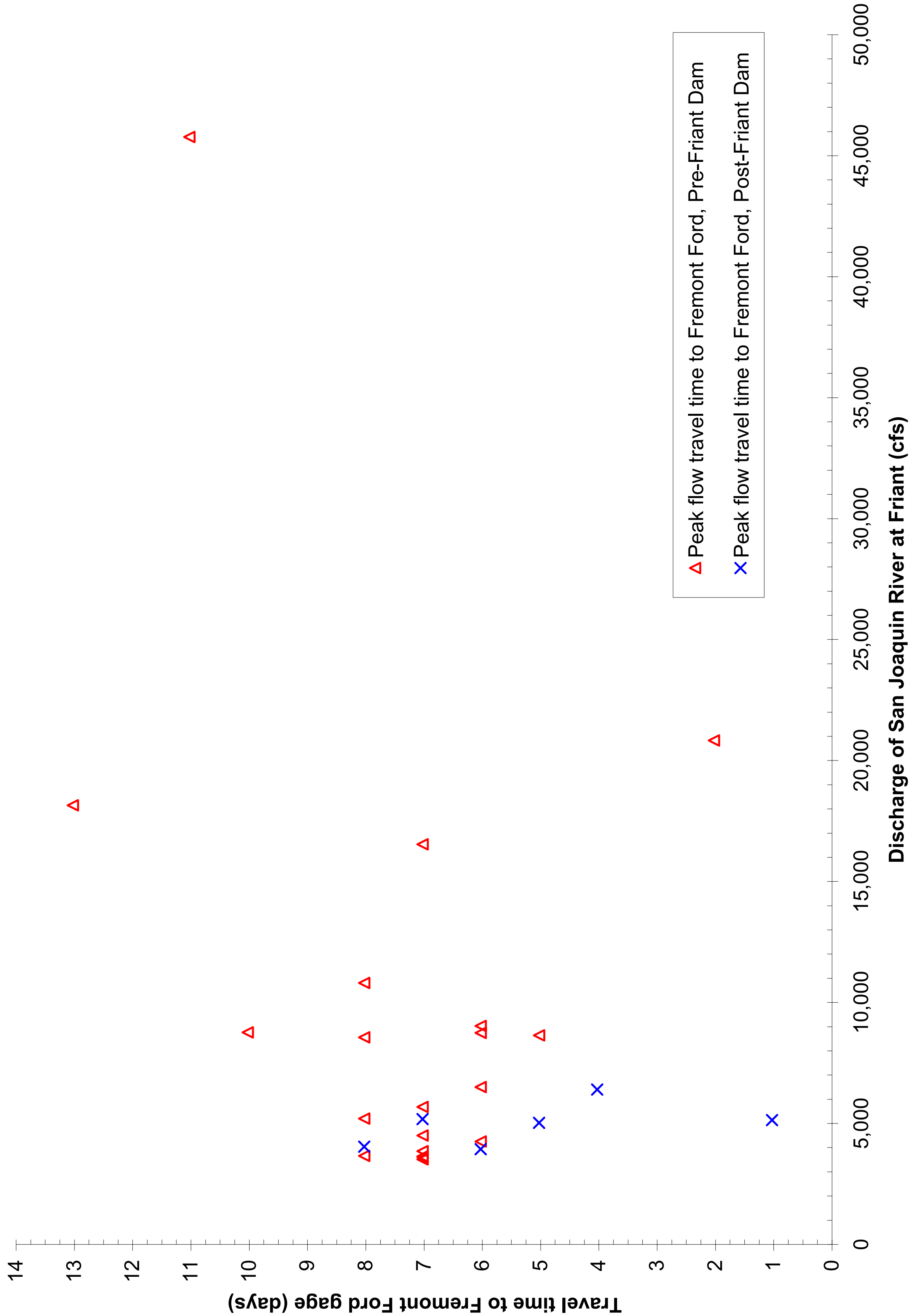

Figure 2-36. Comparison of travel time between the San Joaquin River at Friant gaging station and San Joaquin River at Fremont Ford gaging station under pre-and post-Friant Dam periods. Hydrographs in Figures 2-33 and 2-34 are used.

2.7.1. Historical and Existing Baseflow Routing

Historical baseflows were most likely contained within the San Joaquin River channel(s) between Friant and the Merced River confluence. Most early maps clearly show that baseflows were contained within a single channel of the San Joaquin River, or in two or more secondary channels (e.g., Lone Willow Slough in Reach 2 and 3, Santa Rita Slough in Reach 3, Salt Slough in Reach 3 and 5) as shown on Government Land Office plat maps, Hall (1878) maps, and Derby (1952) maps. Derby's 1852 map shows channels passing from the San Joaquin River to the Fresno Slough; however, review of historical aerial photographs shows that these channels did not convey baseflows as observed in the 1937 aerial photographs, and thus these channels are likely high flow sloughs (see Figure 2-37). There has been some inference that there was baseflow contribution from the Tulare Lake basin groundwater from an anonymous reference in 1873 (as cited in Fox 1987a):

> *the San Joaquin River receives an important accession of volume from underground drainage-probably from the Tulare Lake drainage*

Review of the Hall (1878) and ACOE (1917) maps, combined with descriptions of the artesian springs along the San Joaquin River in Reaches 2-5, suggests that baseflow contribution from groundwater sources was likely dominated by artesian springs along the river corridor rather than underground drainage from the Tulare Lake basin. This baseflow contribution, as well as gaining and losing reaches under historical and existing conditions, is discussed further in Chapter 4.

Under existing conditions, baseflow magnitude and routing has changed considerably as a result of infrastructure development in the San Joaquin Valley (see Chapter 5). Baseflows are still conveyed by the San Joaquin River, but several differences have occurred:

- The magnitude of baseflows has changed, with baseflows decreased in Reach 1, 2, 4, and 5, and baseflows increased in Reach 3 due to Delta-Mendota Canal water deliveries to Arroyo Canal.
- The number of secondary channels conveying baseflows have decreased as they have been converted to agricultural return channels or reclaimed (filled) for agriculture.
- The routing of baseflows has changed drastically as a result of the irrigation flow distribution system.

Current baseflows along the San Joaquin River are summarized in Table 2-11. Estimated unimpaired baseflows at the San Joaquin River at Friant gaging station are also provided in Table 10. Pre-Friant Dam flows were examined at the downstream end of the study reach (at Fremont Ford from 1938-1943), but those baseflows were lower than those at Friant due to agricultural diversions; therefore, unimpaired discharges downstream of Friant were simply listed as “greater than Friant”. Current typical seasonal flow distribution is provided for Friant Dam in Figure 2-38, and at Mendota Pool in Figure 2-39.

2.7.2. Water Budget and San Joaquin River Model

In order to model existing and future flow routing through the study area, a water budget analysis was conducted for subreaches between Friant Dam and the Merced River confluence. This information was also used in the development of the San Joaquin River Model. The San Joaquin River Model was constructed to model the daily or monthly flow patterns (hydrographs) that are required to achieve some of the specified quantitative restoration objectives of the Restoration Study. The daily flow and water budget model components provide the basis for calculations of streamflow and associated riparian conditions that depend on the flow or hydraulic parameters along the San Joaquin River channel.

Table 2-11. Typical seasonal flows in different reaches of the San Joaquin River based on trends observed in USGS gaging station data and from descriptions of flow by local irrigation district staff.

	UNIMPAIRED TYPICAL BASEFLOWS		EXISTING TYPICAL BASEFLOWS		
Reach	Unimpaired summer/fall baseflows (cfs)	Unimpaired winter baseflows (cfs)	Summer flows during the irrigation season (cfs)	Winter flows during the non-irrigation season (cfs)	Comments on existing typical baseflows
1A	340[1]	780[1]	200-300	50-100	Riparian diversions and infiltration losses
1B	340	780	5-200	5-50	Riparian diversions and infiltration losses
2A	>340	>780	0-20	0-20	0-20 cfs flow at Gravelly Ford (upstream end of Reach 2A)
2B	>340	>780	0	0	Downstream of Chowchilla Bifurcation Structure
3	>340	>780	500	200	Delta Mendota Canal water delivered to Arroyo Canal
4A	>340	>780	0	0	Some seepage and flow accretion occurs, but is pumped from river at many locations through reach
4B	>340	>780	0-10	0-10	Control structure at entrance prevents any flows from entering from upstream reach, agricultural return flows re-water channel downstream of Mariposa Bypass
5	>340	>780	0-60	0-60	Agricultural return flows

[1] From median values of hydrograph component analysis at San Joaquin River at Friant gaging station

2.7.2.1. Water Budget Methods

An annual water budget analysis was prepared using the available gage data and results of previous analyses by MEI (2000a, 2000b). The analysis was based on the period of record between 1986 and 1999. The estimated natural flow at Friant Dam was derived from a synthetic record that was provided by the USBR and Mr. Huxley Madeheim. This record represents the best available estimate of the amount of flow that would have occurred at that location in the absence of the upstream storage and flow regulation projects. This is the only location for which an estimate of the unimpaired flows is available. The 1986-1999 period includes a severe six-year drought (in addition to some of the wettest years in the mid to late 1990's), so this period should cover the range of climatic conditions experienced over the long term on the San Joaquin River. The average unimpaired runoff in the 1986-99 period was about 98% of the 1901-2000 average; this period had more winter runoff than the longer term average, and had a greater number of dry and wet years (5 Extremely Wet, 1 Wet, 1 Normal, 1 Dry, 6 Critically Dry). The existing conditions (i.e., 1986-1999) flows in each subreach were estimated as follows:

- **Friant Dam**—from the USGS record of mean daily flows at the Friant gage.
- **Gravelly Ford**—Friant Dam flows modified by the flow loss curves for the Friant Dam to Gravelly Ford reach (Figure 2-4).
- **San Joaquin River upstream from the Chowchilla Bifurcation Structure**—Gravelly Ford flows modified by the flow loss curve for the Gravelly Ford to Chowchilla Bifurcation Structure reach (Figure 2-4).

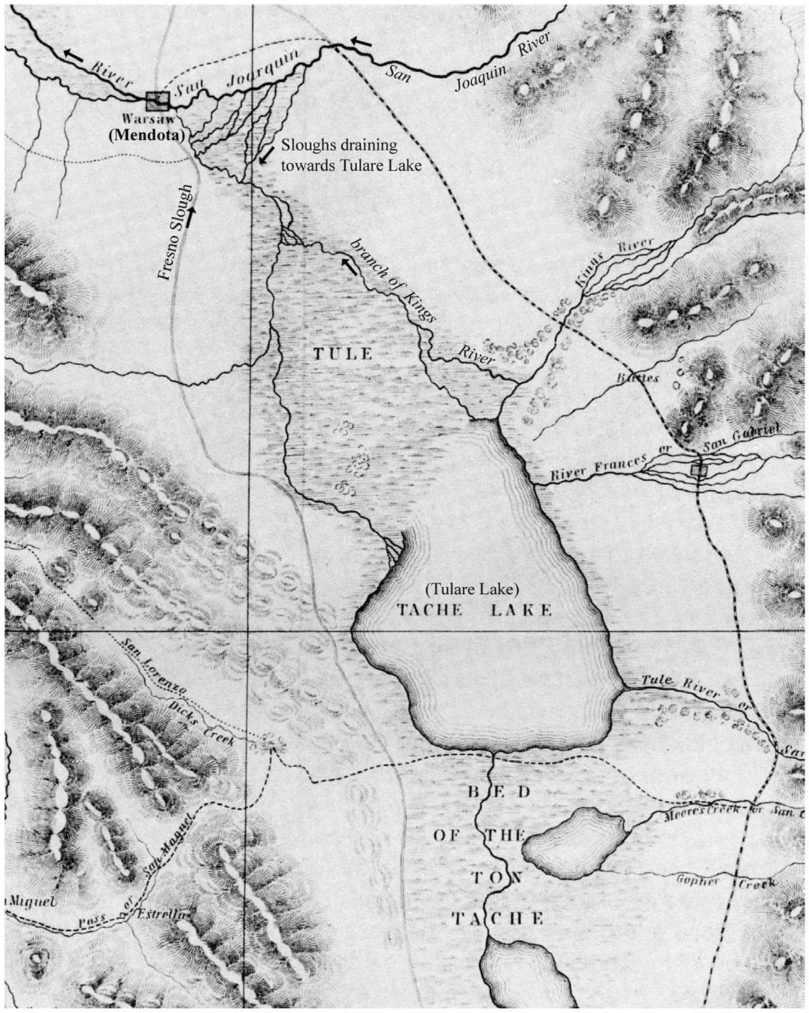

Figure 2-37. 1852 map of the San Joaquin River between present-day Friant and Firebaugh, showing sloughs draining towards Tulare Lake, and Fresno Slough draining towards the San Joaquin River from the Kings River.

- **Chowchilla Bifurcation Structure to head of Mendota Pool**—Estimated flows in the river upstream from Chowchilla Bifurcation Structure, less measured flows in the Chowchilla Bypass where data were available. Where data were not available, flows in the river downstream from the Chowchilla Bifurcation Structure were estimated based on the “initial flow to the river” operating rule.
- **Mendota Dam to Sack Dam**—The San Joaquin River near Mendota gage was used to represent the flows in this subreach. Missing data were estimated by interpolation.
- **Sack Dam to Sand Slough Control Structure (Node 5-6)**—Where available, the flows in this subreach were estimated using the recorded flows at the San Joaquin River near Dos Palos gage. Flows during other periods were estimated using the assumption that all flow in the upstream river would be diverted into the Arroyo Canal up to the approximate canal capacity of 600 cfs.

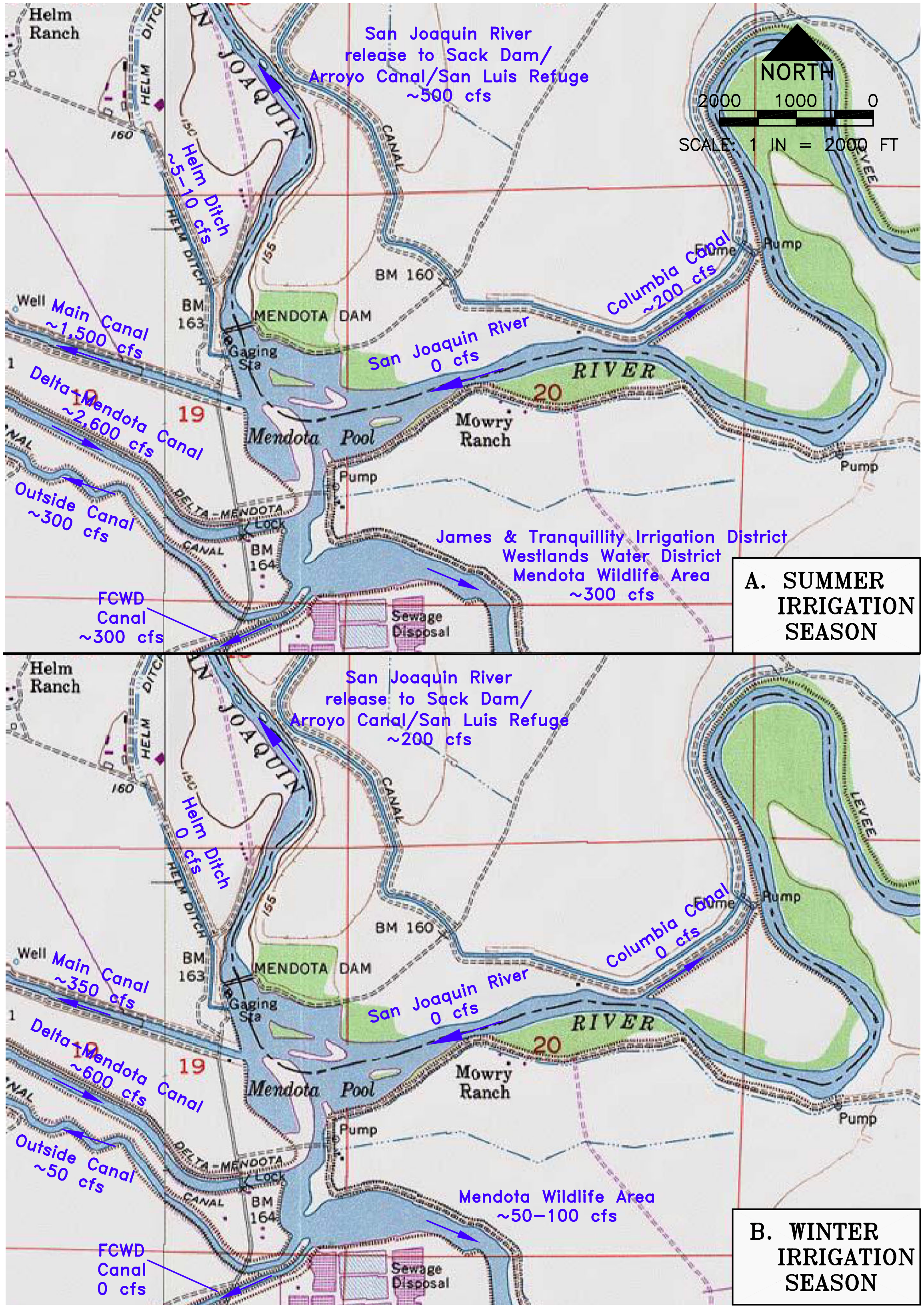

Figure 2-38. Diagrammatic of typical river releases and diversions from Friant Dam during summer irrigation season and winter non-irrigation season.

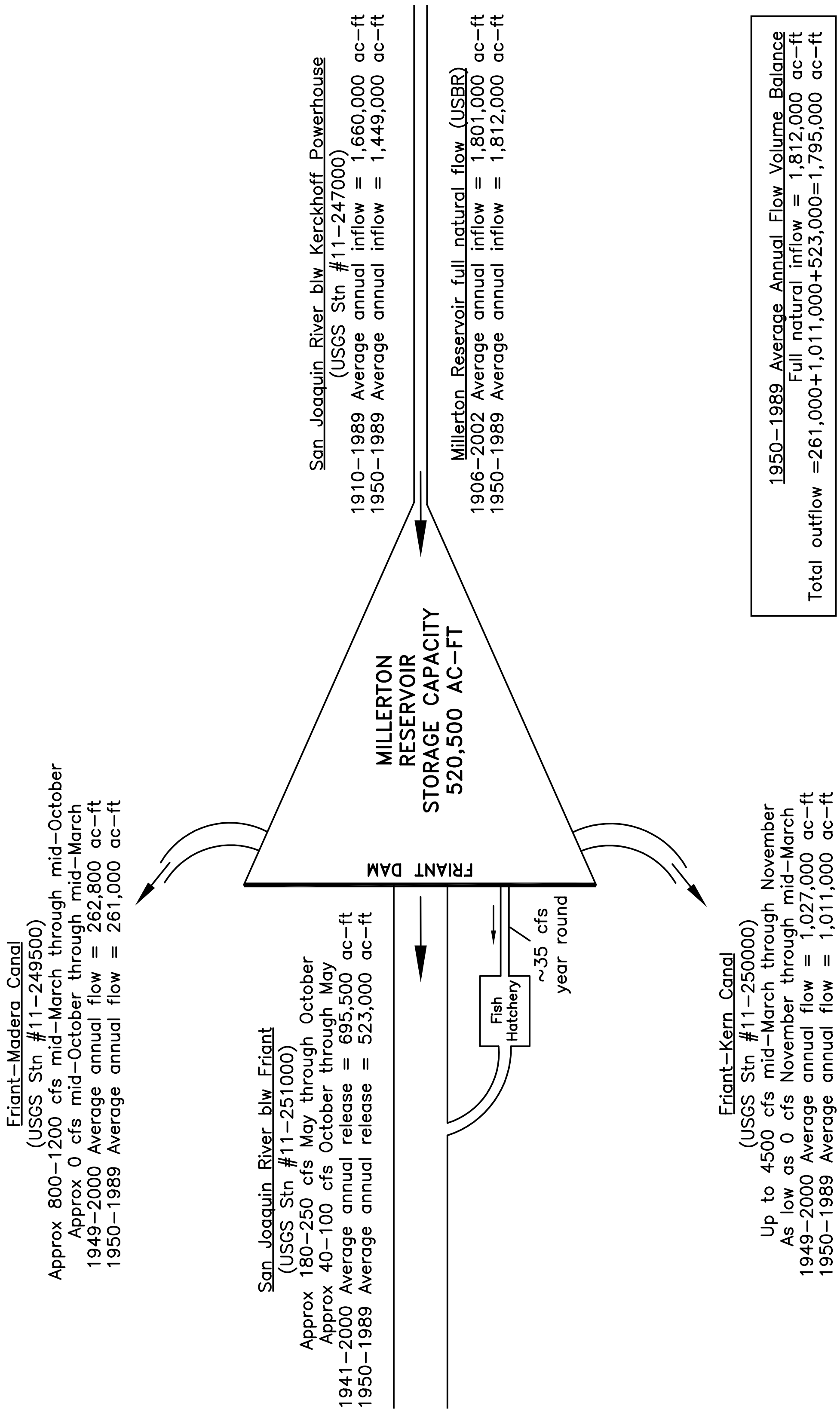

Figure 2-39. Schematic diagram of typical river releases and diversions from Mendota Dam during summer irrigation season and winter season. Winter diversions and releases are largely for wildlife refuges.

- **Sand Slough Control Structure to Mariposa Bypass**—No direct flow records are available for this reach. Consequently, the flow estimates were made by subtracting the flow in the Mariposa Bypass from the estimated flows in the Mariposa Bypass to Bear Creek Reach (see below), with the flows shifted by 1 day to account for the travel time.
- **Mariposa Bypass to Bear Creek**—Flows in this subreach were estimated by subtracting the total flow in Bear Creek at the mouth from the recorded flows at the San Joaquin River near Stevinson gage.
- **Bear Creek to Salt Slough**—The recorded flows at the San Joaquin River near Stevinson were used for this subreach.
- **Salt Slough to Mud Slough—**Flows in this subreach for water years 1986 through 1989 were derived from the San Joaquin River at Fremont Ford Bridge gage record or from the recorded flows in Salt Slough and the recorded flows at the San Joaquin River near Stevinson gage.
- **Mud Slough to Merced River confluence—**Flows in this subreach for water years 1986 through 1995 were estimated by subtracting the recorded flows at the Merced River near Stevinson gage from the recorded flows at the San Joaquin River near Newman.
- **Downstream from Merced River**—Flows downstream from the Merced River were derived from the San Joaquin River near Newman gage record.

The accuracy of the restoration simulations depend on the flow and hydraulic geometry calculations because all other simulated river variables are dependent on these hydraulic parameters (i.e., depth and velocity). The daily flow and water budget model consists of the following elements:

- managed (i.e., controlled) release of water from Friant Dam, Chowchilla Bifurcation Structure (both into the San Joaquin River and into the Chowchilla Bypass), Mendota Pool, Sack Dam, and the Sand Slough gate;
- tributary inflows from Cottonwood, Little Dry, and Bear Creeks; Salt and Mud Sloughs; the Merced River; other local runoff or irrigation returns; and Eastside Bypass return flows during high-flow events, as well as Delta-Mendota Canal inflow to Mendota Pool (considered a tributary inflow that must be specified);
- agricultural diversions (i.e., pumps) along the San Joaquin River, canals that divert from Mendota Pool and Sack Dam (Arroyo Canal), and the flood control diversions into the Chowchilla and Eastside Bypasses (during high-flow events);
- evapotranspiration losses from the water and riparian vegetation along the San Joaquin River channel;
- seepage along the San Joaquin River channel caused by infiltration to groundwater or discharge from the shallow groundwater to the stream channel;
- measured streamflow losses; and
- temporary storage of water in the alluvial deposits along the riparian corridor as streamflow (i.e., stage) increases and subsequently declines during a storm event or pulse flow period. This alluvial storage may occur in ponds along the stream or within the gravel beds of the river alluvium.

The methods and assumptions for estimating these daily water budget terms are described in the remainder of this section.

2.7.2.2. Managed Releases of Water Assumptions

Managed releases of water from Friant Dam, Chowchilla Bifurcation Structure, Mendota Pool, Sack Dam, and the Sand Slough gate can be specified in San Joaquin River Model. Appropriate values for these flows were estimated using measured data. The San Joaquin River flow changes downstream from these release points were estimated in the water budget calculations.

Releases from Friant Dam supply riparian diversions along the San Joaquin River downstream to Gravelly Ford, the downstream end of Reach 1. There is a flow gage below Friant Dam and another flow gage at Gravelly Ford, with a nominal flow target of 5 cfs year-round. The flow through the California Department of Fish and Game Friant Fish Hatchery (currently 35 cfs) is discharged into the San Joaquin River approximately one mile downstream from Friant Dam. The hatchery flow is measured at the Friant Dam flow gage and is included in the USBR records of Friant Dam releases. During dry years, the seasonal pattern of releases can be used to estimate the net effects of diversions, evapotranspiration, and seepage along this 40-mile river segment (i.e., Reach 1). Separating diversions from seepage and evapotranspiration is more difficult.

Higher releases than those necessary for supplying riparian diversion are made from Friant Dam only when large rainfall events and anticipated snowmelt conditions force flood control releases. During high-flow events, the Chowchilla Bifurcation gates are used to divert water from the San Joaquin River into the Chowchilla Bypass and subsequently into the Eastside Bypass floodways. The Eastside Bypass flows return to the San Joaquin River at the Mariposa Slough confluence and at the Bear Creek confluence in Reach 5 (MEI 2000a, MEI 2000b).

The Delta-Mendota Canal delivers water from the Tracy Pumping Plant to the water districts that are collectively known as the exchange contractors. The Delta-Mendota Canal supplies water to the river at Mendota Pool, where a majority of the irrigation canals divert water. Some water is released from Mendota Pool and flows downstream in Reach 3 to Sack Dam and into the Arroyo Canal. Releases from Sack Dam at RM 182 are generally very small (leakage). Normally, most of the flow is diverted into the Arroyo Canal. However, during flood events, the flow past Sack Dam is recorded at the Dos Palos gage. Flood flows are generally diverted into the Eastside Bypass at the Sand Slough Control Structure at RM 168. Releases of water into the San Joaquin River channel downstream of the Sand Slough Control Structure are controlled by a gate; local landowners indicate that these gates have not been opened since at least before the 1997 flood. Flood flows from the Eastside Bypass return to the San Joaquin River in the Mariposa Bypass at RM 147 and the downstream end of the Eastside Bypass (Bear Creek confluence) at RM 136.

Historical daily flow records are available from below Friant Dam, at Gravelly Ford, at the Chowchilla Bifurcation, below Mendota Pool, below Sack Dam at Dos Palos (during high-flow periods), and at the Stevinson gage (downstream of the Eastside Bypass) in Reach 5. The historical flow records can be used to characterize the net flows along the San Joaquin River, but several reaches do not have sufficient concurrent flow data to adequately estimate flow losses (e.g., Reach 4 and Reach 5).

2.7.2.3. Agricultural Diversions Assumptions

Monthly estimates of agricultural diversions from the San Joaquin River are included in the San Joaquin River Model. DFG staff has provided a listing of diversion pumps and canals, based on comprehensive river surveys, but with only limited estimates of the capacity for diversion at each structure. Agricultural diversions are generally operated to satisfy a seasonal demand that follows the evapotranspiration pattern for the riparian vegetation. It is therefore difficult to distinguish between diversions and riparian evapotranspiration.

Table 2-12 gives the locations and sizes of the pumps identified by DFG along the San Joaquin River between Friant Dam and Gravelly Ford. If the diversion pipe size was measured, an assumed velocity of 5 feet per second (ft/sec) was used to calculate the diversion capacity. The actual water velocity in the pump will depend on the pump horsepower and the head (elevation difference) between the river and the discharge. If the horsepower of the pump was recorded (nameplate value), an assumed head of 20 feet was used to estimate the capacity of the diversion.

When aggregated by river mile, the potential diversion capacity between Friant Dam and Gravelly Ford was estimated to be 520 cfs (RM 229), much more than the maximum actual summer diversion rate of up to 200 cfs. The potential diversion capacity is larger than the actual net diversion because not all diversions are continuously operating at full capacity, and agricultural return flows allow re-use. The identified locations of the pumps were used to estimate the location of the main diversions along the San Joaquin River. As indicated in Table 2-12, the simulated diversions were assumed to be located at eight discrete river mile segments where the largest diversions were identified in the DFG survey. The percent of Reach 1 flow loss estimated in the model was longitudinally distributed by the concentration of pumps and their respective proportion of total pumping capacity (last column in Table 2-12).

The Delta-Mendota Canal deliveries and canal diversions from the Mendota Pool were not simulated. The release from the Mendota Dam to the Arroyo Canal, located at Sack Dam (Reach 3) was specified, based on the historical flows measured below Mendota Pool. Almost all of the San Joaquin River flow is diverted into the Arroyo Canal at Sack Dam, except during flood events. For restoration simulations, flow releases from Sack Dam and from the Sand Slough gate are specified. Agricultural diversions downstream of Sack Dam are limited because there is usually little dependable flow downstream of Sack Dam in the summer.

2.7.2.4. Evapotranspiration Loss Assumptions

Evaporation from the water surface of the river and adjacent ponds is a seasonal pattern that can be estimated from the surface area of the water and the measured seasonal evaporation rate (in inches per day [in/day]). Evaporation depends slightly on the water temperature, and the temperature model could calculate the rate of evaporation. However, a regional estimate, based on evaporation pan or meteorological measurements, is used in the model. Table 2-13 shows the average evaporation rates for the San Joaquin River region, calculated from the meteorological data (including effects of air temperature, solar radiation, wind, and humidity). The maximum monthly value in July is about 9 inches (0.30 in/day). The minimum value in December and January is approximately 1.0 inch (0.03 in/day). Evaporation is therefore expected to be about 10 times greater in the summer than in the winter. Transpiration from vegetation along the riparian corridor follows a similar seasonal pattern, although the riparian area and the rate of transpiration are more difficult to estimate. For restoration simulations, the San Joaquin River Model assumes that a fixed additional river width (or acres per mile) with a transpiration rate equal to the specified evaporation rate contributes to the evapotranspiration losses along the San Joaquin River. For the 40 river miles between Friant Dam and Gravelly Ford, which have an estimated river width of 200 feet (i.e., 969 acres), the maximum evapotranspiration loss is approximately 10 cfs.

Table 2-12. Estimates of diversions in Reach 1 from 2001 DFG surveys.

River Mile	Intake Size (Inches)	Horsepower (Hp)	A Estimated Flow From Intake Size (cfs)	B Estimated Flow From Horsepower (cfs)	Maximum of Columns A & B (cfs)	Sum by River Mile (cfs)	Cumulative Percent of Total Diversions	Percent Used in the Model
266.57 L	8		1.74		1.74	1.74	0.31%	
265.73 L	12		3.93		3.93			
265.20 L	7	15	1.34	5.25	5.25			
265.19 R	15	123	6.13	43.05	43.05			
265.13 R	12		3.93		3.93			
265.13 R	12		3.93		3.93			
265.13 R	12		3.93		3.93	64.00	11.51%	
264.75 L	7		1.34		1.34	1.34	11.75%	
263.45 R	12		3.93		3.93			
263.45 R	12		3.93		3.93			
263.06 L	12		3.93		3.93	11.78	13.81%	
262.72 R	6		0.98		0.98			
262.46 L	6		0.98		0.98			
262.46 L	10		2.73		2.73			
262.31 L	10		2.73		2.73			
262.16 R	36	10	35.33	3.50	35.33	42.74	21.30%	20%
261.65 L	8	10	1.74	3.50	3.50			
261.25 L	3		0.25		0.25			
261.21 R	12	25	3.93	8.75	8.75			
261.05 R	24	75	15.70	26.25	26.25			
261.00 L	8		1.74		1.74			
261.00 L	8		1.74		1.74	42.23	28.69%	
260.25 R	7	75	1.34	26.25	26.25			
260.25 R	7	75	1.34	26.25	26.25	52.50	37.89%	
259.95 L	3		0.25		0.25			
259.77 L	9	10	2.21	3.50	3.50			
259.67 L	10		2.73		2.73			
259.48 L	6	7.5	0.98	2.63	2.63			
259.48 L	10	7.5	2.73	2.63	2.73			
259.48 R	6	75	0.98	26.25	26.25			
259.47 L	10	60	2.73	21.00	21.00			
259.20 R	4	5	0.44	1.75	1.75			
259.00 L	7	20	1.34	7.00	7.00			
259.00 R	4	15	0.44	5.25	5.25	73.07	50.69%	30%
258.70 L	12	15	3.93	5.25	5.25	5.25	51.61%	
257.49 R	30	50	24.53	17.50	24.53	24.53	55.90%	5%
256.77 L	8		1.74		1.74			
256.33 R	7		1.34		1.34			
256.32 R	10		2.73		2.73			
256.31 L	3		0.25		0.25	6.05	56.96%	
254.90 R	7	10	1.34	3.50	3.50			
254.90 R	7	10	1.34	3.50	3.50	7.00	58.19%	
253.95 L	13		4.61		4.61			
253.40 L	16	30	6.98	10.50	10.50	15.11	60.83%	5%
252.28 R	8		1.74		1.74	1.74	61.14%	
251.60 R	7		1.34		1.34			
251.57 R	15		6.13		6.13			
251.16 R	7		1.34		1.34	8.80	62.68%	
249.66 R	7		1.34		1.34	1.34	62.92%	
248.00 R	36		35.33		35.33	35.33	69.10%	10%
246.88 R	48	100	62.80	35.00	62.80	62.80	80.10%	10%
245.41 R	36	75	35.33	26.25	35.33	35.33	86.29%	
240.56 L	12		3.93		3.93	3.93	86.98%	5%
230.89 L	5		0.68		0.68			
230.13 R	5		0.68		0.68			
230.06 R	10		2.73		2.73			
230.06 R	10		2.73		2.73	6.81	88.17%	
229.85 R	10		2.73		2.73			
229.56 R	4	10	0.44	3.50	3.50			
229.35 L	8	20	1.74	7.00	7.00			
229.35 L	8		1.74		1.74	14.97	90.79%	
228.89 R	12		3.93		3.93			
228.78 R	24	60	15.70	21.00	21.00			
228.78 R	24	60	15.70	21.00	21.00	45.93	98.84%	15%
227.72 R	10		2.73		2.73	2.73	99.31%	
222.75 R	12		3.93		3.93	3.93	100.00%	
					570.96	570.96		100%

Table 2-13. Average monthly evapotranspiration estimates from California Irrigation Management Information Systems meteorological stations.

Normal Year ETO's from CIMIS webpage
http://wwwdpla.water.ca.gov/cimis/cimis/hq/sjdnorm.htm

CIMIS ID	80			145	56	148
	Fresno	Friant	Kerman	Madera	Los Banos	Merced
Jan	0.9	1.2	0.9	0.9	1	1
Feb	1.6	1.5	1.5	1.4	1.5	1.5
Mar	3.3	3.1	3.2	3.2	3.2	3.2
Apr	4.8	4.7	4.8	4.8	4.7	4.7
May	6.7	6.4	6.6	6.6	6.1	6.6
Jun	7.8	7.7	7.7	7.8	7.4	7.9
Jul	8.4	8.5	8.4	8.5	8.2	8.5
Aug	7.1	7.3	7.2	7.3	7	7.2
Sep	5.2	5.3	5.3	5.3	5.3	5.3
Oct	3.2	3.4	3.4	3.4	3.4	3.4
Nov	1.4	1.4	1.4	1.4	1.4	1.4
Dec	0.6	0.7	0.7	0.7	0.7	0.7
Total	51	51.2	51.1	51.3	49.9	51.4

Evapotranspiration loss rates are expected to be comparable in the other reaches because the meteorological conditions are similar; however, the varying degrees of riparian vegetation along the channel will result in some reach-by-reach variation. The riparian width estimates that are specified in the model for each 1-mile segment will determine the total evapotranspiration losses in these reaches.

2.7.2.5. Seepage Losses Assumptions

Seepage loss along the San Joaquin River is difficult to estimate because the physical properties of the riverbed and alluvial channel below the river are generally unknown. The San Joaquin River Model assumes that the seepage is controlled by the width of the alluvial channel below the river that is saturated with water at low flow. The model specifies a characteristic seepage rate (i.e., infiltration) for each reach. This rate may depend on the soil properties and the head difference thought to control the groundwater flows below the river.

Because the alluvial width and the seepage rate are unknown, the combined seepage loss in cubic feet per second per mile can be used to guide these estimates. The alluvial width can be roughly estimated from the basic geologic description of the river. The model allows the alluvial width to be specified for each mile and the seepage rate to be specified for each reach. For example, a steady-state ("filling" rate is higher when flow changes first occur) seepage rate of 2 in/day has been estimated for Reach 2 between Gravelly Ford and the Mendota Pool, and the alluvial width is assumed to be approximately 500 feet. This alluvial width and seepage rate give a seepage loss of approximately 8.5 cfs per mile, for a total loss of 100 cfs for the 12 miles between Gravelly Ford and the Chowchilla Bifurcation Structure. This magnitude of loss is generally confirmed by the periods of flow data at the Chowchilla Bifurcation Structure (Figure 2-4) and by measurements during the Riparian Restoration Pilot Project in 1999 and 2000. A similar approach of estimating seasonal seepage losses was taken for the reach between Friant Dam and Gravelly Ford, with seasonal values shown in Table 2-14.

Seepage losses in the Mendota Pool and Reach 3 between Mendota and Sack Dam are unknown. Seepage may actually be into the river channel from surrounding agricultural lands (shallow groundwater) in Reaches 4 and 5. The model allows the seepage widths to be estimated for each mile and the seepage rates (positive losses only) to be specified for each reach.

2.7.2.6. Measured Streamflow Losses Assumptions

Measured data were used to estimate streamflow losses used by the San Joaquin River Model. In Reach 2A, the USBR has measured daily streamflow at Gravelly Ford and at the Chowchilla Bifurcation Structure for several years. During periods of no rainfall, the difference between the Friant Dam releases and the flows at downstream locations is a direct measure of the total losses to diversions, evapotranspiration, and seepage. The records from 1987 to 2001 have been graphically evaluated to provide monthly estimates of these flow losses. Because there are no diversions between Gravelly Ford and the Chowchilla Bifurcation Structure, and vegetation density is low resulting in low evapotranspiration rates, the losses along Reach 2A are driven by seepage and are expected to be fairly constant.

Daily streamflow measurements and loss estimates were made for 1987-1999 by subtracting flows measured at Friant with flows measured at Gravelly Ford and at the Chowchilla Bifurcation Structure. This evaluation provided additional details to the flow loss curves presented in Figure 2-4, but this evaluation also illustrated significant variability.

Between the Friant gaging station and Gravelly Ford (approximately 38 river miles), a minimum flow of 105 cfs is needed at the Friant gage to get a measurable flow at the Gravelly Ford gage, suggesting that the minimum seepage loss outside the irrigation season is 105 cfs (2.8 cfs/mile). This correlates well with Figure 2-4. Some years have larger losses (up to 154 cfs) during the winter (non-irrigation) season, perhaps due to some diversion for gravel mining operations in Reach 1. Flow losses increase during the irrigation season as riparian diversions are utilized. Flow losses increase to approximately 130 cfs to 250 cfs during the summer and fall irrigation season.

Between the Gravelly Ford gaging station and Above Chowchilla Bifurcation Structure gaging station (approximately 13 river miles), a minimum of 75 cfs is needed at the Gravelly Ford gage to get a measurable flow at the Above Chowchilla Bifurcation Structure gage, suggesting that the minimum seepage loss outside the irrigation season is 75 cfs (5.8 cfs/mile). This reach has had the greatest depletion in shallow groundwater aquifer due to overdraft, which is likely reflected in the larger unit-length seepage loss rate. This minimum seepage rate also correlates well with Figure 2-4. There do not appear to be as significant seasonal pattern to flow losses between the irrigation season and winter season (as occurred between Friant and Gravelly Ford). Maximum flow losses are approximately 250 cfs, with several years having intermediate "plateaus" of flow loss. These intermediate values of flow losses are likely due to varying degrees of riparian withdrawals in the reach during those times when there are flows in the river.

Losses in 1998 and 1999 are also review specifically, although these two single years do not necessarily reflect normal flow losses due to varying degrees of diversion and groundwater pumping on a year-to-year basis. Based on 1998 pilot project results in 1998, high flows occurred through July. Through July 1998, the combination of large variable local inflows from tributaries and releases from Friant Dam makes flow loss estimates difficult. During August and September 1998, the losses between Friant Dam and Gravelly Ford were about 100–150 cfs, and less for most of the rest of the year. For August through mid-November 1998, the losses between Gravelly Ford and the Chowchilla Bifurcation Structure were relatively constant at about 100 cfs. In 1999, the first year of Friant Dam releases were provided for the riparian vegetation pilot project. A seed dispersal flow of approximately 600 cfs in early July 1999 was followed by an establishment period that had a controlled flow recession through October. Losses from Friant Dam to Gravelly Ford declined from about 150 cfs in July to about 50 cfs in December. Losses between Gravelly Ford and the Chowchilla Bifurcation Structure were about 100 cfs in July, then approximately 80 cfs in August; when Gravelly Ford flows declined to less than 75 cfs, no flow was measured at the Chowchilla Bifurcation Structure.

Lastly, flow losses between the Chowchilla Bifurcation Structure and Mendota Pool (Reach 2B) are considered negligible due to the backwater of Mendota Pool and shallow groundwater recharge by the Mendota Pool backwater.

Table 2-14 provides a monthly summary of the loss estimates from the 1987-2001 daily flow records. For simulation of future San Joaquin River restoration conditions, a monthly value that exceeds most of the measured loss rates was used. The separation of these total losses into the evapotranspiration, diversion, and seepage variables was accomplished with some comparative simulations of the San Joaquin River Model. The seepage rate was set to provide a constant loss that matches the lowest monthly values measured in the November–January periods. The estimated seepage loss from Reach 1 (Friant to Gravelly Ford) is approximately 60 cfs. For the estimated alluvial width of 500 feet along the 40 miles of river, this loss corresponds to a seepage rate of 0.5 in/day. For Reach 2 (Gravelly Ford to Mendota Dam) the seepage loss is estimated to be 120 cfs (20% more than the Gravelly Ford to the Chowchilla Bifurcation Structure loss estimate of 100 cfs). This somewhat contradicts earlier assumptions that flow loss between the Chowchilla Bifurcation Structure and Mendota Dam is negligible; however, this assumption was nonetheless used in the model. This assumed 120 cfs loss corresponds to a seepage rate of 2 in/day for the assumed alluvial width of 500 feet along this 20-mile river reach.

2.7.2.7. Water Budget Results

The water budget analysis indicates that baseflows generally decrease in the downstream direction to Mendota Dam, where flows increase due to contribution of water imported from the Delta-Mendota Canal. Flows are steady downstream to Sack Dam, where all flow is removed from the river. Flows remain at near zero discharge downstream to the Mariposa Bypass, where the annual flow volume increases in the downstream direction as a result of tributary inflows and delivery of flow from the Chowchilla Bypass/Eastside Bypass system back into the mainstem San Joaquin River. Figures 2-40 through 2-42 graphically illustrate the longitudinal variation in average discharge along the reach for the winter baseflow period, spring snowmelt period, and summer baseflow period; however, this figure is based on average computations described below and these “average” conditions do not accurately represent typical flows in this reach. For example, Reach 4B is perennially dry, yet Figures 2-40 through 2-42 suggest that there is a small amount of flow in the reach. The magnitudes of the annual and seasonal average flows are summarized in Table 2-15. The more general flows illustrated in Table 2-10 are typical values based on a more generalized review of USGS gaging records and typical operation of Friant Dam, Mendota Dam, and Sack Dam. The trend of decreasing baseflows in the downstream direction was most likely much different than unimpaired conditions, where artesian springs and downstream tributaries draining the Sierra Nevada augmented baseflows. Examination of flows at the San Joaquin River at Fremont Ford gage between 1938-1943 show a decrease in baseflow, likely due to agricultural diversions (e.g., Mendota Dam was diverting flows in the late 1800’s).

Table 2-14. Monthly Loss Estimates for Reach 1 and Reach 2 based on USGS daily flow records at Friant, and USBR Daily Flow Records at Gravelly Ford and the Chowchilla Bifurcation Structure, all rounded to the nearest 25 cfs.

A. Friant to Gravelly Ford Losses (cfs)

Year	1987	1988	1989	1990	1991	1992	1993	1994	1995	1996	1997	1998	1999	2000	2001
January	40	50	50	75	100	100	100	75		75		75	75	75	75
February	50	75	75	100	125	100		100					75		75
March	50	100	125	125		125		125							
April	100	100	125	150	125	175		150							125
May	125	150	175	175	175	200		175			150		100	100	150
June	150	175	200	200	200	225		225		175	175				
July	175	200	200	225	225	250	200	250		200	200		175	150	
August	150	175	175	200	200	250	175	225		175	150	150	150	150	
September	100	150	150	175	175	225	150	200	75	175	150	150	125	150	
October	100	125	125	150	150	200	125	125	75	150	125	125	100	125	
November	50	100	100	125	125	125	100	100	100	100	100		75	100	
December	50	75	100	100	100	100	75	100	50	75	75		75	100	

B. Gravelly Ford to Bifurcation Losses (cfs)

Year	1993	1994	1995	1996	1997	1998	1999	2000	2001
January						100	75		
February							75		
March							50		
April							75		
May	>75				50		75		
June				100	>150				
July	>100				>100		100		
August	>125		150		75	100	100		
September	>100		100		75	100	75		
October			50		75	100	>50		
November					>100	100			
December					>100				

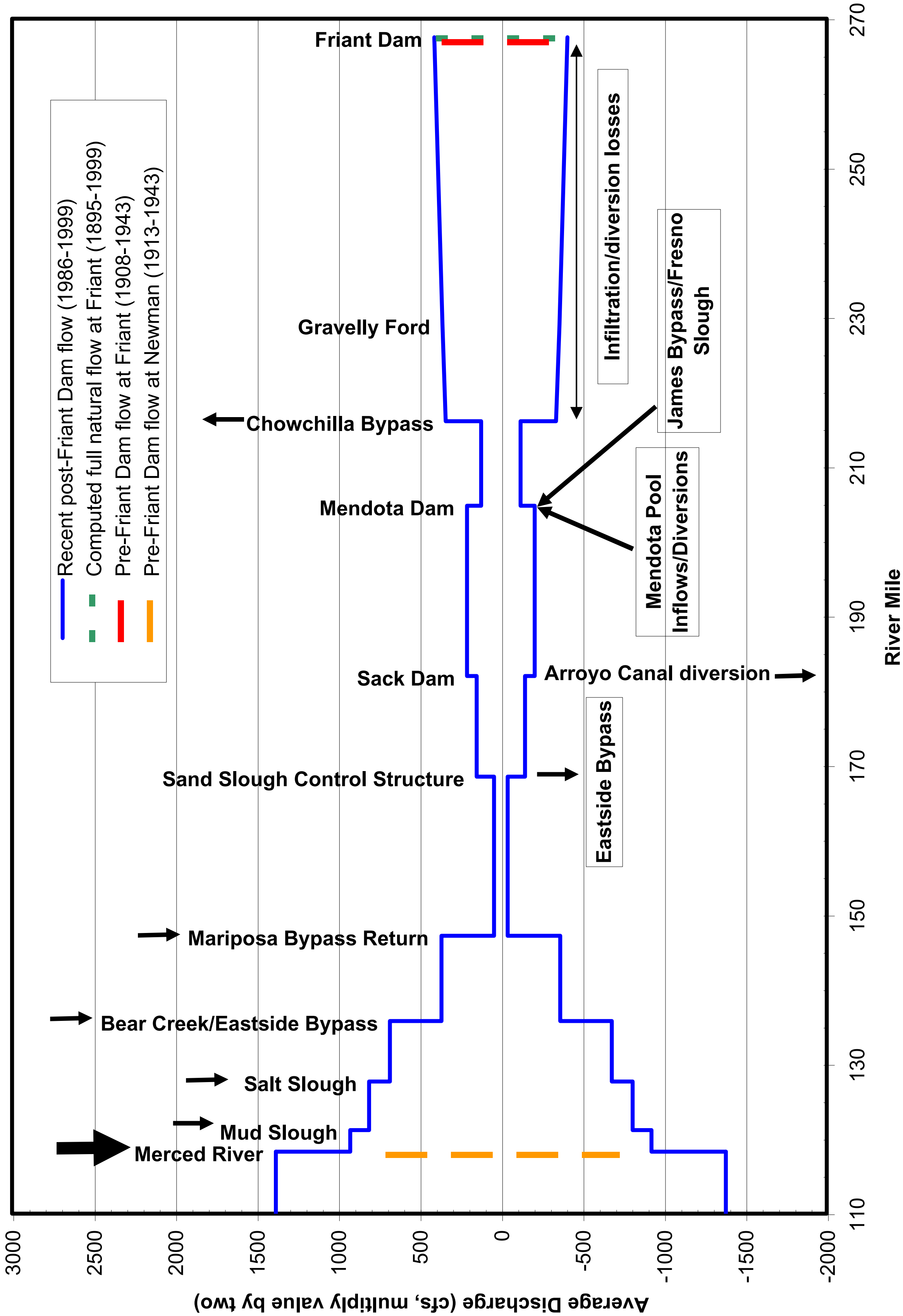

Figure 2-40. Longitudinal variation in average discharge by subreach between Friant Dam and the Merced River for winter baseflow period (December 1-March 31).

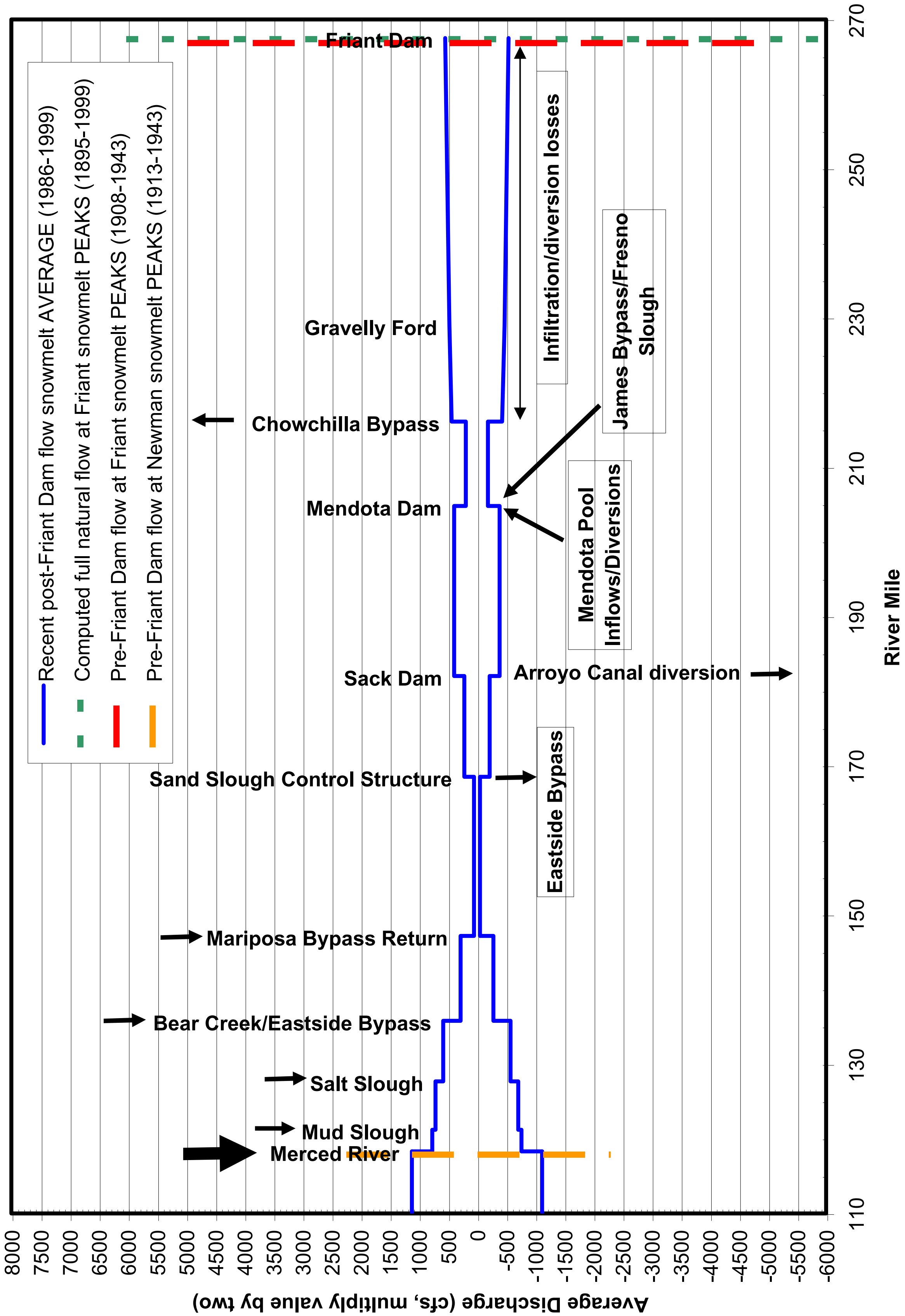

Figure 2-41. Longitudinal variation in average discharge by subreach between Friant Dam and the Merced River for spring snowmelt period (April 1-July 31).

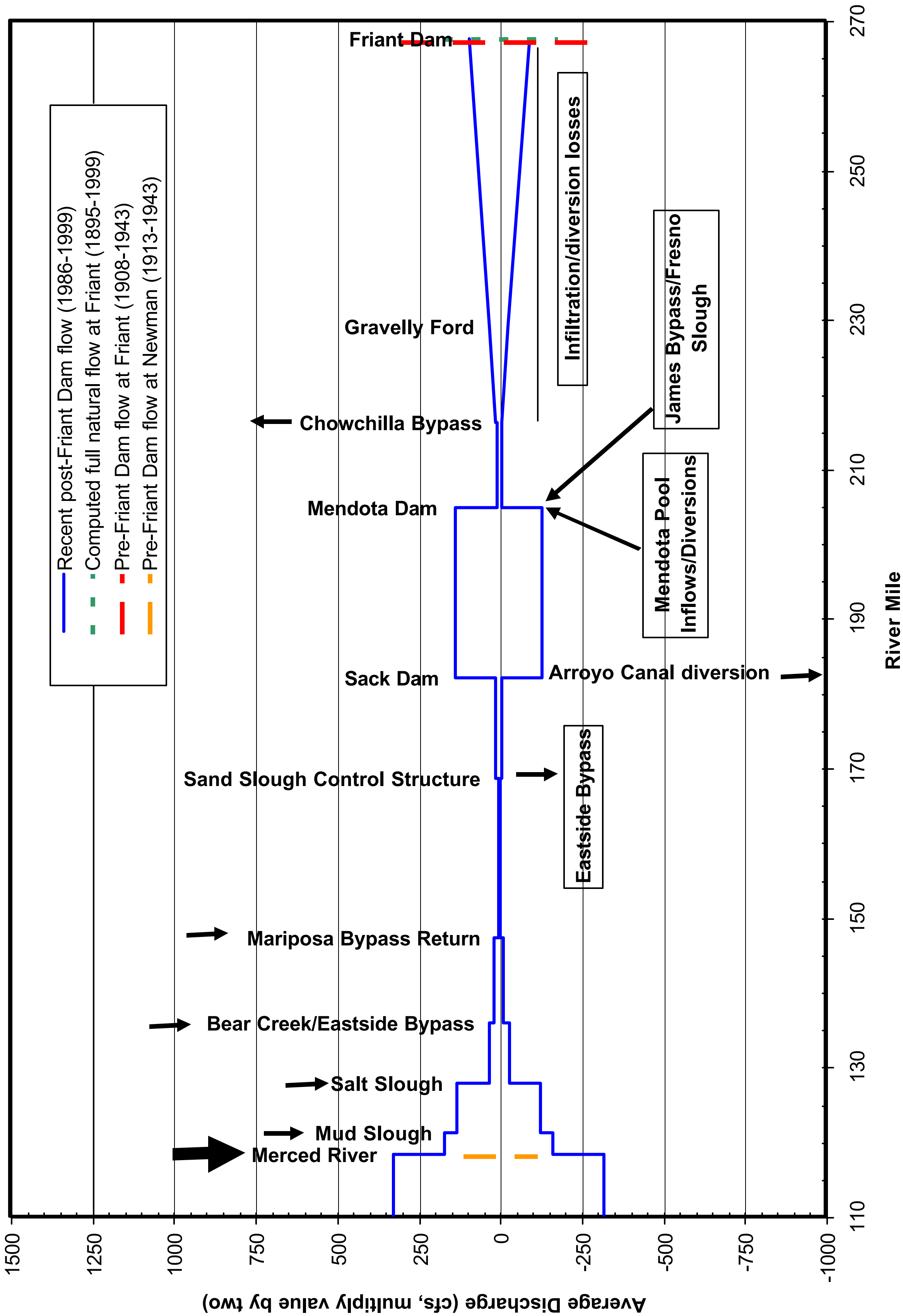

Figure 2-42. Longitudinal variation in average discharge by subreach between Friant Dam and the Merced River for summer baseflow period (August 1-November 31).

Table 2-15. Annual runoff and average annual seasonal discharge by subreach in the San Joaquin River between Friant Dam and the Merced River. "Node" refers to nodes used in the San Joaquin River Model. Note that 1986-1999 data are computed averages, and do not necessarily reflect typical flow conditions for a given reach.

Node	Description	Average Annual Runoff (acre-ft)	Seasonal Discharge Summer Baseflows (cfs)	Seasonal Discharge Winter baseflows (cfs)	Seasonal Discharge Spring Snowmelt (cfs)
Pre-Friant Dam from USGS					
1	Friant Dam (1908-1943)	1,727,000	600[2]	711[2]	9,900[3]
11	downstream from Merced River (1913-1943)	1,866,000	220[2]	1,400[2]	4,437[3]
	Full Natural Flow from Madeheim (1999)				
1	Friant Dam (1895-1999)	1,812,000	340[2]	780[2]	12,000[3]
1986-1999					
San Joaquin River					
1	Friant Dam	504,000	185	816	1,088
2	Gravelly Ford	415,000	55	718	947
3	upstream from Bifurcation Structure	384,000	20	677	869
3-4	Bifucation Structure to Mendota Pool	153,000	15	242	379
4-5	Mendota Dam to Sack Dam	353,000	266	415	782
5-6	Sack Dam to Sand Slough Control Structure	181,000	20	296	435
6-7	Sand Slough Control Structure to Mariposa Bypass	46,000	6	84	101
7-8	Mariposa Bypass to Bear Creek	318,000	31	729	562
8-9	Bear Creek to Salt Slough	621,000	60	1,363	1,155
9-10	Salt Slough to Mud Slough	794,000	255	1,618	1,421
10-11	Mud Slough to Merced River	896,000	332	1,848	1,535
11	downstream from Merced River	1,360,000	645	2,762	2,237
Inflows/outflows					
1-2	Losses between Friant Dam and Gravelly Ford	-89,000	-129	-97.5	-140.1
2-3	Losses between Gravelly Ford and Bifurcation Structure	-31,000	-35	-41.3	-78
3	Chowchilla Bypass	-231,000	-5	-442	-511
4	James Bypass (Fresno Slough)	136,000	1	223	341
4	Gains and losses in Mendota Pool[1]	64,000	250	-50	62
5	Arroyo Canal	-172,000	-246	-119	-347
6	Eastside Bypass	-135,000	-15	-212	-334
7	Mariposa Bypass	272,000	25	645	461
8	Bear Creek	39,000	21	120	21
8	Eastside Bypass	264,000	8	514	572
9	Salt Slough	173,000	195	255	266
10	Mud Slough	102,000	77	230	115
11	Merced River	465,000	312	914	702

Table 2-15. Cont.

[1] The indicated flows represent the combination of imported flows from the Delta-Mendota Canal and other gains and losses associated with flow bypasses and groundwater interaction

[2] Median values, obtained from hydrograph component analysis

[3] Median values of snowmelt PEAK from hydrograph component analysis

This information was used to help develop the San Joaquin River Model. Application of the model to a hydrograph is shown in Figure 2-43, where measured and simulated daily baseflow patterns between Friant Dam and Gravelly Ford are compared for June 2001. The total diversions simulated were 100 cfs, with about 60 cfs of seepage and 10 cfs of evapotranspiration losses. The total depletions between Friant Dam and Gravelly Ford were similar to the data for the first 15 days of June. During the pulse flow event, there was a distinct lag of approximately three days in the flows at Gravelly Ford. In addition, the losses between Friant Dam and Gravelly Ford apparently increased slightly during the pulse flow of 400 cfs. The simulated losses remained the same throughout June. Subsequently, as the flow pulse ended, the flows at Gravelly Ford decreased approximately four days after the drop in flow at Friant Dam. This example suggests that the model reasonably predicts lower flows at downstream gages, but over-predicts higher baseflows at downstream gages. The model also does a reasonable job in predicting the flow attenuation and travel times (Figure 2-43). Further refinements have been made to the model to improve hydrograph predictions.

2.8. FLOOD FLOW ROUTING

This section discusses historic flood flow routing based on historical accounts and maps, then describes existing flood flow routing within the San Joaquin River Flood Control Project. Chapter 5 describes the flood control project in more detail. Existing flood flow routing is described in this report by comparison of discrete hydrographs from several gaging stations between Friant Dam and the Merced River. Finally, a flood routing model has been developed for the study reach in which existing and future high flow hydrographs can be predicted longitudinally. This flood routing model is then used to evaluate historic and existing flood inundation areas.

2.8.1. Historical and Existing Flood Flow Routing

Historic flood routing is fairly straightforward: much of the valley floor along the river corridor was under water, with most San Joaquin River flow routing north to the Delta. There were times, however, when high flows from the San Joaquin River flowed into the Fresno Slough and times when high flows from the Kings River flowed into the San Joaquin River via Fresno Slough. Derby's 1852 map illustrates how this two-way flood flow routing occurred; San Joaquin River flows sometimes exited from the San Joaquin River channel in Reach 2B via high flow sloughs, and connected with Fresno Slough. In our review of the historic literature, primarily Derby's first-hand accounts and map (Derby 1850, 1852) (Figure 2-37) of the Fresno Slough-San Joaquin River confluence during the snowmelt runoff period of 1850, it appears that high water flowed from the San Joaquin River through sloughs to the Fresno Slough, which then carried these flows north back to the San Joaquin River. In traversing west along the divide between Tulare Lake and the San Joaquin River, Derby (1850) states:

> *"We…crossed no less than eight distinct sloughs, one of which we were obliged to raft over, before arriving at the Sanjon [Fresno Slough]. In all of these sloughs a strong current was running southwest, or from the San Joaquin River to the [Tulare] lake. The Sanjon is a large and deep slough about forty miles*

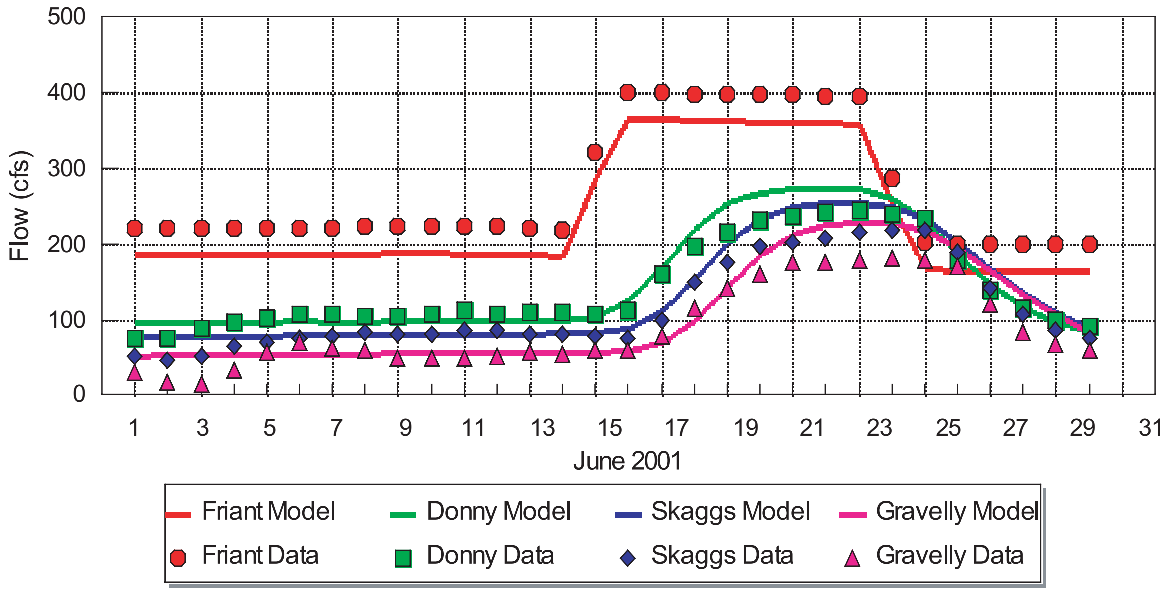

Figure 2-43. June 2001 baseflow pulse on the San Joaquin River to compare flow routing model results with measured flows.

> *in length, connecting the waters of the lake with the San Joaquin River, with which it unites at its great southern bend [at the present location of Mendota]. At this time [May 23, 1850] it was about two hundred and forty feet in width, and with an extremely slow current setting towards the river. I do not think it possible to communicate directly with the lake through this slough. An attempt has been made a week or two previous to our arrival by a party of men in a whaleboat, who examined it for twenty or thirty miles, and found it branching off into innumerable smaller sloughs, which intersected the tule swamp in every direction."*

A portion of high flows from the Kings River certainly flowed through Fresno Slough to the San Joaquin River under historical conditions, and still does occasionally under existing conditions (see Figure 2-37). There was also speculation in the literature on whether the Tulare Lake would rise to the point where it would overflow into the Fresno Slough into the San Joaquin River (as implied on Figure 2-37); however, the elevation of the Tulare Lake surface would have to have risen 30 to 35 feet for this to occur (CDPW, 1931). If this lake overflow did in fact occur, the frequency is not known. Flood flows from streams draining the east side of the valley would empty into the extensive flood basin in Reaches 4 through 5, such that the flood basin was a buffer between the tributary stream and the mainstem San Joaquin River.

The substantial storage capacity of this flood basin had a substantial influence on flood routing through the San Joaquin River valley. Comparing flood peaks for pre-Friant Dam floods between the San Joaquin River at Friant gaging station and the San Joaquin River at Fremont Ford gaging station shows flood peaks were reduced substantially by the large storage capacity of the flood basin even though there was already a substantial number of levees constructed by 1943 (Figure 2-33).

The most significant changes to flood routing under existing conditions are caused by the San Joaquin River Flood Control Project. This project bypasses flood flows from the San Joaquin River at the

Chowchilla Bifurcation Structure and Sand Slough Control Structure, and routes these high flows through the Chowchilla Bypass, the Mariposa Bypass, and the East Side Bypass (Figure 2-44). In addition, the East Side Bypass captures any flood flows from the Fresno River, Chowchilla River, and Bear Creek. The floodway width is much narrower due to confining levees of the flood control project along the river and in the bypasses, and this likely decreases travel time and reduces flood peak attenuation. High flows can still occasionally spill from the San Joaquin River in Reach 2B into Fresno Slough, as happened in 1997 (ACOE 1999), but the reduction in flood magnitude from Friant Dam and levees constructed along Reach 2 greatly reduces the frequency of this occurring. High flows on the Kings River frequently route through James Bypass and Fresno Slough into the San Joaquin River, as illustrated in the James Bypass flood frequency data (Figure 2-14). While flood peak attenuation under existing conditions is likely much less than prior to construction of the San Joaquin River Flood Control Project, flood peak attenuation under existing conditions is still substantial. The following sections evaluate several recent flood hydrographs using gaging stations along the length of the study reach.

The following two sections evaluate 1986 and 1995 flood hydrographs using gaging stations along the length of the study reach. These two years were chosen because they had discrete high flow events that could be easily tracked on gaging records, and these two flood years occurred during a period where there was a larger number of gaging stations through the San Joaquin River and flood control bypasses to provide more calibration points for the flood routing model.

2.8.1.1. Empirical Results of 1986 High Flow Event

During the 1986 high flow event, the peak release from Friant Dam was 7,950 cfs, which occurred on March 11 (Figure 2-45). The recorded peak flow at the Gravelly Ford gage of 7,975 cfs occurred on March 17, 1986. However, the primary component of the rising limb of the Gravelly Ford hydrograph began to level off at about 7,650 cfs on March 12. Comparison of the rising limbs of the Friant and Gravelly Ford hydrographs indicates an approximate 1-day time lag in the flows between the two locations (in contrast to low flow period when it takes 4 to 5 days for flow change at Friant Dam to fully show up at Gravelly Ford). A similar pattern occurred between the Gravelly Ford gage and the measured flows into the head of the Chowchilla Bypass, with an approximately 1-day time lag between Gravelly Ford and the Chowchilla Bifurcation Structure. Inflows to the Chowchilla Bypass peaked at 7,380 cfs on March 22, but the primary part of the rising limb of the hydrograph began to level off at about 6,910 cfs on March 11. The data are based on mean daily flows; thus, the timing of peak and other components of the hydrographs indicated by the data may be up to one day off from the actual timing that occurred in the river.

Measured flows at the Dos Palos gage peaked at 5,030 cfs on March 19. These flows are affected by diversions into the Chowchilla Bypass, inflows and outflows at Mendota Dam associated with the various canals and the James Bypass/Fresno Slough, and diversions into the Arroyo Canal.

The peak discharge at the Stevinson gage near the downstream end of the reach of 17,300 cfs occurred on March 17. At the Fremont Ford gage, which is approximately 8 miles downstream, the peak discharge of 18,100 cfs occurred on March 18, 1986. Comparison of the rising limbs of the hydrographs indicates an approximately 1.7-day time lag.

The rising limb of the Gravelly Ford hydrograph and the early part of the Stevinson hydrographs overlap. Because of the significant distance between the two gage locations, a several-day time lag is expected, which indicates that tributary inflows were responsible for the early part of the rising limb at the Stevinson gage.

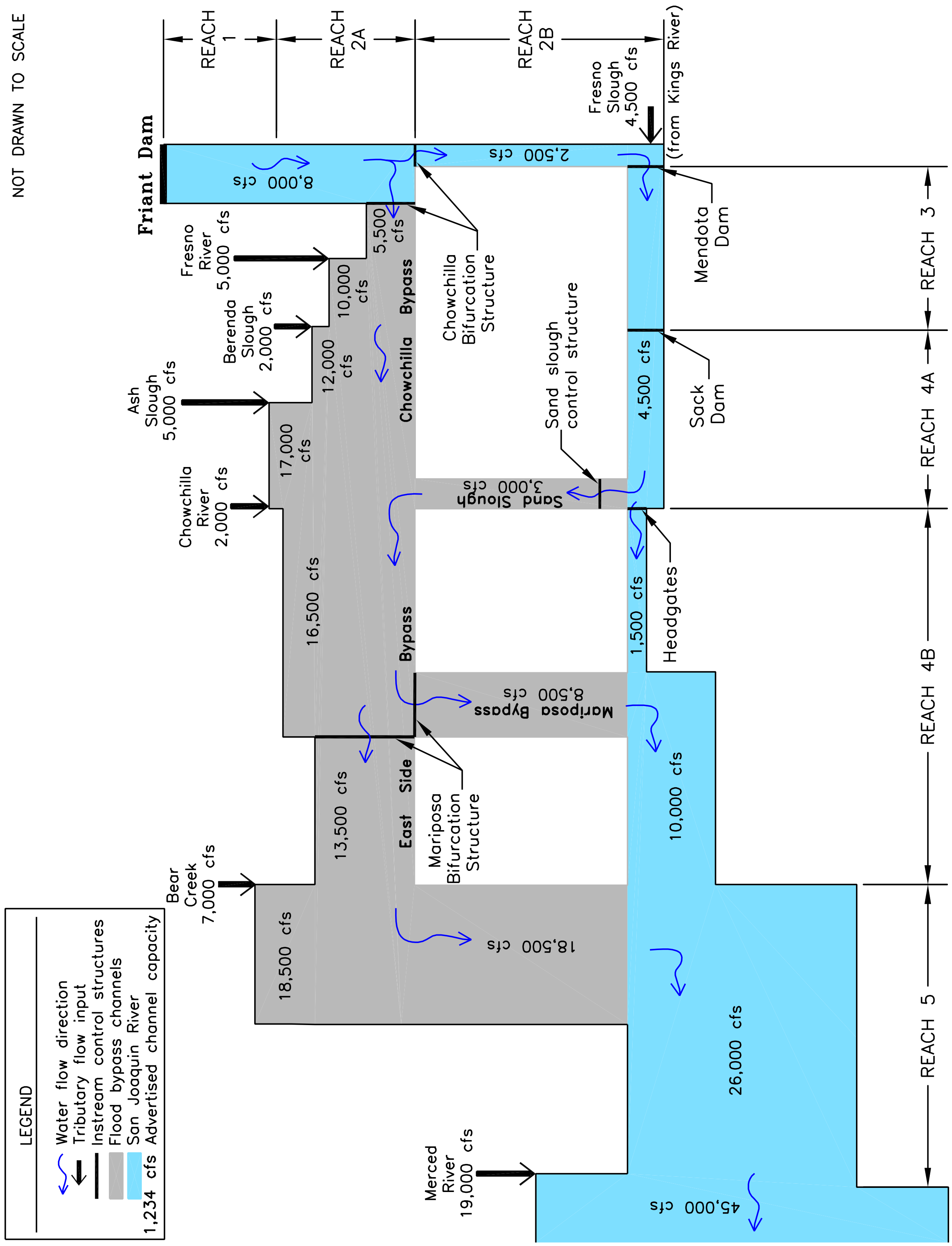

Figure 2-44. Schematic map of structures, flood routing, and reach hydraulic capacity of the San Joaquin River Flood Control Project.

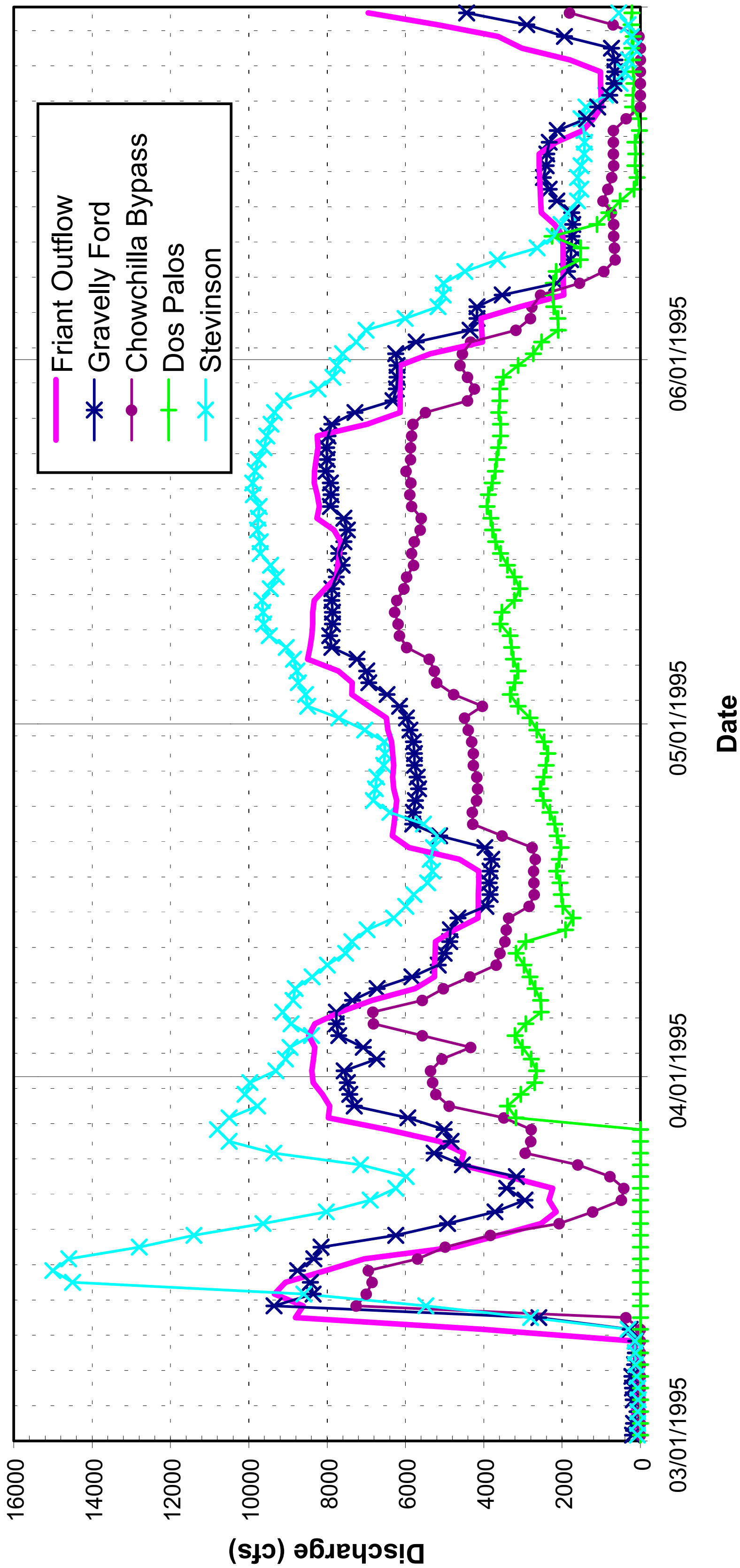

Figure 2-45. Measured mean daily flow hydrographs for the 1986 high flow event at five mainstem San Joaquin River gages.

2.8.1.2. Empirical Results of 1995 High-Flow Event

During the 1995 event, the primary part of the Friant release hydrograph began to level off at about 8,810 cfs on March 11, and the peak of the hydrograph of 9,350 cfs occurred on March 13 (Figure 2-46). At Gravelly Ford, the hydrograph peaked at 9,359 cfs on March 12. Comparison of the rising limbs of the hydrographs indicates an approximately 1-day time lag, which is very similar to the time lag that occurred in the 1986 event. The peak discharge into the Chowchilla Bypass of 7,255 cfs occurred on March 12, and the rising limbs of the hydrograph indicate less than 1 day of time lag between Gravelly Ford and the Chowchilla Bifurcation Structure.

According to the measured flow records, the rising limb of the hydrograph at the Dos Palos gage occurred over a 1-day period from March 27 to 28, and the initial peak of the hydrograph of 3,400 cfs occurred on March 29. The gage records indicate that there was no flow in the river until March 28, which leaves one to suspect that the gage may have been inoperable during the period prior to March 17; thus, the above statement regarding the timing of the rising limb at this location should be treated with caution.

At the Stevinson gage, the peak discharge of 15,000 cfs occurred on March 15, and the early part of the rising limb of the hydrograph exhibits approximately the same timing as occurred at the Gravelly Ford gage. This again indicates that inflows from tributaries closer to the Stevinson gage were responsible for the early rise in flows at that location.

2.8.2. Flood Routing Model

Because the measured hydrographs include inflows from tributaries for which data are not available and the hydrographs do not represent all of the locations of interest, flow routing models were developed and calibrated for each event. These models are not to be confused with the water budget model described in Section 2.7.2. The flow routing models were developed using a combination of the HEC-1 Flood Hydrographs Package and the HEC-2 Water-Surface Profile computer programs (ACOE 1990a and 1990b). The procedures for using these programs to perform river routings are described in Corps Training Document No 30 (ACOE 1990c), and details of the application for this specific project are described in MEI (2000a and 2000b). In general, the procedure involves use of the Modified Pulse storage routing method (Chow 1959), which consists of repetitive solution of the continuity equation assuming that the outflow is a unique function of storage.

When applying this method to rivers, the overall routing reach is subdivided into several subreaches, a storage-outflow relationship is developed for each subreach, and the inflow hydrograph is routed through the overall reach by assuming that the subreaches represent a series of reservoirs, with the inflow to each successive reservoir being the computed outflow from the next upstream reservoir. The storage-outflow relationship for each subreach is developed from the HEC-2 model, based on the total volume of water in the subreach computed from the cross sectional areas and distances between cross sections for each modeled discharge. Calibration of the model is achieved by adjusting the number of reaches and the length of the routing time step until modeled results match, to within a reasonable tolerance, observed hydrographs. Data used in the water-surface profile analysis (HEC-2) were derived from surveys performed by Ayres Associates in 1997 for the ACOE and the USBR, supplemented with additional field survey data collected in 1999, information obtained from plans for various structures along the reach, and where appropriate, from the modern and historical USGS 7½-minute quadrangle maps. Discharge data used in the analysis were taken from available stream gage records along the reach.

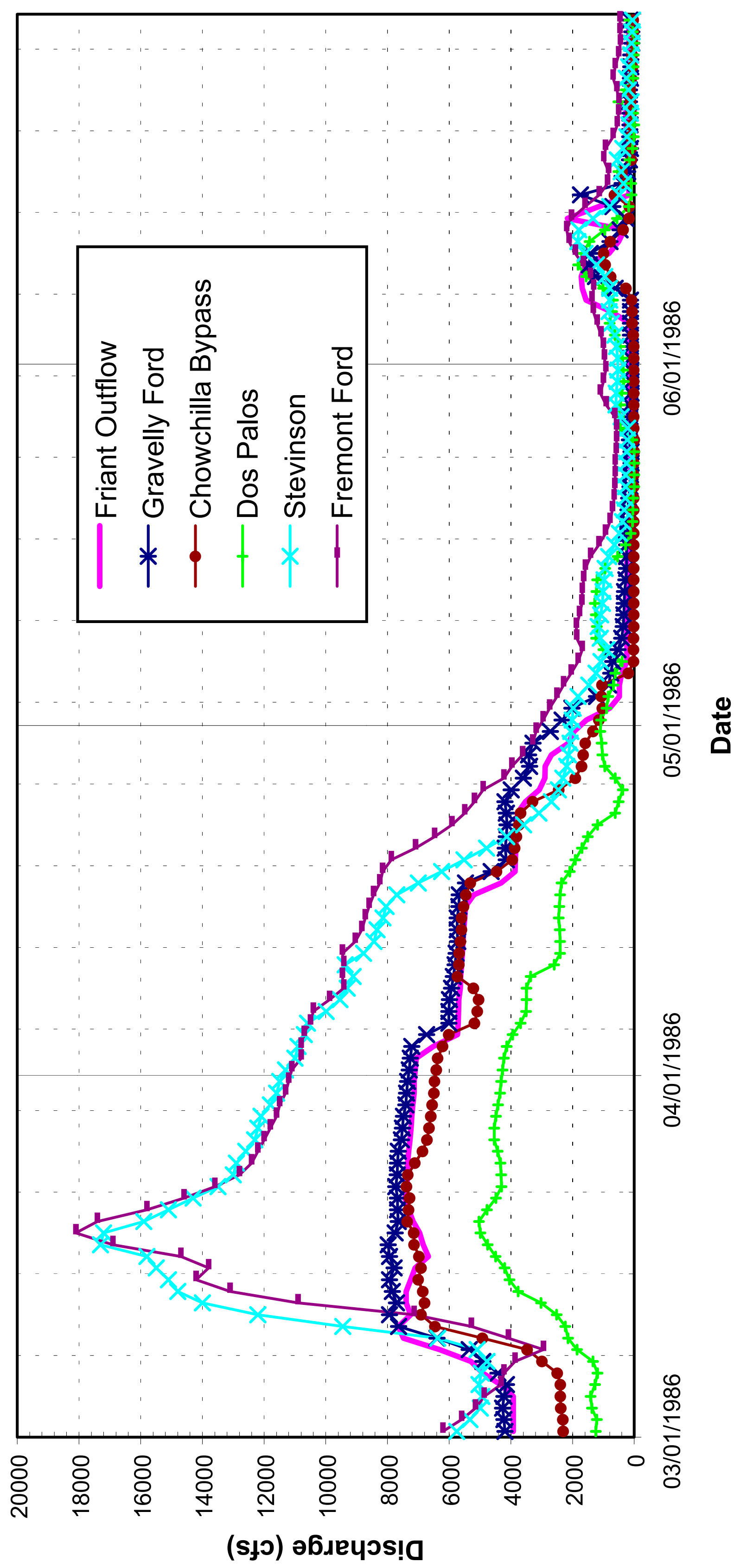

Figure 2-46. Measured mean daily flow hydrographs for the 1995 high flow event at five mainstem San Joaquin River gages.

2.8.2.1. Model Calibration from Friant Dam to Mendota Dam

The flow-routing models were developed and calibrated for the 1986, 1995, and 1999 high flow events to provide a means of evaluating storage and attenuation effects along the study reach. These two high flow events were chosen for calibration because they occurred during a period when many gaging stations were in operation on the mainstem San Joaquin River and Eastside Bypass, which improved calibration. The model for the portion of the reach between Friant Dam and Mendota Dam was initially calibrated using the experimental releases that were made from Friant Dam during June, July, and August 1999. Inflows to the upstream end of the reach were taken from the USGS real-time data at the San Joaquin River below Friant Dam gage, and the flows at Gravelly Ford that were used as a basis for the calibration were taken from real-time flows published on the California Data Exchange web site. The HEC-2 model for the reach includes numerous locations where portions of the overbanks and in-channel gravel pits were blocked from the computations to account for ineffective flow areas to improve the reasonableness of the model results for evaluating the in-channel hydraulics. These ineffective flow areas are important to the flow routing, however, because they store significant amounts of water that can affect hydrograph attenuation and translation through the reach. In addition, the available 2-foot contour mapping on which the cross sections in the HEC-2 model were based covers only a limited amount of the floodplain, and in some cases does not include all of the gravel pits that may affect storage along the reach. For this reason, it was necessary to adjust the storage-outflow relationships that were developed from the calibrated HEC-2 model results to more accurately reflect the flood storage along the reach. The initial adjustment was made by preparing a special version of the HEC-2 model with the encroachments removed so that all of the area below a given water-surface elevation that is represented in the ground profile data in the model would contribute to the computed storage volume. The limits of the storage areas were further adjusted by comparing the extent of flooded areas observed on aerial photographs taken during the period May 23 through May 10, 1993, when releases from Friant Dam ranged from 1,010 to 1,950 cfs, and an aerial videotape taken on May 2, 1995, when the release from Friant Dam was 7,930 cfs. The water-surface elevations in this version of the model were set equal to the computed water-surface elevations from the original version of the model. Because of the uncertainty of the depth in flooded areas along the reach that are beyond the limits of the mapping, additional adjustments to the storage volumes were made to improve overall calibration of the model.

Flow losses to channel percolation and diversion along the reach can be significant, particularly at low flows. The loss relationships between Friant Dam and the Chowchilla Bifurcation Structure (Figure 2-4) were incorporated into the routing model to improve model performance.

The best calibration of the routing model for the 1999 flows was achieved using 18 subreaches between Friant Dam and Gravelly Ford (Table 2-16), and a routing time-step of 1 hour (Figure 2-47). The subreach boundaries were selected based on the volume of storage present in the overbanks, on similarity of hydraulic characteristics and on the location of significant hydraulic structures and controls.

Table 2-16. Subreach boundaries used in the flow-routing models for the San Joaquin River between Friant Dam and Mendota Dam

Flow-routing Subreach	Hydraulic and channel stability Subreach	Downstream boundary stationing (feet upstream of Mendota Dam)	Landmark at downstream portion of Subreach
		399,920	Friant Dam
1	1	309,480	
2	1	302,816	
3	1	295,442	
4	1	283,990	
5	1	274,631	
6	1	266,524	Highway 41 Bridge
7	2	262,344	
8	2	254,139	
9	2	250,742	
10	2	237,280	
11	2	227,429	
12	2	217,109	
13	2	204,174	Highway 99 Bridge
14	3	191,772	
15	3	170,887	
16	3	153,064	
17	3	146,331	
18	4	126,279	Gravelly Ford
19	4	110,187	
20	5	94,987	
21	5	79,986	
22	5	59,770	Chowchilla Bypass Structure
23	6	43,940	
24	6	29,019	
25	6	14,622	
26	6	745	Mendota Pool

After calibration of the model to low flow conditions, the Friant Dam to Gravelly Ford model was expanded to include the reach between Gravelly Ford and Mendota Dam. The modified model used a total of 26 subreaches, including the original 18 subreaches between Friant Dam and Gravelly Ford, and eight additional subreaches between Gravelly Ford and Mendota Dam (Table 2-16). Because only daily flow data were available for the historical flows on which alternative flood release scenarios were based, the routing time-step was increased to 8 hours in this version of the routing model, and the daily flow records were treated as instantaneous flow values. The HEC-1 model internally computes the interpolated discharge values that correspond to each of the 8-hour increments from the daily input values. Trial runs of the model using interpolated values of the inflows that would more closely represent the instantaneous values, and using different time step lengths, indicated that the model results are insensitive to these refinements.

The measured flow record at the San Joaquin River below Friant Dam and at Gravelly Ford for the period March 15 through May 31, 1995, was used to validate the extended model. The validation results indicated that the timing of the computed hydrographs at Gravelly Ford was reasonable, but that the computed discharges were about 5% higher than the measured values (Figure 2-48). Comparison of the measured hydrograph volumes for this period revealed that the flow losses along the reach were about 5% higher than would be indicated by the loss curves in Figure 2-4. This

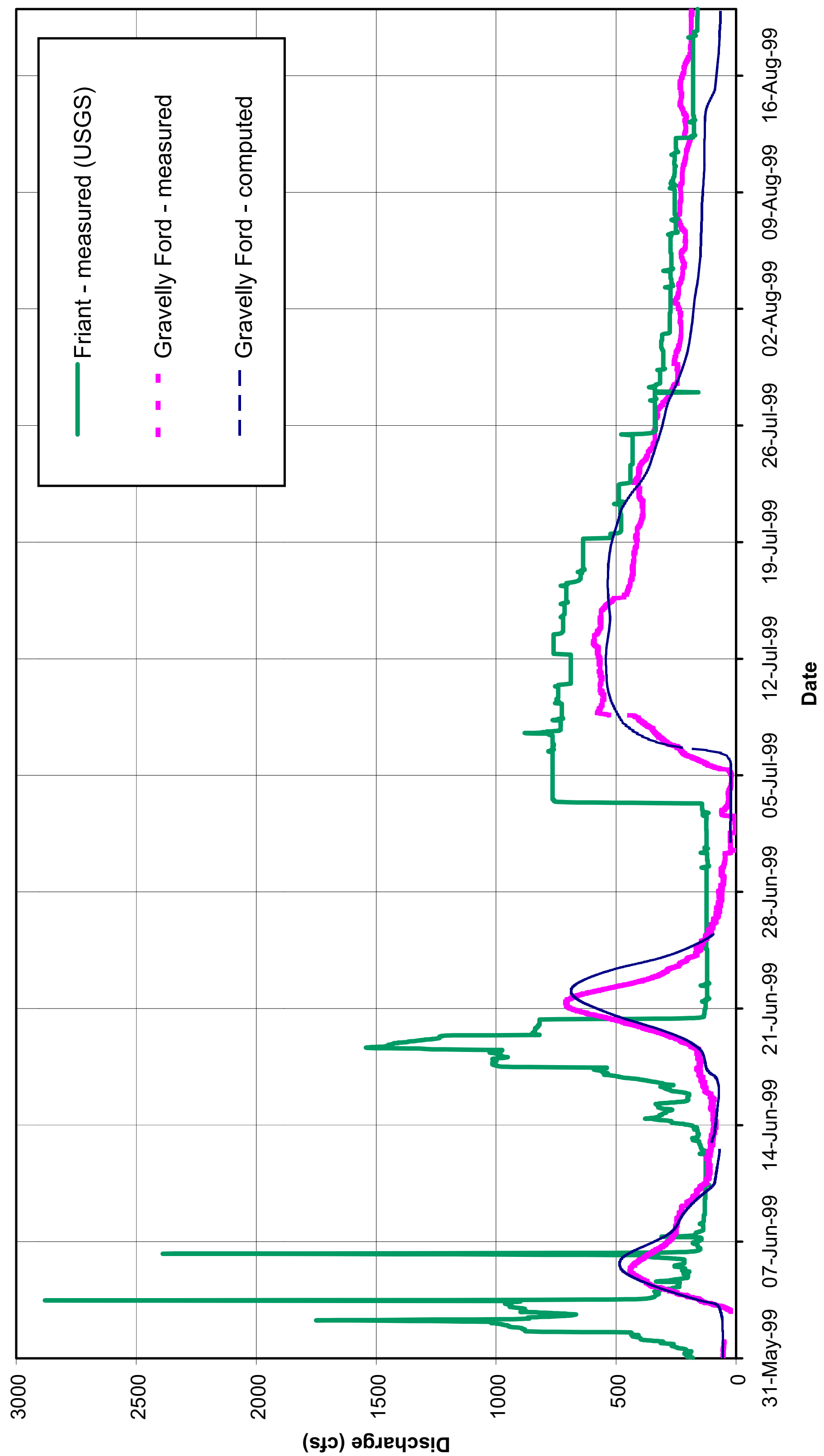

Figure 2-47. Measured and computed mean daily flow hydrographs in the San Joaquin River below Friant Dam and at Gravelly Ford for June 1-August 27, 1999.

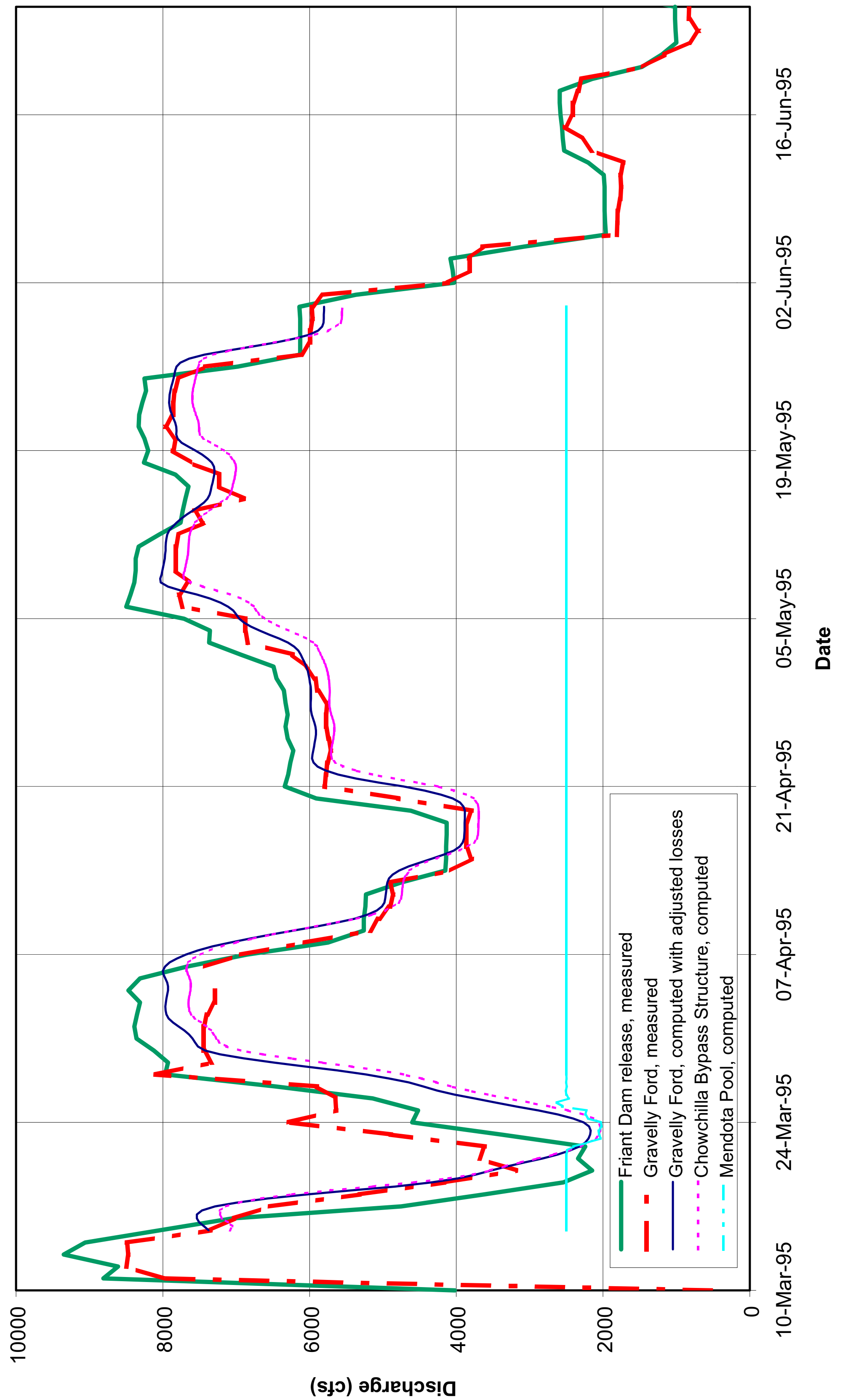

Figure 2-48. Measured and computed mean daily flow hydrographs in the San Joaquin River below Friant Dam and at Gravelly Ford for March 15-May 31, 1995.

apparent discrepancy may be attributable to a variety of factors, including error in the measured flows at Gravelly Ford, the possibility that additional flow loss occurred in the reach associated with levee breaches that are not accounted for in the storage-outflow relationships, and uncertainty in the percolation loss relationships at higher flow. Figure 2-49 shows the results of applying the routing model to the 1986 Friant Dam release hydrograph. Based on the available data, the results obtained from the modified model are believed to provide a reasonable basis for estimating changes in the flood release hydrographs as they move downstream along the reach, assuming that major levee breaches that increase the flood attenuation do not occur. Given the history of this reach, such breaches are likely; thus the routed results provide discharges at each point along the reach that represent the upper limit of the discharge that is likely actually to occur under existing conditions.

2.8.2.2. Model Calibration between Mendota Dam and the Merced River

Procedures similar to those described above were used to develop the flow routing model for the reach between Mendota Dam and the Merced River. Details of the model development can be found in MEI (2000b). This model covers the mainstem of the San Joaquin River and the entire Chowchilla Bypass/Eastside Bypass flood control system (Figure 2-2 and Figure 2-44). The reach between the Chowchilla Bifurcation Structure and Mendota Dam was included in the extended model because MEI obtained additional data after completion of the initial Friant Dam to Mendota Dam study to assist in calibration and definition of the measured flow split at the Chowchilla Bifurcation Structure.

Table 2-17 summarizes the routing subreaches used in the overall routing model and includes the number of subreaches used for each subreach. Where a hydraulic analysis was available (all the mainstem reaches plus Bear Creek), the storage-outflow relationship for each subreach was developed from the HEC-2 model output, based on the total volume of water in the subreach computed from the cross-sectional areas and distances between cross sections for each modeled discharge. At other locations such as the Eastside Bypass system, a typical cross section representing the subreach was input to the model, with the storage-outflow relationships developed internally based on normal-depth calculations.

Table 2-17. Summary of Reaches used in the HEC-1 Flow-Routing Model of the San Joaquin from the Chowchilla Bifurcation Structure to the Merced River

Routing	Description	Length (miles)	Number of Routing Subreach	Method *
SJ1	Mainstem, Chowchilla Bifurcation Structure to Mendota Dam	11.2	4	Hydraulic Analysis
SJ2	Mainstem, Mendota Dam to Sack Dam	22.4	6	Hydraulic Analysis
SJ3	Mainstem, Sack Dam to Sand Slough Control Structure	13.6	6	Hydraulic Analysis
SJ4	Mainstem, Sand Slough Control Structure to Mariposa Bypass	21.1	10	Hydraulic Analysis
SJ5	Mainstem, Mariposa Bypass to Bear Creek	11.6	5	Hydraulic Analysis
SJ6	Mainstem, Bear Creek to Salt Slough	6.9	4	Hydraulic Analysis
SJ7	Mainstem, Salt Slough to Mud Slough	7.8	3	Hydraulic Analysis

Table 2-17. cont.

Routing	Description	Length (miles)	Number of Routing Subreach	Method *
SJ8	Mainstem, Salt Slough to the Merced River	3.1	1	Hydraulic Analysis
CB1	Chowchilla/Eastside Bypass, Chowchilla Bifurcation Structure to the Diversion from Mainstem at the San Slough Control Structure	31.9	14	Normal Depth
EB1	Eastside Bypass, Diversion from Mainstem at the Sand Slough Control Structure to Mariposa Bypass	9.1	4	Normal Depth
EB2	Eastside Bypass, Mariposa Bypass to Bear Creek	6.6	3	Normal Depth
MB1	Mariposa Bypass	4.4	2	Normal Depth
BC1	Bear Creek	4.1	2	Hydraulic Analysis

* Method used to develop storage curves: Hydraulic Analysis from HEC-2 modeling; Normal Depth - from typical cross section

Initial routing parameters (number of routing subreaches and time-step length) were specified for each routing subreach based on the routing performed for the Friant Dam to Mendota Dam reach (MEI 2000). The time-step length was set to 12 hours with subreach lengths varying from 6,100 to 16,100 feet. Because of unknown flow splits at diversion points and unknown tributary inflows and flow losses, verification of the routing parameters could not be carried out for all of the individual routing reaches. Therefore, verification was carried out only for reaches without significant unknown tributary or diversion flows and where measured flows existed at each end of the reach. Figure 2-50 shows the results for the reach from the Mendota gage to the Dos Palos gage for the 1995 runoff period (March through May). Diversions into the Arroyo Canal were based on recorded values. The timing and basic shape of the routed hydrograph matches the measured hydrograph at the downstream end reasonably well. Differences in the magnitudes of the flows, particularly during the latter portion of the simulation, may reflect inaccuracies in the gage records and reported diversions into the Arroyo Canal. These differences could not be minimized through adjustments to the model and the routing parameters as originally specified were taken as reasonable for the section of the river between the Mendota gage and the Dos Palos gage.

Figure 2-51 and Figure 2-52 shows the routed versus computed 1986 and 1995 hydrographs, respectively, for the Stevinson gage. The computed flows are based on the recorded flows at the Chowchilla Bifurcation Structure (Chowchilla Bypass at the head and San Joaquin River below the bifurcation) routed through the system with the estimated losses at Mendota and estimated tributary inflows to the Eastside Bypass above the El Nido gage accounted for. The figure shows that recorded flows are consistently greater than the routed flows in the early portion of each hydrograph, indicating ungaged tributary inflow below the El Nido gage. A 5-day moving average of the computed flow differences was used to develop the estimated inflow hydrographs for the eastside tributaries between the El Nido gage and Bear Creek. The inflows were assumed to end on April 14 in 1986 and April 4 in 1995.

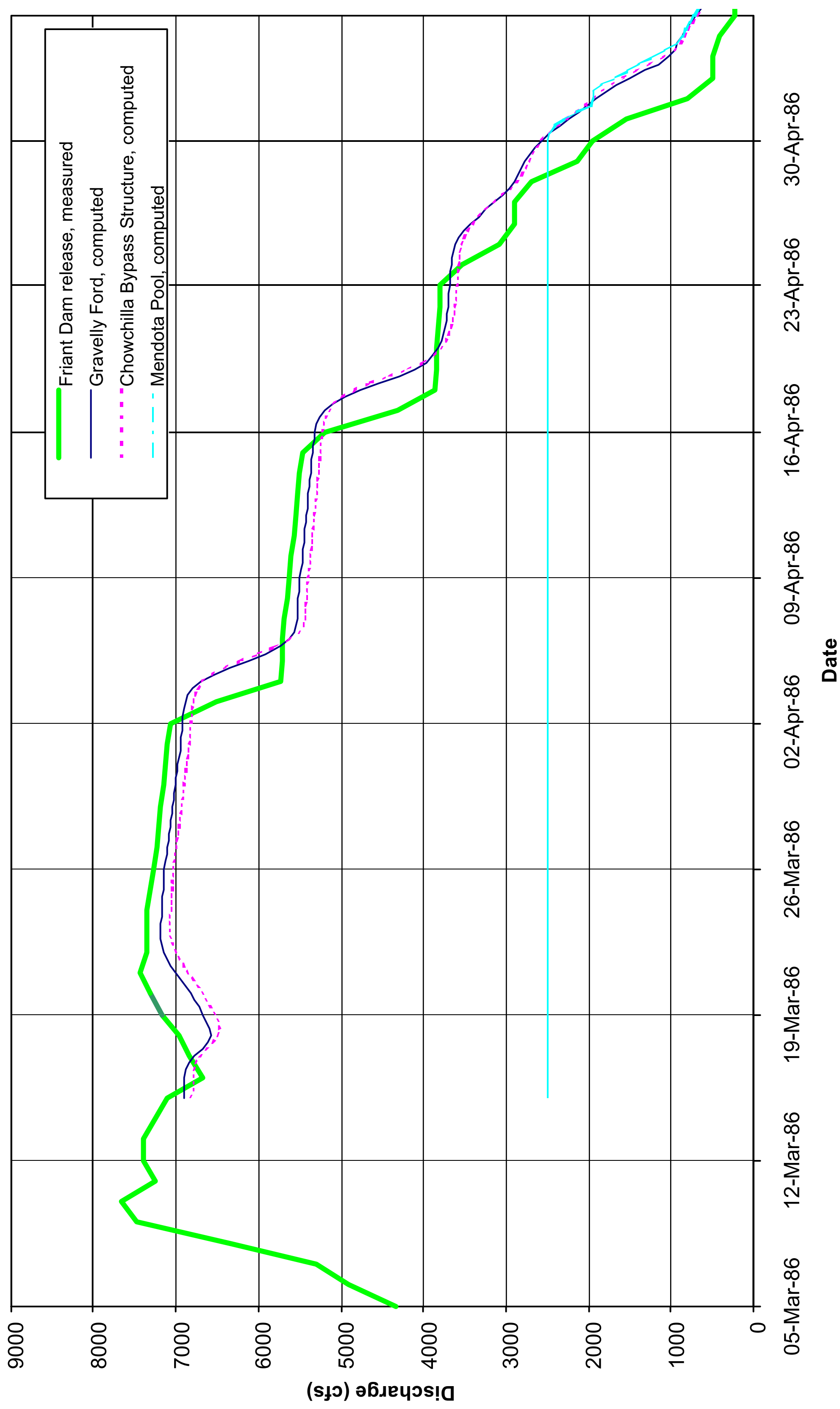

Figure 2-49. Measured and computed mean daily flow hydrographs in the San Joaquin River below Friant Dam and at Gravelly Ford for March 15-May 7, 1986.

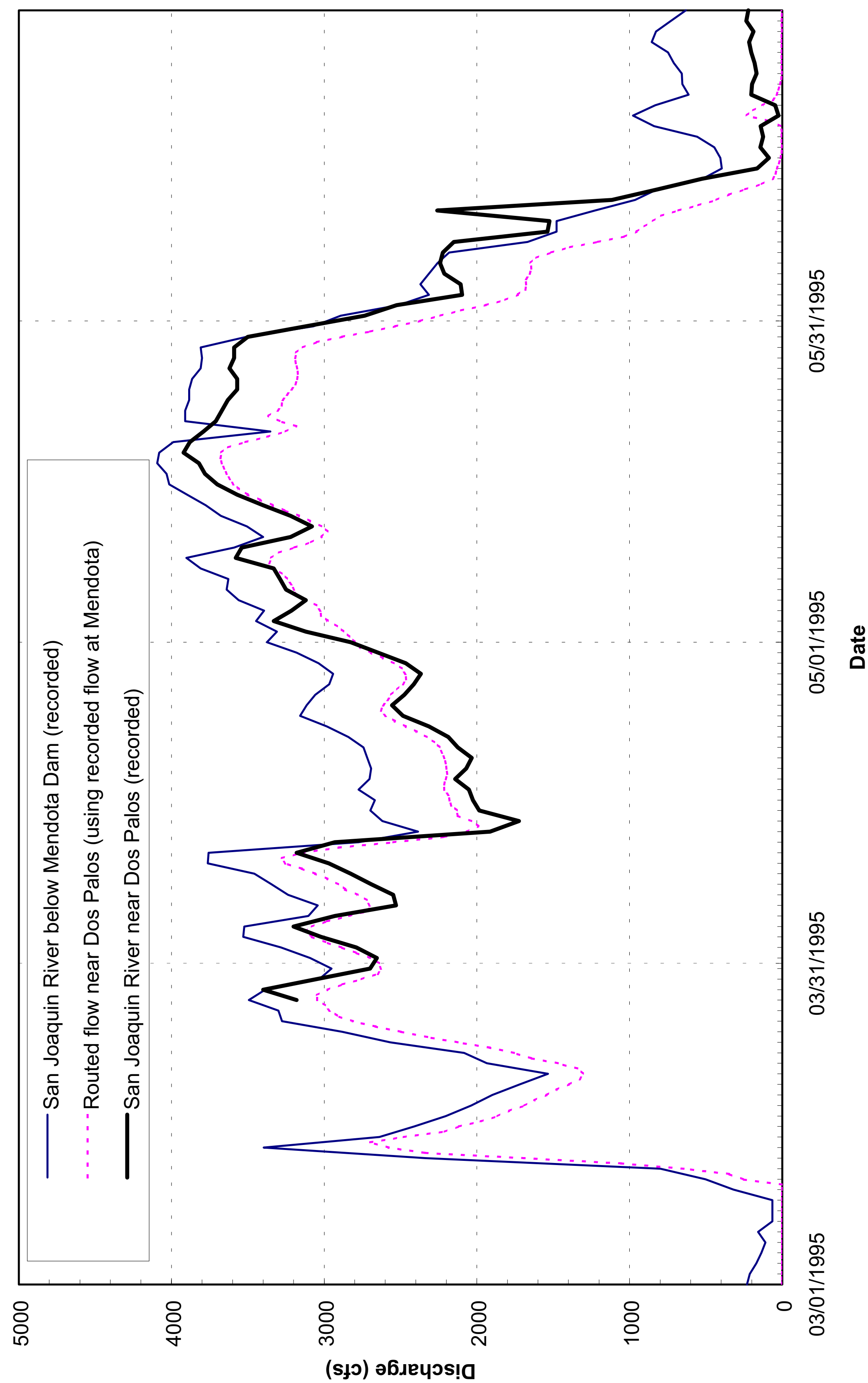

Figure 2-50. Measured and computed mean daily flow hydrographs in the San Joaquin River below Mendota Dam and at the Dos Palos gaging station for March 1-May 31, 1995.

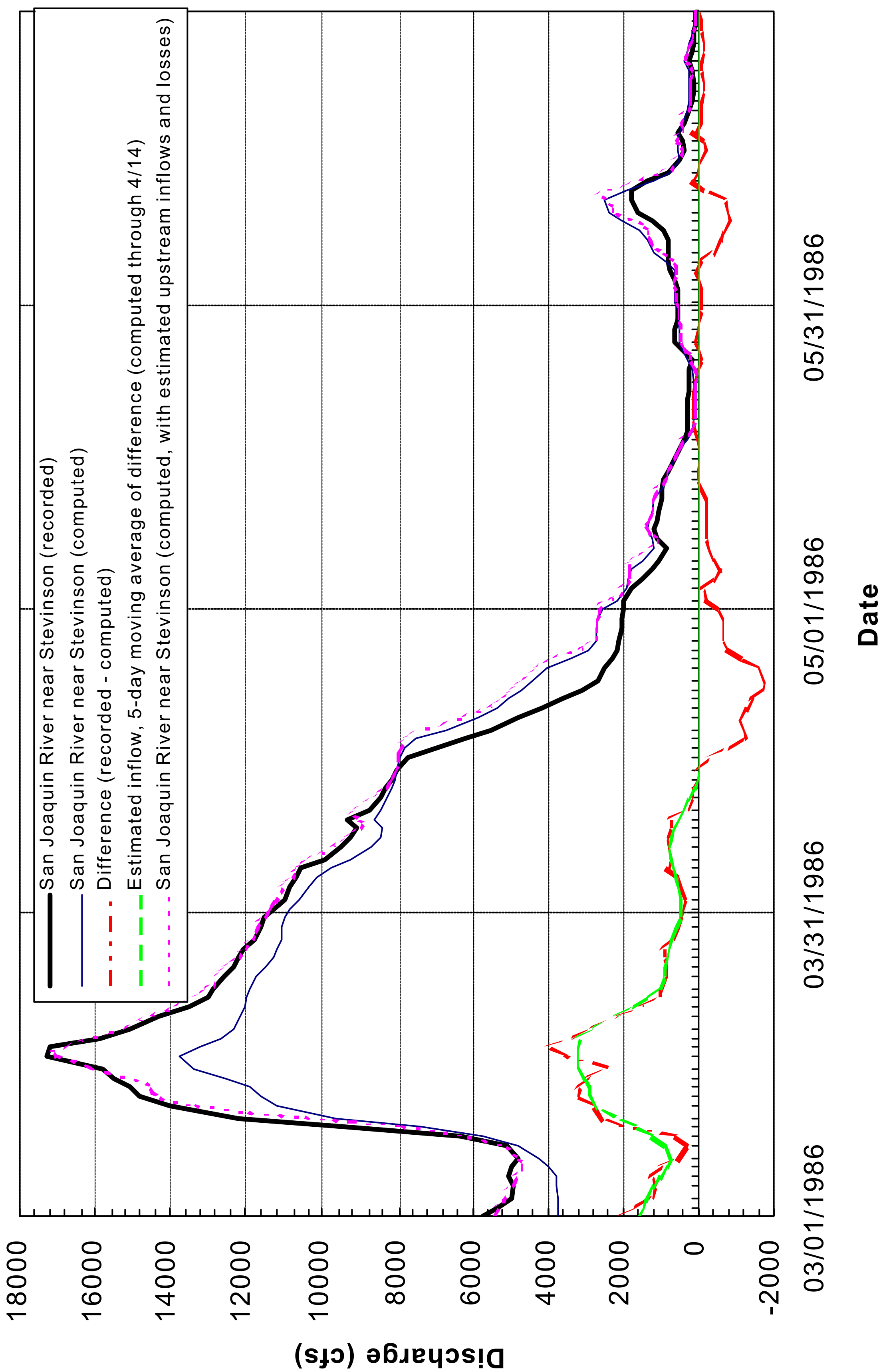

Figure 2-51. Measured and computed mean daily flow hydrographs in the San Joaquin River below Mendota Dam and at the Stevinson gaging station for March 1-May 31, 1986.

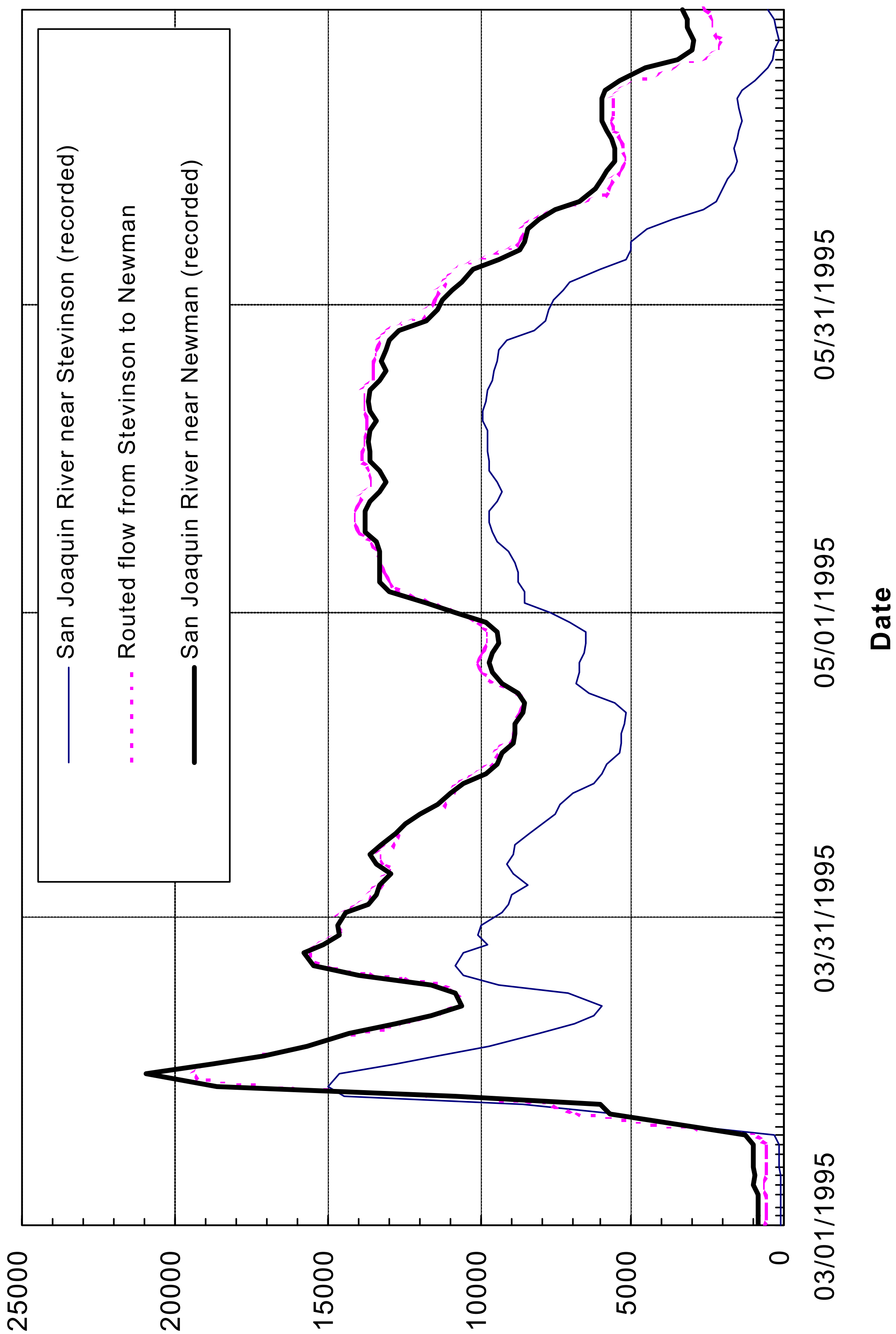

Figure 2-52. Measured and computed mean daily flow hydrographs in the San Joaquin River below Mendota Dam and at the Stevinson gaging station for March 1-May 31, 1995.

Figure 2-53 and 2-54 show the routed versus computed 1986 and 1995 hydrographs, respectively, for the Newman gage. Inflows for Salt Slough, Mud Slough, and the Merced River are known for each event. The plot shows that the computed hydrographs match the measured hydrographs at the downstream end reasonably well, verifying the routing parameters for the section of the river from the Stevinson gage to the Newman gage. Based on these results, it was assumed that the routing parameters developed in a similar manner for the other sections of the river and bypass system are reasonable.

Ungaged inflows into the Eastside Bypass system occur at various locations, and an apparent flow loss occurs near Mendota Dam during high flows. These inflows and losses were concentrated at three locations in the routing model: (1) Overflow losses at Mendota Dam, which represent the apparent losses near the dam during high flows; (2) Eastside tributaries 1, which represent ungaged inflows to the bypass system between the Chowchilla Bifurcation Structure and the El Nido gage; and (3) Eastside tributaries 2, which represent ungaged inflows to the bypass system between the El Nido gage and the mouth of Bear Creek. The unknown flows at each of these locations were estimated for both the 1986 and 1995 runoff periods by comparing computed flows (routed flows from known points upstream) with recorded flows.

The model was also calibrated at the gaging station below Mendota Dam using 1986 and 1995 flows. The computed flows are based on recorded flows in the river below the Chowchilla Bifurcation Structure routed to Mendota Dam and added to the recorded inflows from the James Bypass/Fresno Slough. For each time period, measured flows at the Mendota gage are in general much lower than the computed flows, indicating significant flow losses. Assuming accuracy in the gage records, these losses are likely a result of outflows into the various irrigation canals that connect to the river at Mendota Pool. The losses were estimated as the difference between the computed and measured hydrographs, with the computed hydrographs lagged by 1 day for each time period to more accurately align with the recorded hydrographs. A 5-day moving average of the computed differences was used to smooth out the estimated loss hydrograph. Computed negative values represent net irrigation inflows.

Figure 2-55 and Figure 2-56 show 1986 and 1995 computed versus recorded flows at the El Nido gage on the Eastside Bypass, respectively. The computed flows are based on recorded flows at the head of the Chowchilla Bypass, the routed flows at Mendota with the losses accounted for, recorded (1995) or estimated (1986) diversions into the Arroyo Canal, and the estimated flow split at the Sand Slough Control Structure (see below). For the 1986 time period, the hydrographs match reasonably well, indicating minimal tributary inflow. The inflow was assumed to be zero for this time period. For 1995, the computed hydrograph is in general lower than the recorded hydrograph prior to about April 6, but shows a less consistent variation after this, which is attributable largely to the timing of the hydrographs. The computed difference for the period March 1 to April 6, smoothed using a 5-day moving average, was used to develop the estimated inflow hydrograph for 1995 for the eastside tributaries between the Chowchilla Bifurcation Structure and the El Nido gage.

2.8.2.3. Flow Routing Results: Attenuation and Storage Effects under Existing Conditions

Results obtained from the calibrated flow routing model for the 1995 event were used to evaluate the attenuation and storage effects along the reach under existing river conditions. Figure 2-57 shows the measured flows at the Friant gage and the routed hydrographs at eight points along the reach for the period between March 1 and April 1, 1995. The routed hydrographs show an approximately 2-day time lag in flows between Friant Dam and Gravelly Ford and a ½-day time lag between Gravelly Ford and the Chowchilla Bifurcation Structure. The peak discharge among these three locations attenuates

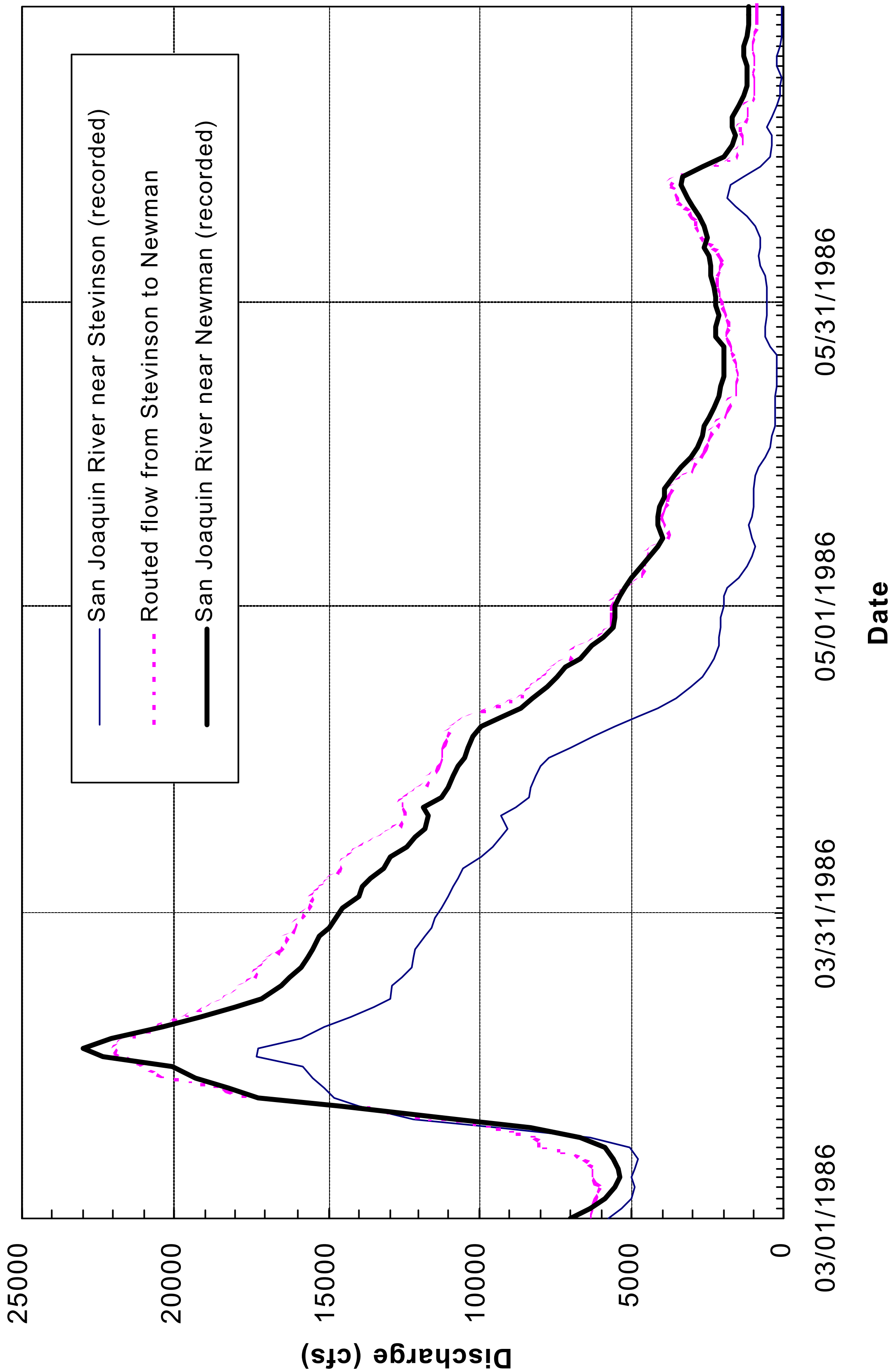

Figure 2-53. Comparison of measured and computed mean daily flow hydrographs at the San Joaquin River near Newman gaging station for March 1-May 31, 1986.

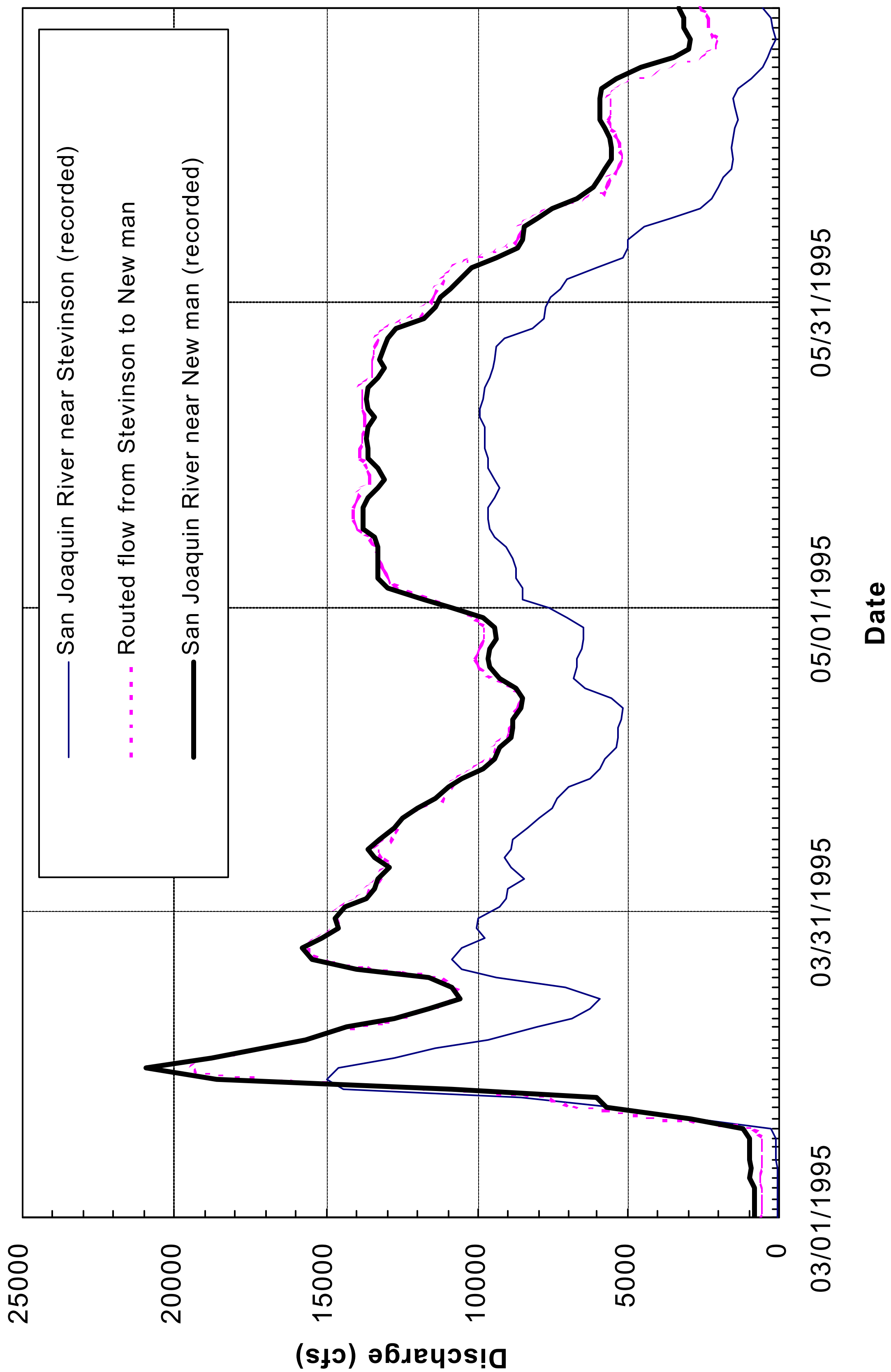

Figure 2-54. Comparison of measured and computed mean daily flow hydrographs at the San Joaquin River near Newman gaging station for March 1-May 31, 1995.

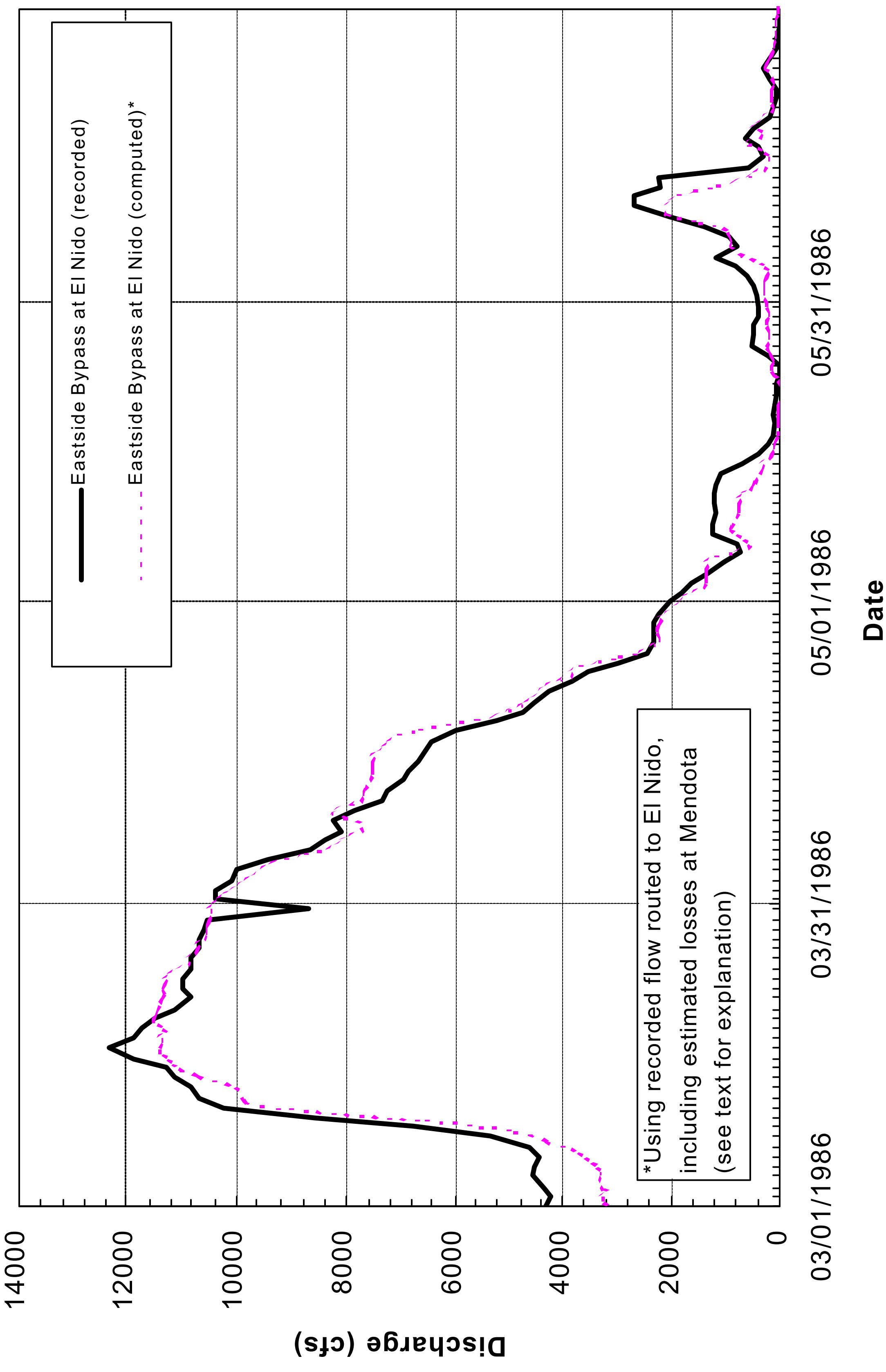

Figure 2-55. Comparison of measured and computed mean daily flow hydrographs at the East Side Bypass at El Nido gaging station for March 1-July 1, 1986.

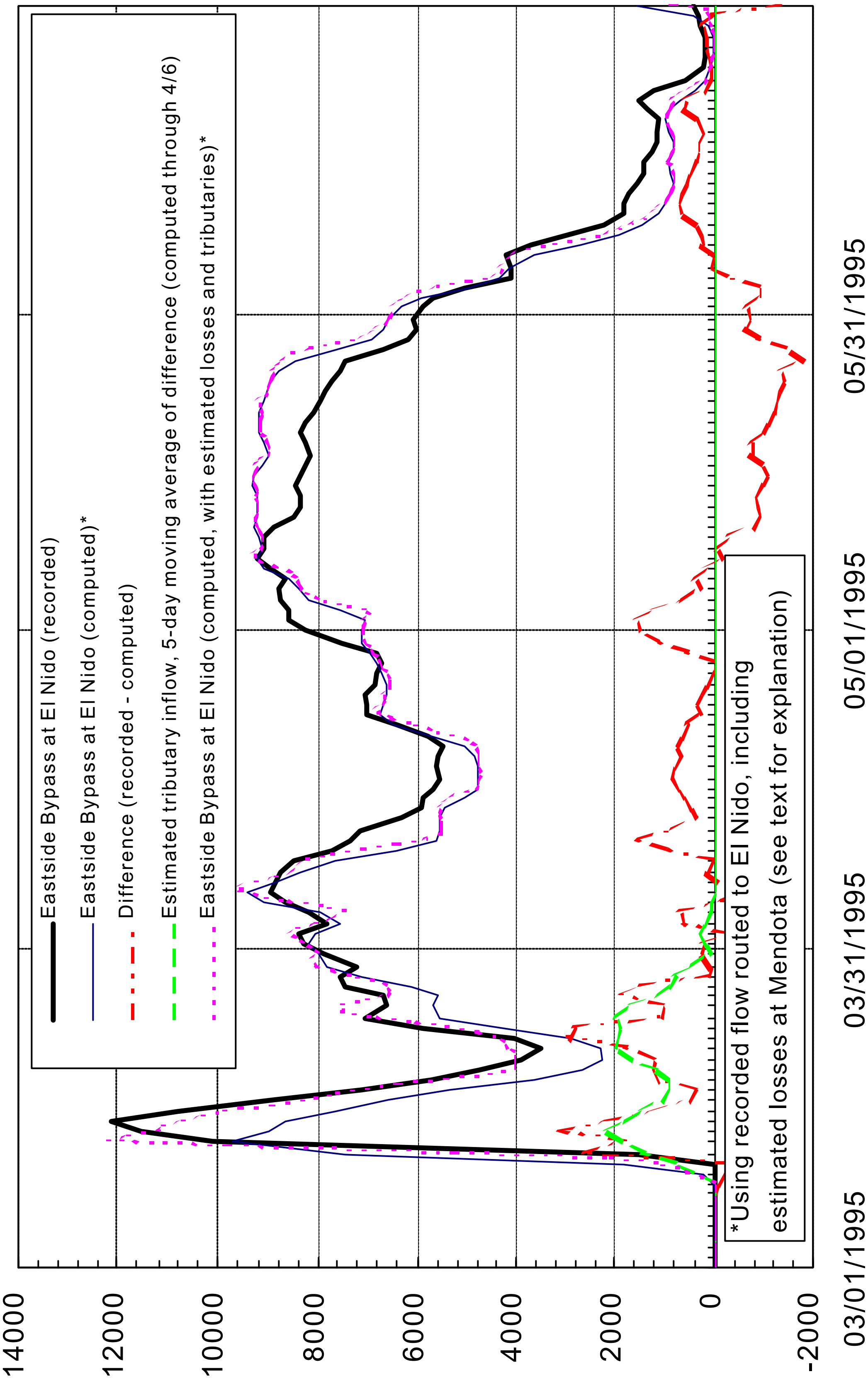

Figure 2-56. Comparison of measured and computed mean daily flow hydrographs at the East Side Bypass at El Nido gaging station for March 1-May 31, 1995.

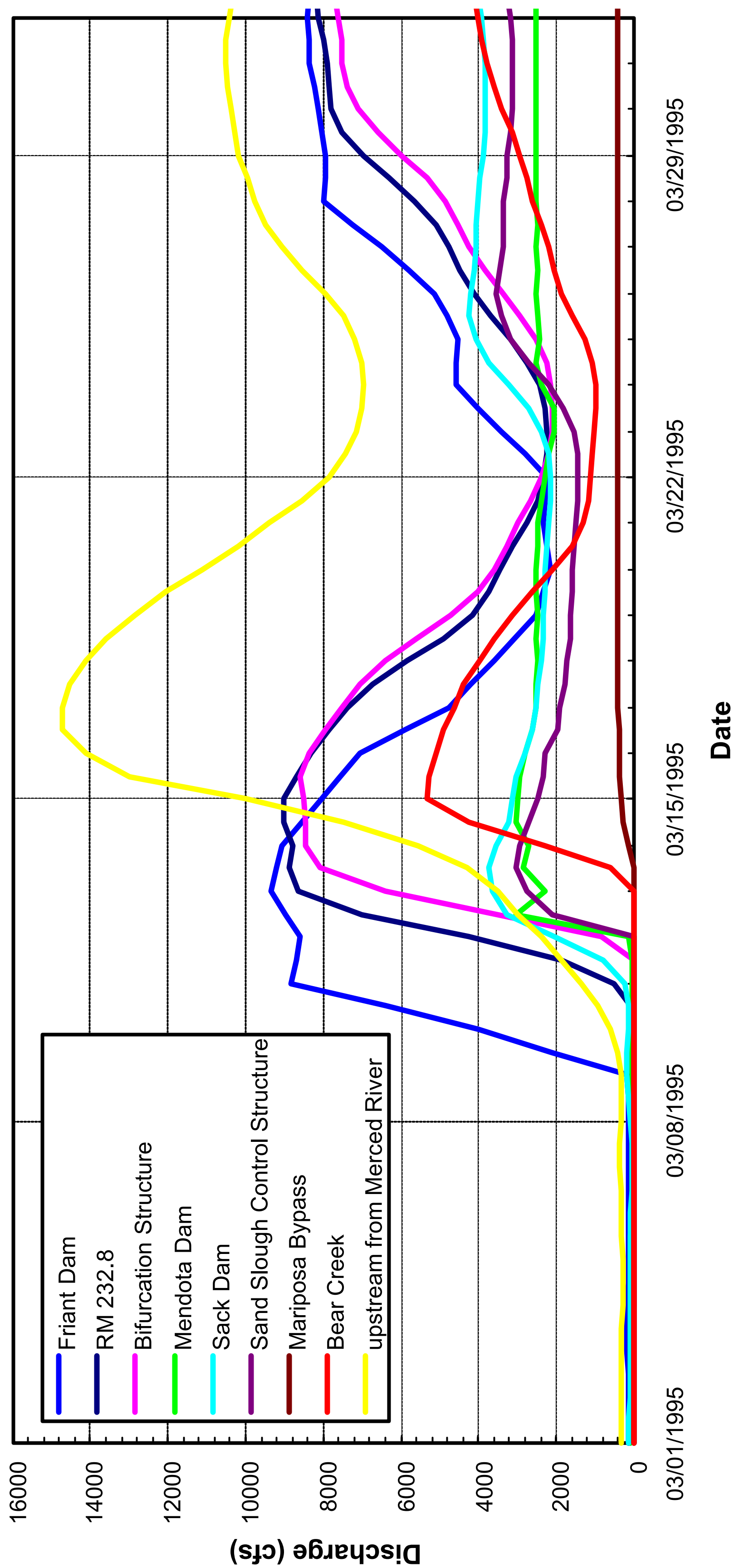

Figure 2-57. Measured flows between March 1 and April 1, 1995, at the Friant gage and the routed hydrographs at eight points along the reach between Friant Dam and the Merced River for existing river conditions.

from 9,350 cfs at Friant Dam to 9,000 cfs at Gravelly Ford to 8,576 cfs at the Chowchilla Bifurcation Structure (Table 2-18). The hydrographs for locations downstream from the Chowchilla Bifurcation Structure show the combined effects of diversions from the main river (e.g., Chowchilla Bypass, losses at Mendota Dam, Arroyo Canal, Eastside Bypass at Sand Slough Control Structure), inflows from the various tributaries along the reach, as well as the routing and attenuation effects in this portion of the overall reach.

Table 2-18. Summary of flood peak attenuation for existing and historic conditions for the 1995 high flow hydrograph. All flood peak magnitudes include tributary inflows for the 1995 high flow.

	Existing conditions		Historic conditions	
Gaging location	**Flood peak magnitude (cfs)**	**% flood peak attenuation from Friant (cfs)**	**Flood peak magnitude (cfs)**	**% flood peak attenuation from Friant (cfs)**
At Friant gage	9,350	0.0	39,300	0.0
At Gravelly Ford	9,000	-3.7	32,700	-16.8
At Chowchilla Bifurcation Structure	8,575	-4.7	28,060	-14.2
At Mendota Dam	3,000	N/A	25,930	-7.6
At Sack Dam	3,700	N/A	25,930	0.0
At Sand Slough Control Structure	3,000	N/A	25,000	-3.6
At Mariposa Bypass confluence	400	N/A	21,800	-12.8
At Bear Creek confluence	5,300	N/A	20,300	-6.9
Upstream of Merced River	14,700	N/A	25,000	+23.2

[1] Model diverts flow into bypasses based on operational rules, flood peak attenuation cannot be computed.

2.8.2.4. Flow Routing Results: Attenuation and Storage Effects under Historical Conditions

A routing model was also developed for historical conditions prior to construction of the bypasses, diversions, and levee system based on the 1914 CDC mapping. This model was used to estimate the characteristics of the historical flood hydrographs along the reach. Inflows at the upstream end of the reach at the present location of Friant Dam were taken from the full natural flow record for the 1995 event. The model used the same routing parameters as the existing conditions model to ensure that the results would be comparable. In addition, the tributary inflows that were used in the existing conditions model were also used in the historical conditions model, but the eastside tributaries that are intercepted by the Chowchilla Bypass and Eastside Bypass were input to the river in their approximate historical locations. Diversions into the bypasses and canals along the reach were eliminated from the model. Although the existing tributary inflows are likely quite different from what they would have been in the absence of human influences, the resulting routing model provided a reasonable approximation of the changes in mainstem hydrograph shape along the reach.

Results obtained from the historical conditions model for the period between March 1 and April 1, 1995 are presented in Figure 2-58 for the same eight locations that were presented for the existing conditions model. The hydrographs attenuate significantly along the upstream portion of the reach between Friant Dam and the present location of Mendota Dam, with a peak discharge at Friant Dam of about 39,300 cfs compared to 28,060 at the present location of the Chowchilla Bifurcation Structure, and about 25,930 cfs at Mendota Dam (Table 2-18). The lag time between each of the locations varies from about ½ day to a full day.

2.8.3. Historical Inundation Pattern and Frequency

As described above, the San Joaquin River historically flooded frequently, particularly in Reaches 2-5. Flows during drier years may not have spilled out onto floodplains and floodbasins, whereas wetter years may have inundated Reaches 2-5 for long periods (months). The combined effects of flood flow regulation by upstream dam, levees along the San Joaquin River, and the San Joaquin River Flood Control Project has greatly reduced the magnitude, frequency, and duration of inundation along the study reach. In an effort to quantify the degree of change in inundation, the flood routing model was used to estimate historical and existing inundation patterns for three index floods.

2.8.3.1. Methods

Peak flow-stage relationships were quantified under historical and existing flood conditions to characterize the pre- and post-flood control periods and the pre- and post-dam periods. The areas inundated for various flows were determined for these periods to show the combined effect of levee confinement downstream of Friant Dam and flood frequency changes as a result of flood flow regulation from upstream dams.

The areas inundated for three historical flood flows were calculated using the 1914 mapping, cross sections, and water surface profiles (ACOE 1917). The 1914 profiles show water surfaces associated with discharges of 5,700 cfs and 9,800 cfs, and for an unknown discharge at the "highest known water surface." To better quantify the effects of the various flood control measures throughout the study reach, the study area was divided into 4 subreaches:

1. Herndon to Chowchilla Bifurcation Structure (Reaches 1B–2A)
2. Chowchilla Bifurcation Structure to Mendota Dam (Reach 2B)
3. Mendota Dam to Sand Slough Control Structure (Reaches 3–4A)
4. Sand Slough Control Structure to Merced River (Reaches 4B–5)

Because the profile for the highest known water surface did not extend to the railroad bridges at Herndon, the upstream reach was truncated at cross section 7 (RM 247.4), approximately 8 miles downstream of the Herndon Railroad Bridge. For each cross section, the water-surface elevation for each of the flows was measured from the profiles. These water-surface elevations were then drawn on the cross sections and the water-surface widths were measured. At numerous locations for the two highest water profiles (9,800 cfs and the "highest known water surface"), the width was greater than the extents of the cross-section plots. The measured widths at these locations are therefore reported as "greater than" the cross-section limits.

The incremental area of inundation between cross sections was calculated by multiplying the measured width and the average of the left and right overbank distances between the cross sections. The overbank distances between the cross sections were measured on the 1914 mapping at approximately the limits of the water surface. Because the detail of the 1914 contours and mapping was not sufficient to accurately map the floodplain, maps showing areas of inundation were not produced.

The areas inundated for the historical flood flows were also calculated for existing conditions to assess the effect of flood control measures and other changes that have occurred throughout the project reach. The water-surface widths were determined from the existing hydraulic model runs for the 5,700-cfs discharge and the 9,800-cfs discharge, assuming the 5,700 cfs and 9,800 cfs values represented Friant Dam releases. The highest known water surface was not included in the present conditions analysis because the discharge is not known. Previously assumed loss rates and operating

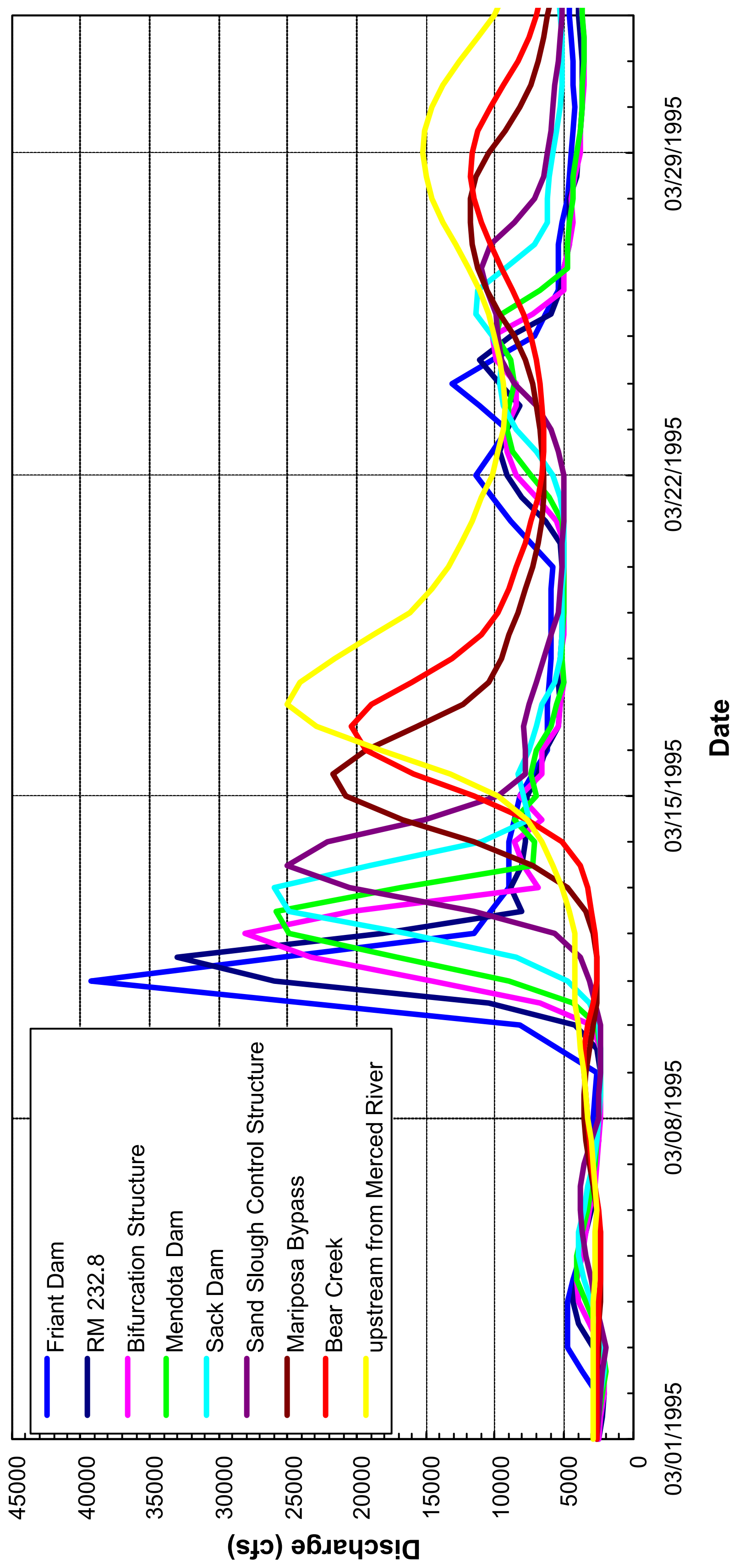

Figure 2-58. Estimated full natural flows between March 1 and April 1, 1995, at the Friant gage and the routed hydrographs at eight points along the reach between Friant Dam and the Merced River for historic river conditions.

rules for the bifurcation structures, control structures, and Mendota Dam were used to determine what discharge remains in the San Joaquin River throughout the reach. It was assumed that flows are limited to 2,500 cfs in the San Joaquin River downstream of the Chowchilla Bifurcation Structure when upstream river flows are less than 8,000 cfs, with flows increasing to 6,500 cfs when the discharge in the upstream river is 12,000 cfs. Discharges remaining in the San Joaquin River after accounting for the various inflows and outflows are summarized in Table 2-19. The incremental areas were calculated by multiplying the water surface width and the overbank distances obtained from the hydraulic model and summed to represent the inundated areas for each of the subreaches.

To evaluate the combined effects of Friant Dam flow regulation and levee confinement on the inundated areas resulting from floods, the inundated areas were calculated in a similar fashion for flows with post-dam frequencies similar to the frequencies of the historical flood events. The historical flood events of 5,700 cfs and 9,800 cfs have pre-Friant Dam recurrence intervals of approximately 1.3 years and 2 years, respectively. Although the discharge and the return period corresponding to the highest known water surface are unknown, for the purposes of this study, it was assumed the discharge had a pre-Friant Dam recurrence interval of 10 years. Under post-Friant Dam conditions, the 1.3-year event below Friant Dam is approximately 240 cfs, the 2-year event is approximately 1,000 cfs, and the 10-year event is approximately 8,000 cfs. The discharges were also adjusted throughout the study reach to include losses and the effects of the assumed operating rules of the bifurcation structure, control structures, and Mendota Dam. The discharge remaining in the San Joaquin River for the three events is summarized in Table 2-19.

Table 2-19. Summary of discharges remaining in the San Joaquin River under present conditions.

			Discharge Below Friant Dam (cfs)					
Section Number	River Mile	Reach	240 cfs	1,000 cfs	5,700 cfs	8,000 cfs	9,800 cfs	Location
596	266.5	1A	240	1,000	5,700	8,000	9,800	<=Friant Dam
225	242.5	1B	149	909	5,609	7,909	9,709	<=Herndon Railroad Bridge
122	235	1B	151	911	5,610	7,909	9,709	
121	235	1B	151	911	5,610	7,909	9,709	<=U/S Limit of "Highest Known Water Surface" Profile
a186	223.6	2A	63	782	5,429	7,714	9,506	<=Chowchilla Bifurcation Structure
a96	215.1	2B	50	728	2,500	2,500	4,006	
								<=Mendota Pool
764	203.7	3	50	728	2,500	2,500	4,006	
474	181.2	4A	1	214	2,020	2,020	3,556	<= Sand Slough Control Structure
302	167.7	4B	1	9	70	70	130	

Table 2-19. cont.

Section Number	River Mile	Reach	Discharge Below Friant Dam (cfs) 240 cfs	1,000 cfs	5,700 cfs	8,000 cfs	9,800 cfs	Location
257	164.4	4B	2	10	71	71	130	
252	164	4B	1	9	70	70	130	<=Mariposa Bypass
36	146.6	4B	1	26	373	373	1,013	
7	144.3	4B	1	26	373	373	1,013	Bear Creek
M234	135	5	1	66	910	910	2,416	
M146	128.2	5	21	282	1,213	1,213	2,756	
M117	125.8	5	40	564	2,425	2,425	5,512	Salt Slough
M116	125.7	5	21	283	1,213	1,213	2,756	
M88	123.7	5	28	333	1,335	1,335	2,901	Mud Slough
M87	123.6	5	35	385	1,458	1,458	3,046	
M6	117.3	5	35	385	1,458	1,458	3,046	Merced River
M5	117.3	5	50	728	2,750	2,750	5,009	

2.8.3.2. Results

The inundated areas for the historical flows are summarized for the 1914 conditions and the present conditions in Table 2-20, illustrating the effects of implemented flood-control measures. The results also include the effects of the large number of diversions along the project reach. Results indicate that the flood control and diversions reduce the area of inundation by an average of about 25% for the 5,700-cfs discharge and by a factor of about 10 for the 9,800-cfs discharge. The reach from Herndon to the Chowchilla Bifurcation Structure shows the smallest reduction in flooded area because there is no flow diverted upstream of this reach under both 1914 and existing conditions. Under existing conditions, the effects of flow diversions become more pronounced downstream of Chowchilla Bypass.

Table 2-20. Summary of inundated areas for 5,700 cfs, 9,800 cfs, and "highest known water surface" under (1) 1914 topographic conditions, and (2) existing topographic conditions and flood control system operation rules.

		Inundated Area at Q=5,700 cfs (acres)		**Inundated Area at Q=9,800 cfs (acres)**		**Inundated Area at Highest Known WSE (acres), Unknown Discharge**	
Reach	**RM Limits**	**1914**	**Existing**	**1914**	**Existing**	**1914**	**Existing**
Herndon to Chowchilla	227.7-247	1,319	1,276	>4,133	1,590	>15,846	?
Chowchilla to Mendota	216.7-227.7	726	420	>6,241	1,931	>8,074	?
Mendota to Sand Slough	169.7-216.7	1,530	1,235	>26,356	1,578	>30,414	?
Sand Slough to Merced	130-169.7	2,029	1,437	>16,436	2,872	>53,084	?

Table 2-21 illustrates the combined effects of Friant Dam flow regulation and levee confinement downstream by summarizing the inundated areas for the pre- and post-Friant Dam 1.3-, 2.0-, and 10-year flood events. The present inundated areas are also controlled by the diversions throughout the project reach. The results indicate that the combined effects of Friant Dam and levee confinement are very significant. For the 1.3-year event, the area inundated under present conditions is about an order of magnitude less than the area inundated under the 1914 conditions, and almost two orders of magnitude less for the 2.0- year and the 10-year events.

The subsidence that has occurred in the project reach should not confound the analysis of the inundated areas under the 1914 conditions with respect to the present topography. The analysis of the 1914 flood conditions is based on pre-subsidence topography, and the analysis of the present flood conditions is based on 1997 topography, which accounts for the subsidence. Under present conditions, the subsidence creates a concave shape in the longitudinal profile, resulting in more inundated area at the flatter downstream end of the profile and less inundated area in the steeper upstream end of the profile.

Table 2-21. Summary of inundated areas for the pre- and post-Friant Dam 1.3, 2.0, and 10-year recurrence interval floods under (1) 1914 topographic conditions, and (2) existing topographic conditions and flood control system operation rules.

		Inundated area at approximately 1.3-year event (acres)		**Inundated area at approximately 2.0-year event (acres)**		**Inundated area at approximately the 10-year event (acres)**	
Reach	RM Limits	1913 (Q=5,700 cfs)	Existing (Q=240 cfs)	1913 (Q=9,800 cfs)	Existing (Q=1,000 cfs)	1913 (Unknown Discharge)	Existing (Q=8,000 cfs)
Herndon to Chowchilla	227.7-247	1,319	350	>4,133	626	>15,846	1,461
Chowchilla to Mendota	216.7-227.7	726	238	>6,241	338	>8,074	439
Mendota to Sand Slough	169.7-216.7	1,530	417	>26,356	627	>30,414	1,578
Sand Slough to Merced	130-169.7	2,029	495	>16,436	616	>53,084	2,872

2.9. SUMMARY

The surface water hydrology of the San Joaquin River has undergone tremendous changes since surface water development began in the mid- to late-1800's, which in turn has caused corresponding changes to fish, riparian, and wildlife populations, as well as the fluvial geomorphic processes responsible for creating and maintaining the San Joaquin River ecosystem. The information presented in this chapter begins to document some of these changes, which will provide useful insights to understand how key biota and geomorphic processes have changed, as well as strategies that may improve future restoration efforts. In addition to gathering and summarizing existing data on surface water hydrology, analyses conducted within this chapter illustrated several key findings on changes to surface water hydrology:

- The average annual volume of water released to the San Joaquin River downstream of Friant Dam was reduced from 1,812,000 acre feet to 695,000 acre feet, a 62% reduction in yield. Because the amount of reservoir storage provided by Millerton Reservoir and other upstream reservoirs is relatively small compared to the unimpaired water yield during wetter water years, much of the post-Friant Dam water releases to the river are flood control releases.

These flood control releases are still much smaller than unimpaired conditions, but they are large enough to provide significant restoration opportunities (e.g., riparian restoration flows, geomorphic process flows, fish rearing and migration flows).

- Native San Joaquin River water no longer flows through all reaches of the San Joaquin River. Flows in the lower San Joaquin River (Reaches 3-5) are provided by Delta-Mendota Canal water (Reach 3), and agricultural return flows of Delta-Mendota Canal water (Reach 4 and Reach 5). The current baseflow regime and agricultural diversion infrastructure leaves several reaches dewatered year-round (Reach 2 and portions of Reach 4).
- The contribution of flow from the Kings River via Fresno Slough still occurs, but likely at a much lower magnitude, frequency, and duration compared to unimpaired conditions.
- Tributary flow contribution (baseflow and floodflows) to the lower San Joaquin River are significantly reduced by upstream dams and the flood control project.
- The magnitude, duration, and frequency of flood flows have been dramatically reduced. Ecological impacts of the reduced flood flow regime and flood control project include reduced geomorphic magnitude, duration, and frequency of fluvial geomorphic processes; reduced magnitude, duration, and frequency of overbank flows; reduced area of overbank inundation; reduced recruitment of riparian and wetland vegetation; and higher water temperatures during certain times of the year.
- The large storage capacity of the historic flood basin in Reach 3 through Reach 5 significantly reduced flood peaks; the reduced floodplain storage and increased hydraulic efficiency of the existing flood control project likely reduces flood wave travel time and reduces the degree of flood peak attenuation compared to unimpaired conditions.
- The life history strategy of riparian vegetation, wetland vegetation, native fish, waterfowl, and other biota evolved to the unimpaired flow regime. Changes to the flow regime have interfered with these life history strategies with varying and poorly known impacts. The conceptual relationships between hydrology, fluvial geomorphology, and the biota in this chapter (as well as Chapters 3, 7, and 8) provide opportunities for future restoration strategies to develop an ecosystem approach to restoring the San Joaquin River, increase mutual benefits to target species, and improve overall probability of success of the restoration effort.

2.10. LITERATURE CITED

Cain, J.R., 1997. Hydrologic and Geomorphic Changes to the San Joaquin River between Friant Dam and Gravely Ford and Implications for Restoration of Chinook Salmon (*Oncorhynchus tshawytscha*), M.S. thesis, Department of Landscape Architecture, University of California, Berkeley, 143 pp.

California Department of Public Works (CDWP), 1931. *San Joaquin River basin, Bulletin No. 29*, Sacramento, CA.

California Department of Water Resources (DWR), 1998. *The California Water Plan Update*, Volumes 1 and 2, Sacramento, CA.

Chow, V.T., 1959. *Open Channel Hydraulics*. McGraw-Hill Book Co., New York, 680 p.

Derby, G.H., 1850. The topographical reports of Lieutenant George H. Derby, in *Quarterly of the California Historical Society*, Vol. 11, No. 2, June 1932.

Derby, G.H. 1852. Report to the Secretary of War, Report on the Tulare Valley, Senate Executive Document no. 110, 32nd Congress, 1st session.

Dunne, T. and L.B. Leopold, 1978. *Water in Environmental Planning*, W.H. Freeman and Company, New York.

Fox, P., 1987a. *Freshwater inflow to San Francisco Bay under natural conditions*, Appendix 2 to State Water Contractors Exhibit 262, California State Water Resources Control Board Hearings on the Bay-Delta.

Fox, P., 1987b. *Rebuttal to David R. Dawdy Exhibit 3 in regard to Freshwater inflow to San Francisco Bay under natural conditions*, State Water Contractors Exhibit 276, California State Water Resources Control Board Hearings on the Bay-Delta.

Hall, W. H., 1886. Topographic and irrigation map of the San Joaquin Valley, Sheets 2 and 3. California State Engineers Department. Sacramento, CA.

Madeheim, H., 1999. Full natural flow estimates at Friant Dam, developed from USAN model.

Mussetter Engineering, Inc., 2000a. *Hydraulic and Sediment Continuity Modeling of the San Joaquin River from Friant Dam to Mendota Dam, California*. Prepared for the U.S. Bureau of Reclamation, Fresno, California, Contract No. 98-CP-20-20060, MEI Project No. 98-13, March.

Mussetter Engineering, Inc., 2000b. *Hydraulic and Sediment Continuity Modeling of the San Joaquin River from Mendota Dam to the Merced River, California*. Prepared for the U.S. Bureau of Reclamation, Fresno, California, Contract No. 99-CS-20-2080, MEI Project No. 99-12, September.

Poff, N. L., J. D. Allan, M.B. Bain, J.R. Karr, K.L. Prestegaard, B.D. Richter, R.E. Sparks, and J.C Stromberg, 1997. The Natural Flow Regime, *Bioscience*, 47(11): 769-784 pp.

Reclamation Board, 1969. Operation and Maintenance Manual for San Joaquin River and Chowchilla Canal Bypass Automatic Control Structures and Appurtenances, Part III.

San Luis Canal Company, 1969. *Operation and Maintenance Manual*, Parts II and III, Section 5100.

Stanford, J. A., J. V. Ward, W.J. Liss, C.A. Frissell, R.N. Williams, J.A. Lichatowich, and C.C. Coutant. (1996). A general protocol for restoration of regulated rivers, *Regulated Rivers: Research and Management,* Vol. 12, 391-414.

Trush, Dr. William, Personal communication, 2002, field reconnaissance of Little Dry Creek watershed.

U. S. Army Corps of Engineers (ACOE), 1917. San Joaquin River, California—Herndon to Head of Delta. Part I in 48 sheets. The Third San Francisco District, in cooperation with the Department of Engineering, State of California, and in collaboration with the California Debris Commission. San Francisco, CA.

U.S. Army Corps of Engineers (ACOE), 1980. *Friant Dam and Millerton Lake, San Joaquin River, California, Report on Reservoir Regulation for Flood Control*, Sacramento District, December 1955 (Revised August 1980).

U.S. Army Corps of Engineers (ACOE), 1990a. HEC-1, Flood Hydrograph Package, Version 4.0, Hydrologic Engineering Center, Davis, California.

U.S. Army Corps of Engineers (ACOE), 1990b. HEC-2, Water Surface Profiles, Version 4.6.0, Hydrologic Engineering Center, Davis, California.

U.S. Army Corps of Engineers (ACOE), 1990c. *River Routing with HEC-1 and HEC-2*, Training Document No. 30, Hydrologic Engineering Center, September, 25 pp.

U.S. Army Corps of Engineers (ACOE), 1993. *San Joaquin River Mainstem, California, Reconnaissance Report*, Sacramento District, Sacramento, California, January.

U.S. Army Corps of Engineers (ACOE), 1999. *Sacramento-San Joaquin Comprehensive Study Post Flood Assessment*, Regulated Flood Flow Frequency Analysis for the Sacramento/San Joaquin River Basins and Delta Tributaries, March, 10 pp.

U.S. Government Land Office, 1855. Plat maps along the San Joaquin River.

USGS, 2000. Water resources data for California, 1910-2000 for various gaging stations within the San Joaquin Valley.

USGS, 1998. Water Quality in the San Joaquin-Tulare Basins California, 1992-1995, *USGS Circular 1159*, Washington D.C.

USGS 1982. *Guidelines for determining flood flow frequency*, Bulletin 17B, Interagency Advisory Committee on Water Data, Hydrology Subcommittee, Washington DC.

USGS, 1975. *Water resources data for California*, 1910-1975 for Chowchilla River and Fresno River gaging stations.